ΕΘΝΙΚΟ ΜΕΤΣΟΒΙΟ ΠΟΛΥΤΕΧΝΕΙΟ
ΣΧΟΛΗ ΗΛΕΚΤΡΟΛΟΓΩΝ ΜΗΧΑΝΙΚΩΝ
ΚΑΙ ΜΗΧΑΝΙΚΩΝ ΥΠΟΛΟΓΙΣΤΩΝ
ΤΟΜΕΑΣ ΗΛΕΚΤΡΙΚΗΣ ΙΣΧΥΟΣ

Εφαρμογή Ημιαγωγών Ισχύος από Καρβίδιο Πυριτίου σε Υβριδικά Ηλεκτρικά Οχήματα

ΔΙΠΛΩΜΑΤΙΚΗ ΕΡΓΑΣΙΑ

Αντώνιος Δ. Αντωνόπουλος

Επιβλέπων : Στέφανος Ν. Μανιάς
Καθηγητής Ε.Μ.Π.

Αθήνα, Ιούλιος 2007

ΕΘΝΙΚΟ ΜΕΤΣΟΒΙΟ ΠΟΛΥΤΕΧΝΕΙΟ
ΣΧΟΛΗ ΗΛΕΚΤΡΟΛΟΓΩΝ ΜΗΧΑΝΙΚΩΝ
ΚΑΙ ΜΗΧΑΝΙΚΩΝ ΥΠΟΛΟΓΙΣΤΩΝ
ΤΟΜΕΑΣ ΗΛΕΚΤΡΙΚΗΣ ΙΣΧΥΟΣ

Εφαρμογή Ημιαγωγών Ισχύος από Καρβίδιο Πυριτίου σε Υβριδικά Ηλεκτρικά Οχήματα

ΔΙΠΛΩΜΑΤΙΚΗ ΕΡΓΑΣΙΑ

Αντώνιος Δ. Αντωνόπουλος

Επιβλέπων : Στέφανος Ν. Μανιάς
Καθηγητής Ε.Μ.Π.

Εγκρίθηκε από την τριμελή εξεταστική επιτροπή την 23η Ιουλίου 2007.

.....	.....	.....
Σ. Μανιάς	Α. Κλαδάς	Σ. Παπαθανασίου
Καθηγητής Ε.Μ.Π.	Καθηγητής Ε.Μ.Π.	Λέκτορας Ε.Μ.Π.

Αθήνα, Ιούλιος 2007

.....
Αντώνιος Δ. Αντωνόπουλος

Διπλωματούχος Ηλεκτρολόγος Μηχανικός και Μηχανικός Υπολογιστών Ε.Μ.Π.

Περίληψη

Στη διπλωματική αυτή εργασία παρουσιάζεται η σχεδίαση ενός μετατροπέα ισχύος από Καρβίδιο Πυριτίου (SiC) με εφαρμογή σε υβριδικά ηλεκτρικά οχήματα. Προορίζεται για το σύστημα BAS (Εναλλάκτης και εκκινητής, οδηγούμενος από ιμάντα) της General Motors που χρησιμοποιείται σε ήπιας μορφής υβριδικά αυτοκίνητα. Το καρβίδιο του πυριτίου αποτελεί μια καινοτομία, η οποία φαίνεται να έχει πολλά πλεονεκτήματα συγκρινόμενη με την τεχνολογία του πυριτίου που είναι κοινή σήμερα. Η σχεδίαση αυτή επικεντρώνεται στις διάφορες λειτουργίες του συστήματος BAS και την αντίστοιχη συμπεριφορά του ηλεκτρικού μετατροπέα. Στόχος είναι να υπολογίσουμε τις απώλειες του μετατροπέα κατά τη διάρκεια ενός τυποποιημένου κύκλου οδήγησης και να αποφασίσουμε αν είναι δυνατό να χρησιμοποιήσουμε το σύστημα ψύξης του κινητήρα εσωτερικής καύσης ώστε να ψύξουμε επίσης τους ημιαγωγούς, κάτι που είναι ανέφικτο χρησιμοποιώντας κοινούς ημιαγωγούς από πυρίτιο. Αν τελικά αυτό φανεί δυνατό, προχωράμε υπολογίζοντας την κατάλληλη ψύκτρα για το μετατροπέα μας και ελέγχουμε αν όντως μπορεί μια τέτοια ψύκτρα να βρεθεί στην αγορά ή οι απαιτήσεις μας είναι εξωπραγματικές.

Λέξεις κλειδιά: Belt-driven Alternator and Starter (BAS), Καρβίδιο πυριτίου (SiC), Διπολικό τρανζίστορ ένωσης (BJT), Αντιστροφέας ισχύος, MATLAB-Simulink, Κύκλος οδήγησης, Απώλειες ισχύος.

Abstract

This thesis is about the design of a Silicon Carbide power converter that can be used in hybrid electric vehicle applications. It is intended for a BAS (Belt driven Alternator and Starter) in a mild hybrid car. Silicon Carbide is an innovative technology that seems to have many advantages compared to the silicon that is commonly used today. This design estimates on the different functions of a BAS and the converter's behavior in each case. The aim is to estimate the converter's losses over a standard driving cycle and decide if it is possible then to use the combustion engine's cooling system to cool the semiconductors as well. If this is achievable then we have to estimate a heat sink for that converter and see if there is such heat sink on the market, or our demand is extreme.

Keywords: Belt-driven Alternator and Starter (BAS), Silicon Carbide (SiC), Bipolar Junction Transistor (BJT), Inverter, MATLAB-Simulink, Driving Cycle, Power Losses.

Acknowledgements

The present thesis was carried out during the spring semester of 2007, at the Industrial Electrical Engineering and Automation department of Lund Institute of Technology. Hoping not to forget anyone, I would like to thank:

- Professors Mats Alaküla and Hans Bängtsson (IEA, LTH) for giving me the chance to work on that project and supervising me on my thesis
- Professors Stefanos Manias and Stavros Papathanasiou (NTUA) for their guidance throughout my whole studies, the inspiration and the encouragement to occupy with electric power and power electronics
- Lars Hoffmann, Tommy Lindholm (SAAB) and Bo Hammarlund (TranSiC) for their assistance and the information they provided for this project
- All the people at IEA for their hospitality and especially Avo Reinap, Gunnar Lindstedt, Jonas Ottosson, Martin Andersson and Oscar Haraldsson for the priceless time they dedicated on me and the knowledge they provided on the HEV subject
- My opponents, Ann Åkesson and Joakim Rydh for their comments, recommendations and questions of course.
- Professor Ioannis Vardoulakis for his guidance and the people at Geolab (Ioannis-Orestis, Stefanos-Aldo, Sotiris, Manolis, Eleni, Ioannis) for their friendship and support throughout the past 5 years
- My family, Diamantis, Zoi and Panagiota for their love and support all these years and last but not least, all my friends in Greece, Sweden and the rest of the world

Lund, 21 June 2007

Antonios Antonopoulos

Table of contents

1. Introduction

1.1 Thesis' outline

This master thesis is about designing a power converter for a mild hybrid electric vehicle. The distinctive feature of this converter is that it consists of bipolar junction transistors, based on silicon carbide. The idea to use silicon carbide in a vehicle application derived from its advantages in high temperature operation. Compared to a normal silicon junction, that cannot operate over 120^{o}C, a silicon carbide junction is reliable even up to 300^{o}C. The temperature under a car's hood can reach up to 130 or 140^{o}C under severe conditions, temperatures that normal silicon cannot withstand. As a result, silicon carbide is a promising technology not only in high voltage applications, but in high temperature ones as well.

The first step was to decide on some characteristics of the electric machine that is going to be used in this application. There are many possible designs, but the most suitable one seems to be the synchronous machine with a magnetization circuit in series. Then we needed to consider the power of that machine that compromised better between the demanded torque and the cost. Another important factor of the machine design is if it is going to be a round (traditional) rotor machine or a claw pole one. In case of a claw pole machine we have to decide for the number of poles as well.

Knowing some technical characteristics, we proceed to a simulation of the complete hybrid, using the MATLAB Simulink package, to see how this model behaves on duty. This hybrid car model exists at the IEA department, but needs the appropriate changes to simulate a BAS system. Apart from our main goal, which is the inverter design, we can evaluate the BAS' efficiency and the improvement it causes to the combustion engine's behavior.

After running the simulations, we are in place to estimate the power flow over the inverter during a standard driving cycle. That power, together with the components' characteristics, leads us to calculate the power losses over the semiconductors. Apart from the losses on normal driving, our electric machine has to operate as starter as well, so we have to investigate how the inverter operates during the starter function. This is the only period where the inverter uses a different modulation than the square pulse and as a result we cannot omit it.

Last but not least, the most important part is to investigate how these losses affect the junction temperature of the components and to estimate an appropriate heat sink for the converter that will cool the semiconductors efficiently with a water temperature of 130°C. All calculations in this thesis are done for both a 112 V battery voltage and a 300 V one. The aim is to conclude on the design that would be more appropriate, as silicon carbide components have proven to be more efficient in higher voltage applications so far.

1.2 The mild hybrid vehicle

It is worth writing a small description of the mild hybrid car. The word "mild" is used referring to the electric machine of a vehicle, which is considerably low power, compared to a full hybrid vehicle. The power range of a mild hybrid's machine is from 5 up to 20 kW. This kind of machines are not able to provide enough power for a pure electric, zero emission driving, but can take advantage of regenerative braking and are able to assist the ICE in heavy accelerations, when more torque is needed. This results in consuming less fuel than a normal car. Higher scale hybridization can result in even lower fuel consumption, however, it increases the initial cost of such a car. In figure 1.1 we can see a comparison of how an electric motor can function, depending on its size and how the cost rises correspondingly to the machine's size. The image is taken from a SAAB hybrid presentation [1].

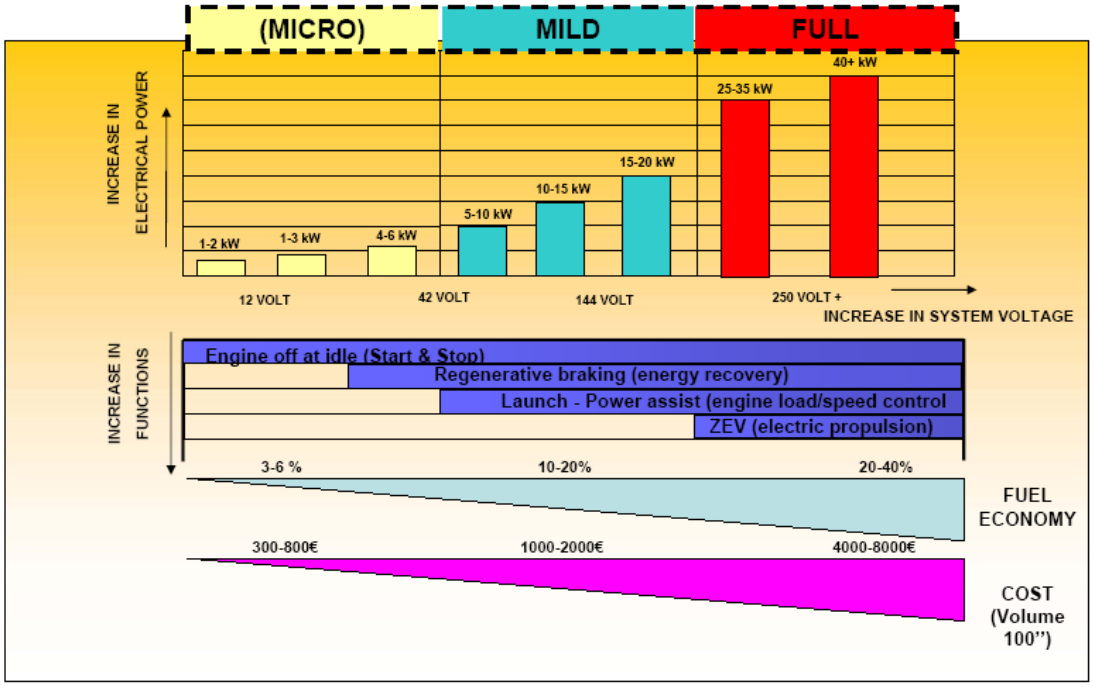

Figure 1.1: Hybrid systems and their attributes

Running some simulations to decide the least fuel consuming configuration we result to figure 1.2 for a gasoline combustion engine [Haraldsson-Andersson, 2007]:

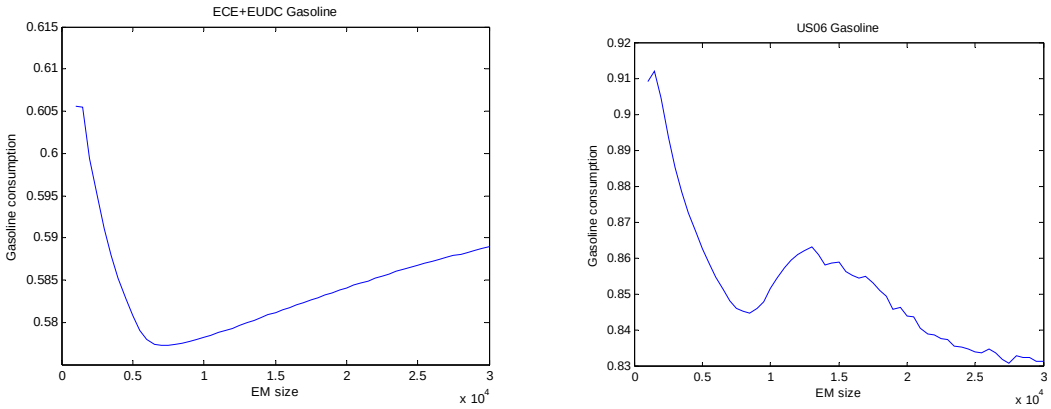

Figure 1.2: Fuel consumption (lt/10km) over different EM sizes with the NEDC and US06 cycle, gasoline engine

It is shown that the most fuel saving configuration relies on a 7-8 kW electric machine. Going from an 8 to a 5 kW machine would cost a lot in fuel saving, but could reduce the initial cost even more. We conclude then to a 5 kW electric machine as the most appropriate for a low cost mild hybrid vehicle.

1.3 Silicon Carbide Bipolar Junction Transistors

As stated at the beginning, the power semiconductors that are going to be used are made of doped SiC wafers. The reason for that choice is that we can reduce the cost if we are able to use the engines cooling circuit in order to cool the semiconductors as well. To introduce SiC technology we are going to present some advantages in comparison to Si. These information were provided from TranSiC, a leading company in developing transistors in silicon carbide.

Silicon Carbide has a bandgap almost three times wider than Si, meaning that the electrons need higher activation energy to jump to the conduction band. As a result, SiC junctions can operate at higher temperature, without any unwanted conduction.

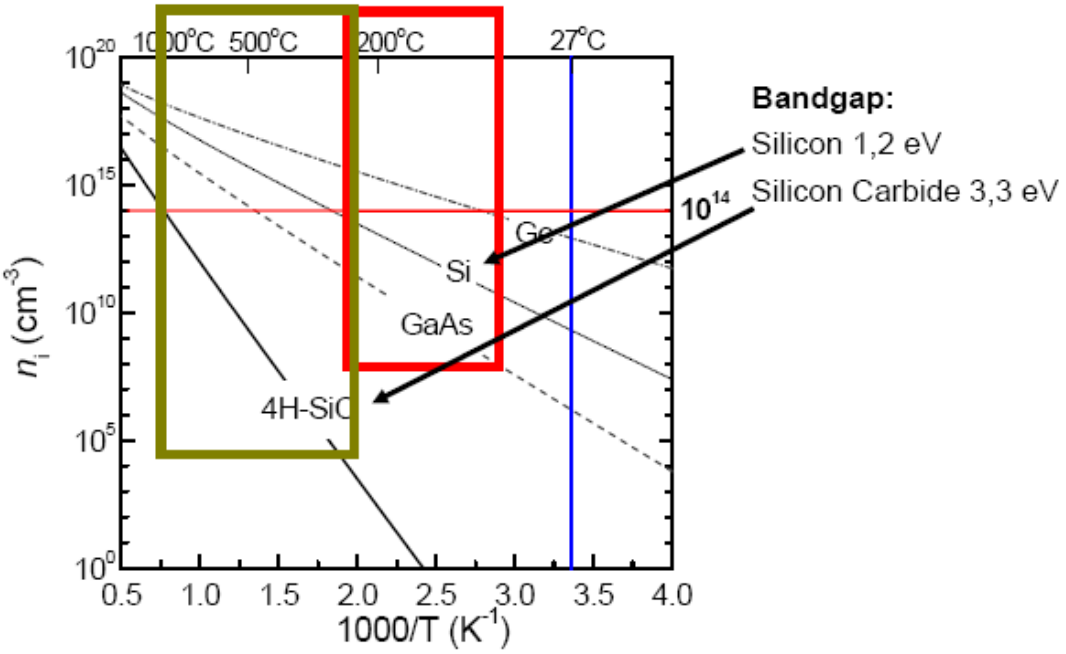

Figure 1.3: Si and SiC bandgap

Another advantage is that its electric breakdown field is almost ten times higher than silicon's, so either it can withstand much higher electric field, or we can make the transistor thinner. By making it thinner we achieve much better switching characteristics, as turn-on and turn-off times are smaller, thus having lower switching losses over the transistors. A comparison between the characteristics of a Si IGBT and a SiC BJT is shown in table 1.1.

Table 1.1: Comparison between a Si IGBT and a SiC BJT characteristics

	V_F @1A	Turn-on loss 800 V 1 A Inductive RT	Turn-off loss 800 V 1 A Inductive RT	T_{max}	DC drive current
SiC BJT	0,52 V	0,03 mJ	0,006 mJ	pack. limited	10 mA
Si IGBT IGDP01N120H2	2,25 V	~ 0,05 mJ	~ 0,05 mJ	150 °C	0

To conclude with this quick reference to silicon carbide power semiconductors, we present a figure where we can make out the different doped layers of a 4H-SiC transistor [Haraldsson-Andersson, 2007].

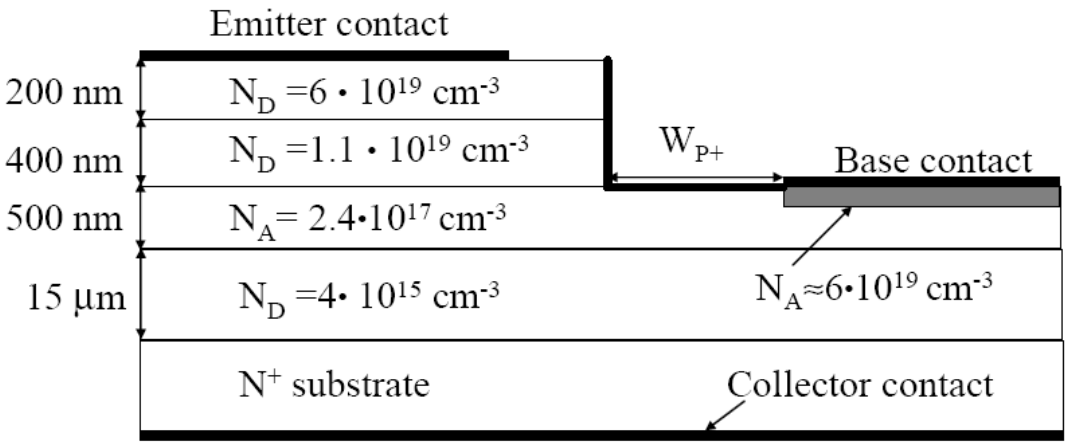

Figure 1.4: A cross section of one finger of a SiC BJT

2. Design parameters of the EM for the BAS application

2.1 Parameters of the Electric Machine

To start with the main part of the thesis, we are specifying some parameters for the electric machine design. At first, the battery and, hence, the DC link voltage. The desired potential is as low as possible, because it will reduce the battery dimensions. For several reasons we are not allowed to look into a design under 100 Volts, so we end up to a battery voltage level of 112 Volts. It would be interesting to detect any advantages or disadvantages of a higher voltage design, as the silicon carbide semiconductors prove to be more efficient in higher voltages. So we are going to investigate a second design, the 300 Volts standard.

The BAS operating principle is based on the existence of a belt that connects the electric machine's shaft to the combustion engine's main shaft. There is a gear ratio of 3:1 between the ICE and the EM, so the electric motor's speed is always three times higher than the ICE's. Considering that a normal car's ICE can reach speeds up to 6500 rpm, the EM has to be able to reach the speed of 19500 rpm. In a 6 pole machine design the electric frequency can reach up to 975 Hz, as:

$$f_e = \frac{pn_{EM}}{60}$$

The electric machine has three different operating modes. The first is to start the ICE, as the BAS operates as an integrated starter. The second is to provide extra torque during accelerations either when the ICE cannot provide the torque required, or when it is not efficient for the ICE to provide it. The third role is to take advantage of the energy produced over a deceleration and charge the battery with that amount of energy.

As a starter, it has to be able to start the ICE under the most severe circumstances, which occur under very low temperatures. We assume that even under -40°C, the maximum amount of torque needed will never be more than 180 Nm. Knowing that $n_{EM} = 3n_{ICE}$, $p = 3$ (pole pairs) we can estimate the ratio between the angular frequency of the ICE ω_{ICE} and the electrical angular frequency of the EM $\omega_{e,EM}$:

$$\left.\begin{aligned}\omega_{ICE} &= \frac{\pi n_{ICE}}{30}\\ \omega_{e,EM} &= \frac{p\pi n_{EM}}{30}\end{aligned}\right\} \Rightarrow \omega_{e,EM} = \frac{3\pi 3n_{ICE}}{30} = 9\omega_{ICE}$$

The power that flows from the EM to the shaft is equal to the power received from the ICE (ignoring any friction losses), so if the torque the ICE needs to start is 180 Nm, then the electrical torque that the EM is asked to provide is:

$$\left.\begin{aligned}P_{shaft} &= T_{ICE}\omega_{ICE}\\ P_{EM} &= T_{EM}\omega_{e,EM}\end{aligned}\right\} \overset{\substack{P_{shaft}=P_{EM}\\ 9\omega_{ICE}=\omega_{EM}}}{\Rightarrow} T_{ICE} = 9T_{EM} \Rightarrow T_{EM} = 20Nm$$

This value is important when we try to estimate the magnetic flux of the machine. Knowing the initial torque and assuming a constant torque period before the field weakening area, we can estimate the base speed of the EM:

$$\omega_{base} = \frac{P}{T} = \frac{5kW}{20Nm} = 250\,rad/s \Rightarrow n_{base} = \frac{30\omega_{base}}{p\pi} = 795{,}77rpm$$

$\frac{n_{base}}{n_{\max}} = \frac{795{,}77rpm}{19500rpm} = 0{,}041$ or 4,1% of the maximum speed.

The field weakening area starts at 795 rpm for the EM, or at 265 rpm for the ICE. In electrical frequency units, this is translated to 39.79 Hz. During the field weakening area, we operate the inverter in square pulse mode. During the starting period, from 0 up to 40 Hz, we use a pulse width modulation, as we want to keep the torque constant. Actually, from 36 up to 40 Hz, the modulation is between the PWM and the square pulse modulation and the area is called the overmodulation area.

For the square pulse mode the line to line output voltage can be estimated by:

$$V_{LL,\max}^{rms} = \frac{\sqrt{6}}{\pi}V_{dc} \approx 0.78V_{dc}\,,$$

which is 87.4V for the 112V design and 234V for the 300V design. On the other hand, the PWM phase uses a special reference signal that is estimated by subtracting from a normal sinus half the sum of the maximum and the minimum value of the corresponding 3 phase signal.

$$V_{a,ref} = u_{a,ref} - \frac{1}{2}\left(\max\left(u_{a,ref}, u_{b,ref}, u_{c,ref}\right) + \min\left(u_{a,ref}, u_{b,ref}, u_{c,ref}\right)\right)$$

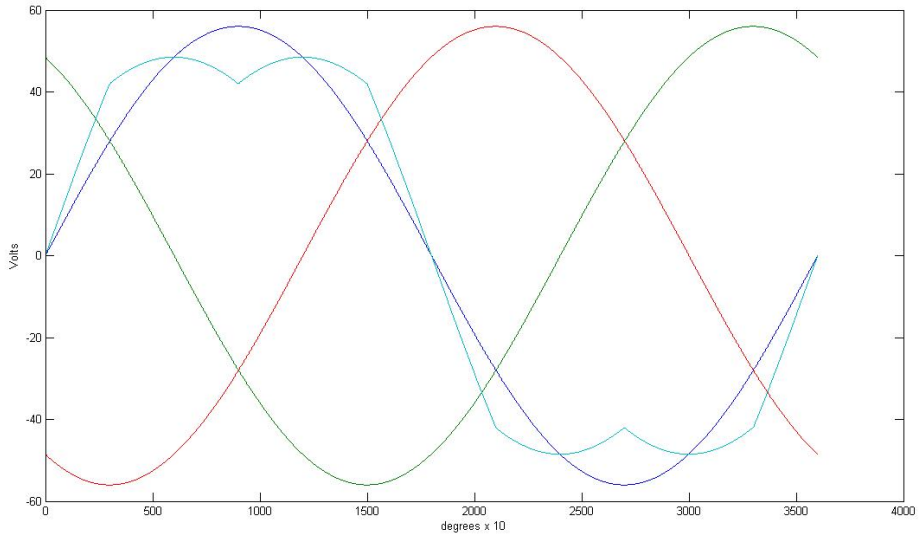

Figure 2.1: Construction of the reference signal

The $V_{a,ref}$ is shown in light blue, while the sinusoidal waveforms correspond to the phase signals u_a, u_b, u_c. This reference allows us to achieve higher voltages over a pulse width modulation, according to the equation:

$$V_{LL}^{rms} = \frac{\sqrt{6}}{\pi}\frac{\pi}{4}\frac{2}{\sqrt{3}}V_{dc} = \frac{1}{\sqrt{2}}V_{dc}$$

The highest line to line voltage in each design is 79.2 Volts for the 112 Volts DC link and 212.1 Volts for the 300 Volts DC link.

The silicon carbide transistors are able to withstand high voltage, over 1 kV, but cannot stand high current [3]. It is important then to estimate the current that flows through each phase and then decide how many semiconductors we are going to use in parallel in each phase leg. Before estimating the current, we need to estimate the magnetic flux of the machine. For the electric machine, at the point where the field weakening effect starts, we have: $n_{base} = 795{,}77 rpm \Rightarrow \omega_{base} = 250\, rad/s$. The input (line to line) voltage of the motor is 87,4V/234V and the power produced is 5 kW. We can assume that the EMF of the EM almost equals the input voltage, so we can estimate the machines magnetic flux, that is:

$$\Psi = \frac{EMF}{\omega_{base}}$$

The corresponding values for each design are 0.35Wb for the 112V and 0.936Wb for the 300V. We also know the torque the EM can produce at this operation point, so we can also estimate the phase current that causes this flux:

$$i_{phase} = \frac{T}{\Psi\sqrt{3}},$$

that means 33.03A for the 112 V design and 12.34A for the 300V. There is also a matter concerning the input voltage, which is not really constant and is dependant on the SOC. The battery voltage can be from $V_{bat} - 20\%$ up to $V_{bat} + 10\%$, so we can have maximum current values that are presented in table 2.1:

Table 2.1: Maximum and nominal current

112V design	*300V design*
V_{in}=87.4V	V_{in}=234V
$i_{nom,RMS}$=33.03A	$i_{nom,RMS}$=12.34A
$i_{max,RMS}$=41.3A	$i_{max,RMS}$=13.57A

Considering that a SiC BJT cannot drive currents higher than 5A, we conclude to an inverter that consists of 72 transistors (12 per module, 24 per phase leg) in the 112V design and 24 BJTs in the 300V design. As for the free wheeling diodes, their forward current is not significantly higher than the transistors' [4], so a good approach would be to place one diode per transistor in any design. A first conclusion that comes from this chapter is that the cost to build an inverter for the low voltage design is three times higher than the higher voltage design as we need three times more components.

Before closing this chapter, we can present the torque and power characteristics of the electric machine and the improved torque and power characteristics of the hybrid vehicle. By adding the electric motor we accomplish much better torque values over the low combustion engine's speed, where its own torque is considerably low. BAS shows that it can improve a vehicle's performance, as the increased low speed torque results into faster accelerations.

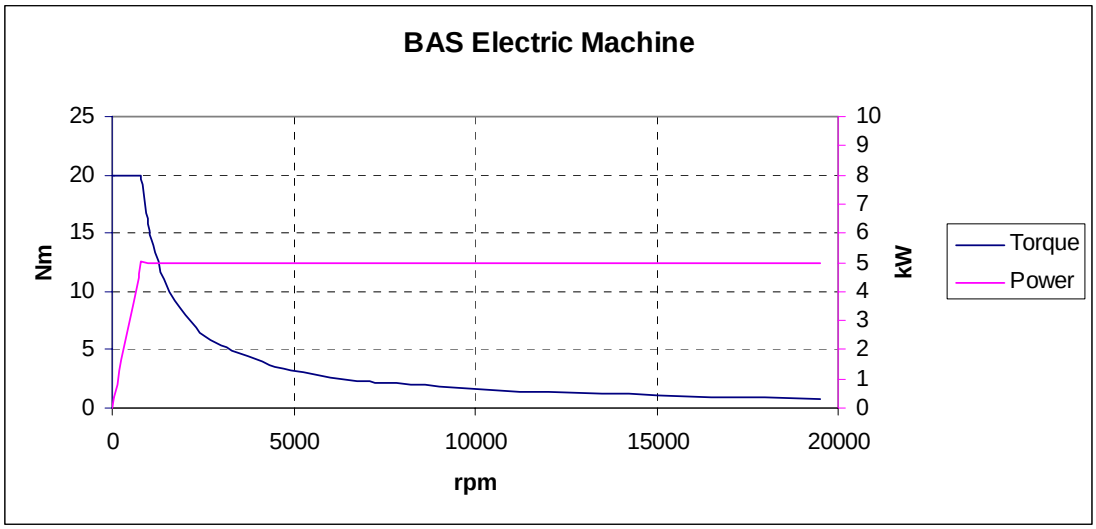

Figure 2.2: EM torque and power graph

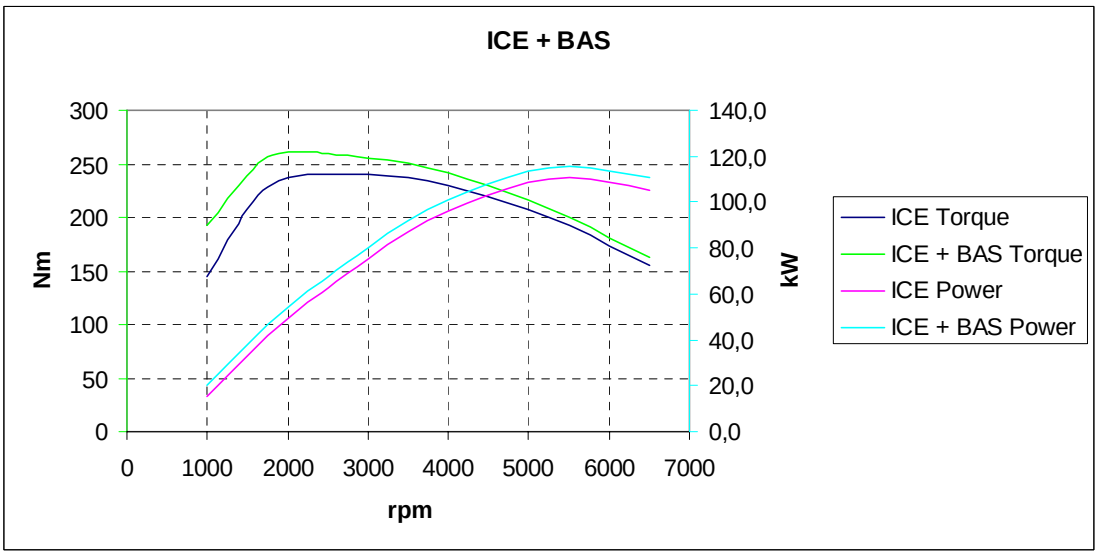

Figure 2.1: Improved vehicle's characteristics

2.2 The Series Magnetized Synchronous Machine

There are several types of machines that can be used for our application. A synchronous machine is preferred as it is a widely known machine, easy to control and is commonly used as an electrical power generator. Its advantages are high torque and power density and high efficiency. We can either use an electrically magnetized or a permanent magnetized synchronous machine. In a permanent magnet machine there is a limit for how much negative flux the magnets can withstand before they are demagnetized. This is thus a limit for the operating region flexibility of the PMSM. Loosing the control of a deeply field-weakened PMSM can result in very high voltages that may damage power electronics and control electronics [Bergh, 2006].

The request for high initial torque leads to a deep field weakening area of the machine. As we are not able to use a PMSM, we will use an electrically magnetized synchronous machine. Our system runs solitarily, so it is not desired to have an extra external source to magnetize the machine. Our only alternative is to use a series magnetized synchronous machine. This is an electrically magnetized synchronous machine that uses the phase currents for exciting the field winding circuit. In such a machine the open end of an EMSM connected in Y is the input to a three phase diode bridge rectifier. The rectifier then supplies energy to the field winding via slip rings. As a result, the field winding current is strictly dependant on the synchronous machine phase currents and the conduction state of the diode bridge rectifier. The operating principle can be seen in figure 2.4. It reminds much of a series magnetized direct current machine. It is important to note that the field winding inductance of a SMSM is lower than the field winding inductance of an EMSM [Bergh, 2006].

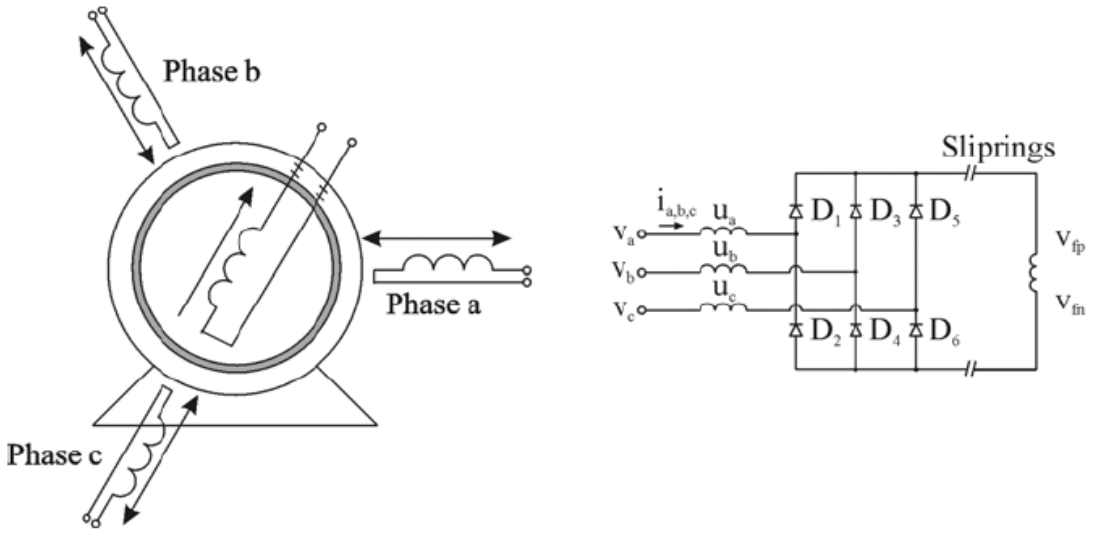

Figure 2.4: Principle of the Series Magnetized Synchronous Machine and circuit configuration

3. The Simulink BAS model

3.1 Describing the old model

After concluding to the design characteristics of the electric machine that is more suitable to use as an integrated alternator and starter, we would like to run some simulations and see how a hybrid car with these characteristics behaves. There is an existing simulink model of a parallel hybrid vehicle that is used in the Hybrid Electric Vehicle's course at LTH, developed by Mats Alaküla. In this chapter we are going to describe the model's function and at the end we are going to run some simulations to show the benefits of the mild hybrid.

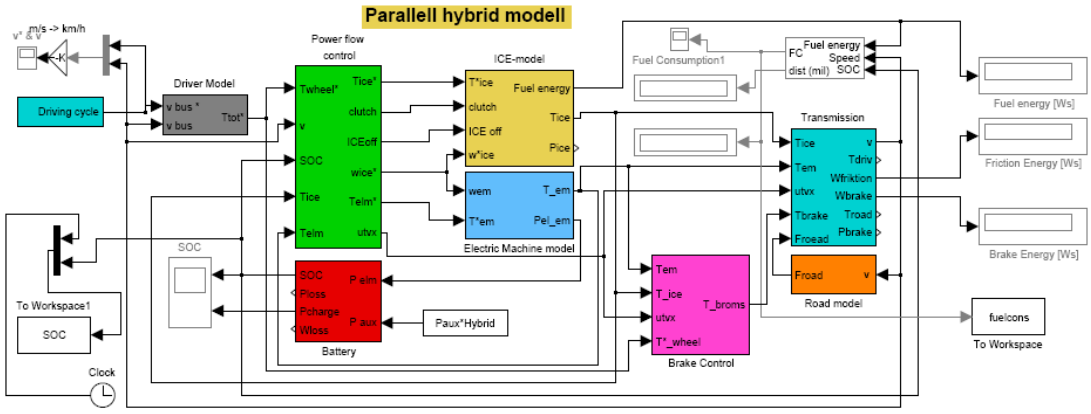

Figure 3.1: The parallel hybrid model

This model takes as input the desired speed of the vehicle, for example a specific driving cycle. It uses some technical specifications of a normal car, such as the wheel radius, the vehicle weight, the gear ratios etc. We determine the combustion engine's power, the battery's energy and the electric machine's power as well. Considering these characteristics, with the help of MATLAB, we built an optimal torque graph over the ICE's speed. The model's aim is to operate the ICE as close as possible to its optimal torque. In case of low efficiency operation, the controller stops the combustion engine and moves the car using the electric machine. This is how we decide to turn off the combustion engine.

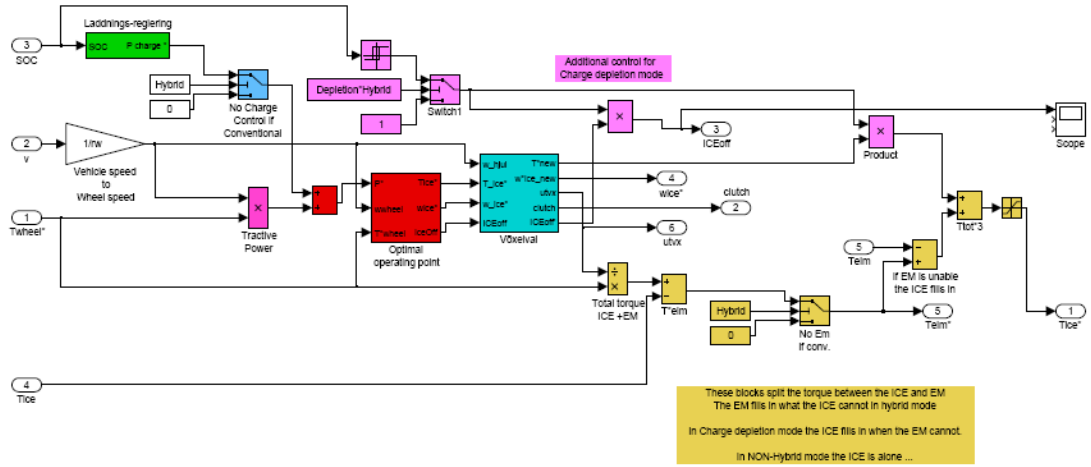

Figure 3.2: The power flow control unit

Another controller is used to control the battery's state of charge. We use the regenerative braking energy to charge the battery as the main charging energy, but we can also charge the battery by operating the ICE in higher power than needed if this leads to better efficiency.

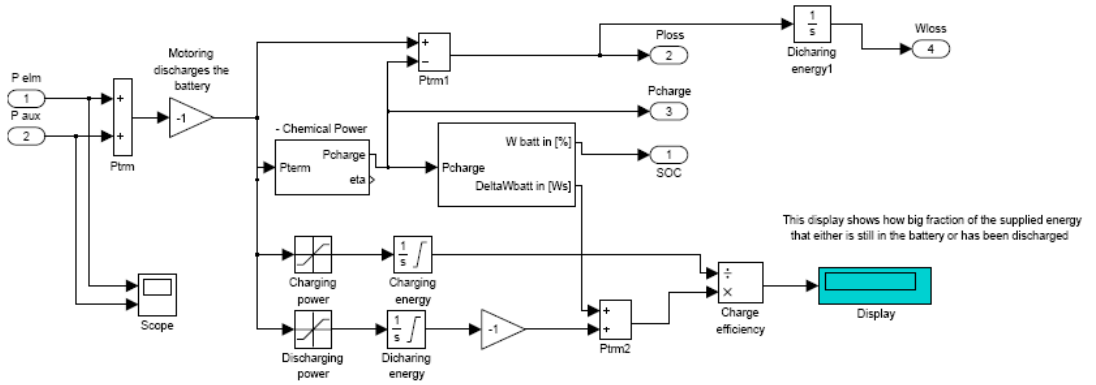

Figure 3.3: The battery model

The two most important models in this simulation are, of course, the ICE and the EM model. The combustion engine operates when needed and always at as high efficiency as possible. On the other hand, the electric machine can operate either separately or in connection to the ICE, depending on the operation. Their technical specifications are initiated by an M-file (appendix B1) we have to run before starting the model.

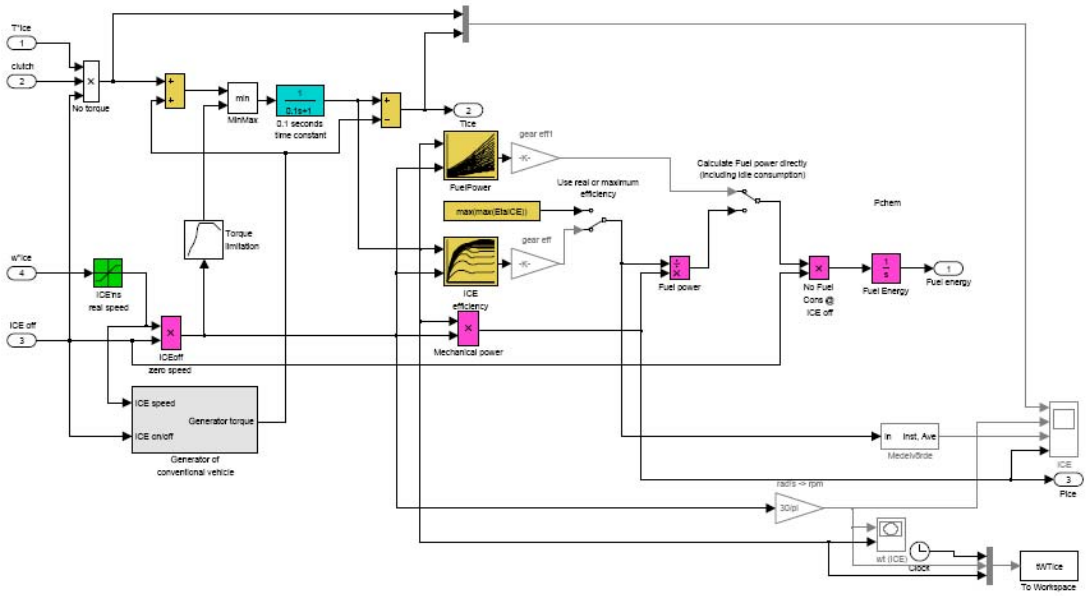

Figure 3.4: The ICE model

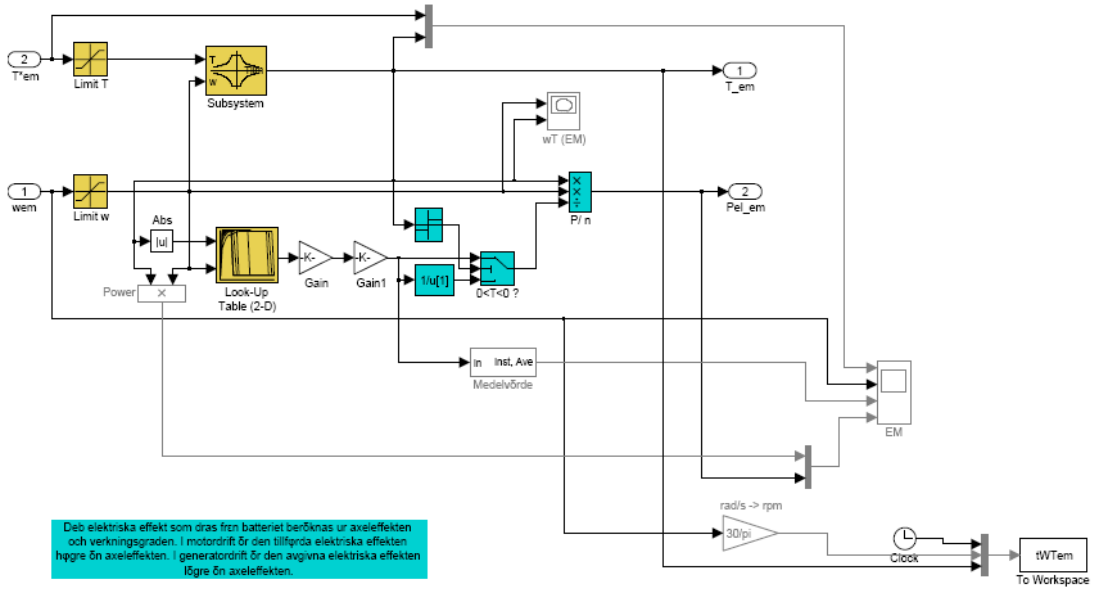

Figure 3.5: The EM model

3.2 The modified BAS model

As stated above, the previous model corresponds to a parallel hybrid model. Apart from the technical specifications we need to change for our mild hybrid, there are several other things to alter in order to make it operate like the real BAS system. The BAS idea is not based on the existence of any clutch between the two machines. Contrarily, there is a belt connecting the ICE and the EM and there is a gear ratio of 3:1 as well. It is not possible then to operate separately one of the two machines.

Furthermore, we cannot move the car using only the power produced from the electric motor, as it is too small for that operation. As a result, the ICE must always operate when the car is moving. We can use the EM, however, as an extra torque producer when accelerating the car if it increases the efficiency of the ICE and as a generator to charge the battery during a regenerative deceleration.

To consume less fuel, we introduce a "stop & go" function, which has the role to turn off the ICE when the car is not moving. That means that both engines are not operating and that we have to start the ICE before the driver asks for acceleration, because the driver should not become aware of that function. So when the driver releases the brake, we have the time (around 0.5 second) to start the ICE, using energy from the battery and turning it into kinetic energy on the electric motor. The modified simulink model is presented in figure 3.6:

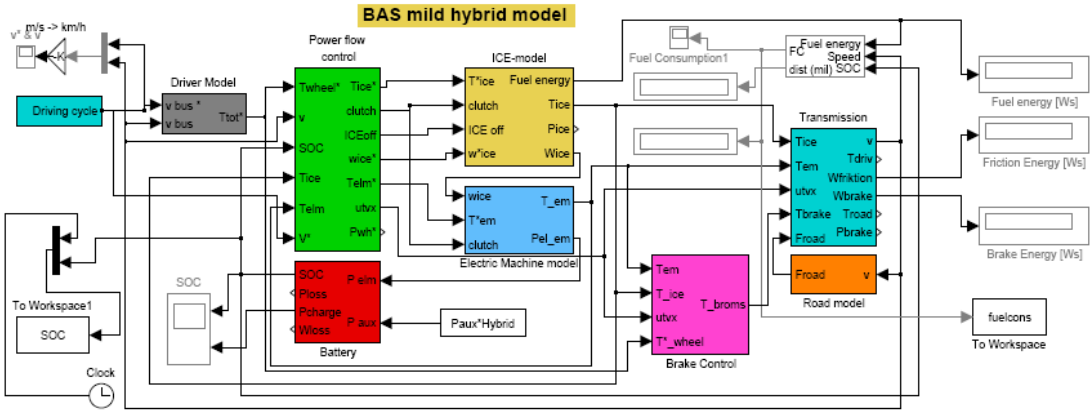

Figure 3.6: The BAS mild hybrid model

In that model we use directly the wheel speed as the criterion for the combustion engine's on or off state, instead of checking the combustion engine's efficiency. As stated above we turn off the ICE when the car is standing still. In addition to that, we have also changed the electric machine's speed. Now it is connected to the same shaft as the ICE is, so to estimate the EM's speed we use the ICE's speed as input and multiply it by the factor of 3 (gear ratio). This is done into the electric machine's model, as shown in figure 3.7.

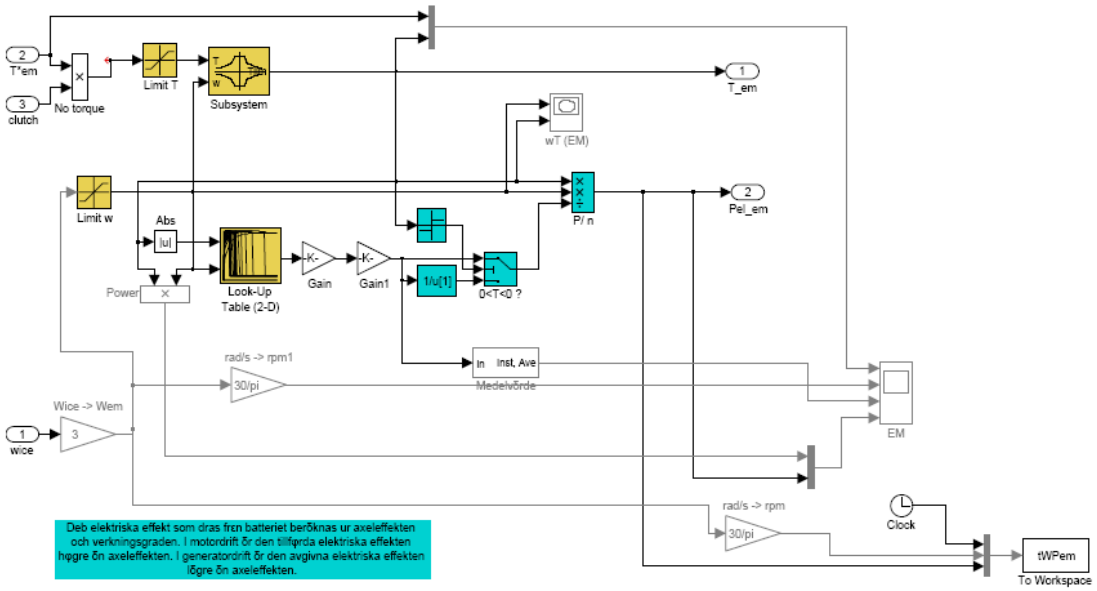

Figure 3.7: The alternated EM model for BAS

An important output of that model is the electric machine's power state that is exported to the workspace. This power is going to be used to calculate the losses over the power converter used between the EM and the battery, as this is the power transferred to and from the electric machine. These are the most important modifications made to the existing simulink model.

3.3 The initialization M-file

There is an M-file, completely presented in appendix B1, which is used to initialize some variables needed for the model to operate. These variables have to do mostly with technical specifications of the internal combustion engine, the electric machine and the vehicle itself. We present some of the more important specifications that were determined with the contribution of Lars Hoffman and Tommy Lindholm from SAAB.

To make our simulations we had to consider a specific car model. This model is a "SAAB 9-3 2.0 lt" with a gasoline engine. Its torque and power graph are shown in figure 3.8. The electric machine's power is 5 kW, as specified above. We choose a 25 kg battery with an energy density of 100 Wh/kg. The state of charge reference value is 70% and our aim is not to fall below that value at the end of a cycle.

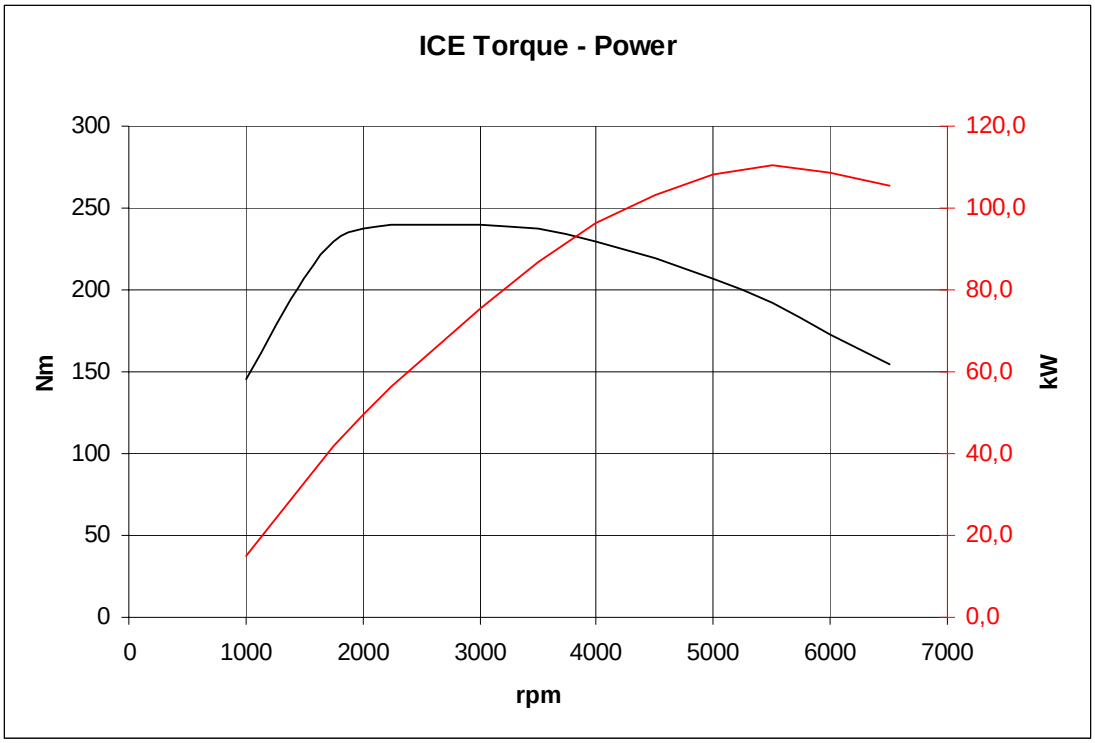

Figure 3.8: Torque and power graph of a SAAB 2.0 lt, gasoline engine

We have auxiliary power consumption on the vehicle, which reaches up to 0.6 kW. As every power consumption in a car needs DC voltage, we supply this power directly from the battery, without interfering with the inverter. Last but not least, we need some information about the gear ratios and the wheel dimensions in order to specify the exact combustion engine's speed at every moment. These information are provided once again by SAAB and presented in table 3.1. Wheel dimensions are: 225/45 R17, which give a radius of 31.7 cm.

Table 3.1: Gear ratios

wheel		**225/45 R17**
Gear	Gear Ratio	Total Gear Ratio
1st gear	13,6818	8,5
2nd gear	7,1591	16,2
3rd gear	4,5036	25,8
4th gear	3,4119	34,0
5th gear	2,5215	46,0
Back	13,0964	8,9

3.4 Running a simulation

We are going to run this model for the two driving cycles to see how the fuel consumption is decreased with the use of a small electric machine. Running the initiation file at first, we produce figures 3.9 and 3.10. In figure 3.9 we see the efficiency of the electric machine,

depending on power or torque. Turning the figure appropriately we can have a torque – power graph as well.

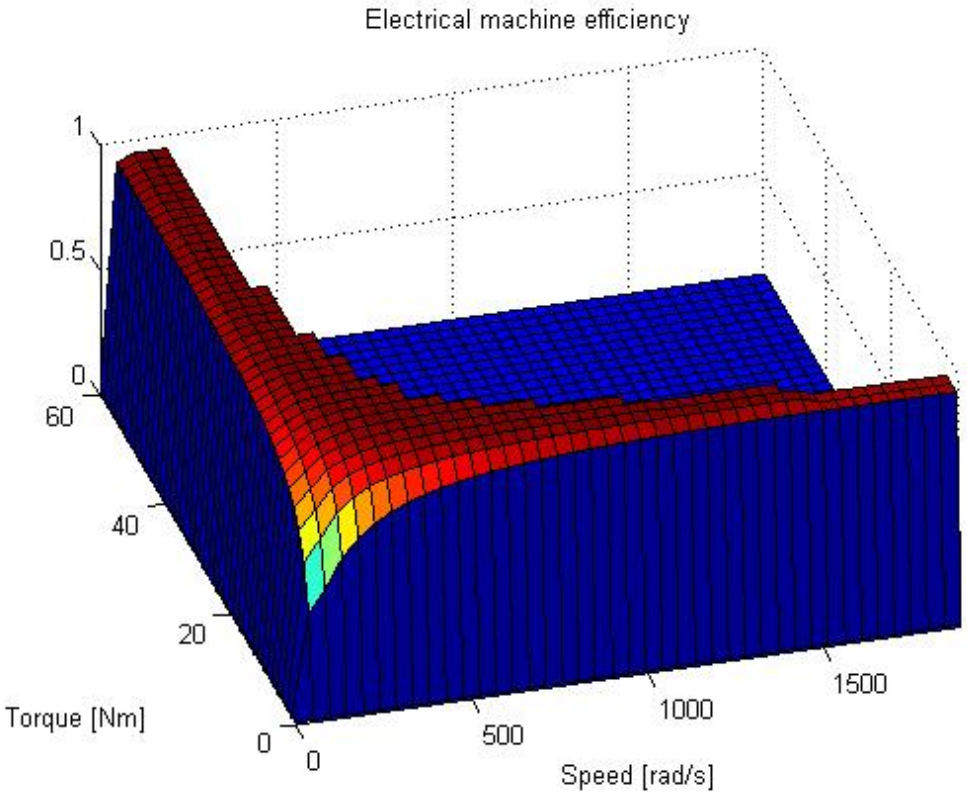

Figure 3.9: Electrical machine efficiency, over torque and power

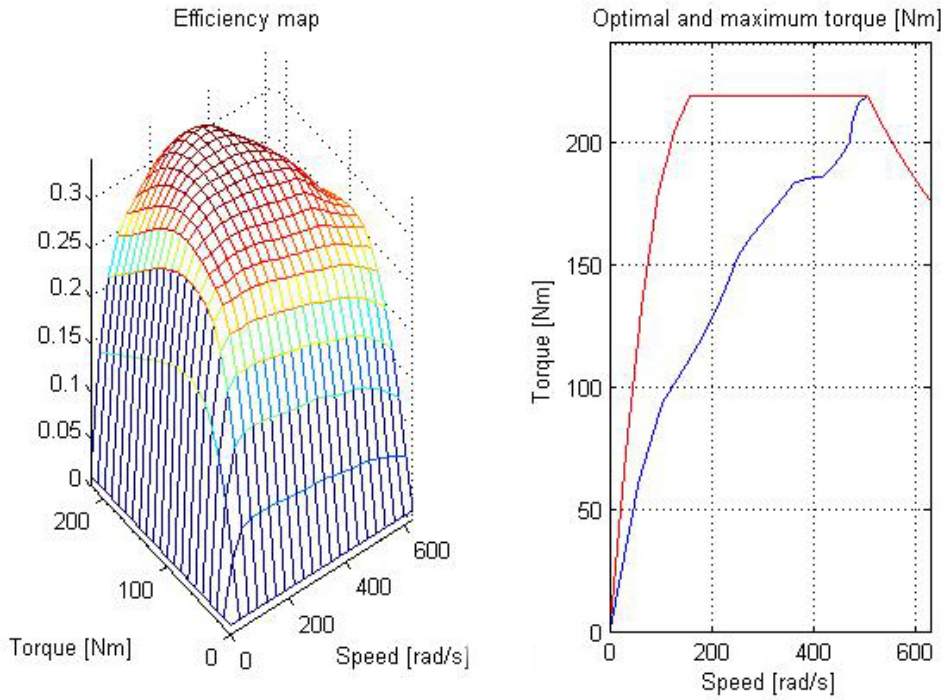

Figure 3.10: Improved efficiency map (left), maximum and optimal torque (right)

Figure 3.10 shows an efficiency map of the ICE that is much better than the corresponding without the contribution of the BAS. The right part of the same figure is a torque diagram. The red line is an approximation of the maximum torque the ICE can produce (the actual maximum torque is shown in figure 3.8), while the blue line is the optimal torque. We want to operate as close as possible to the optimal torque, as there we can achieve the best efficiency of the ICE.

It is time to run the BAS model now. We are going to run it for the two driving cycles, the NEDC and the US06. There are many parameters we can check, but the most important are the power consumed or generated by the electric machine and the battery's state of charge. We present them in the next graphs and then we make a comparison of the fuel consumption results for the two cycles, as it is important to know how profitable in fuel terms the BAS design is.

3.4.1 NEDC

The battery's SOC does never fall significantly, because of the battery's size and its controller. Over an urban driving cycle we take advantage of the decelerations, so we do not lose any charge of the battery.

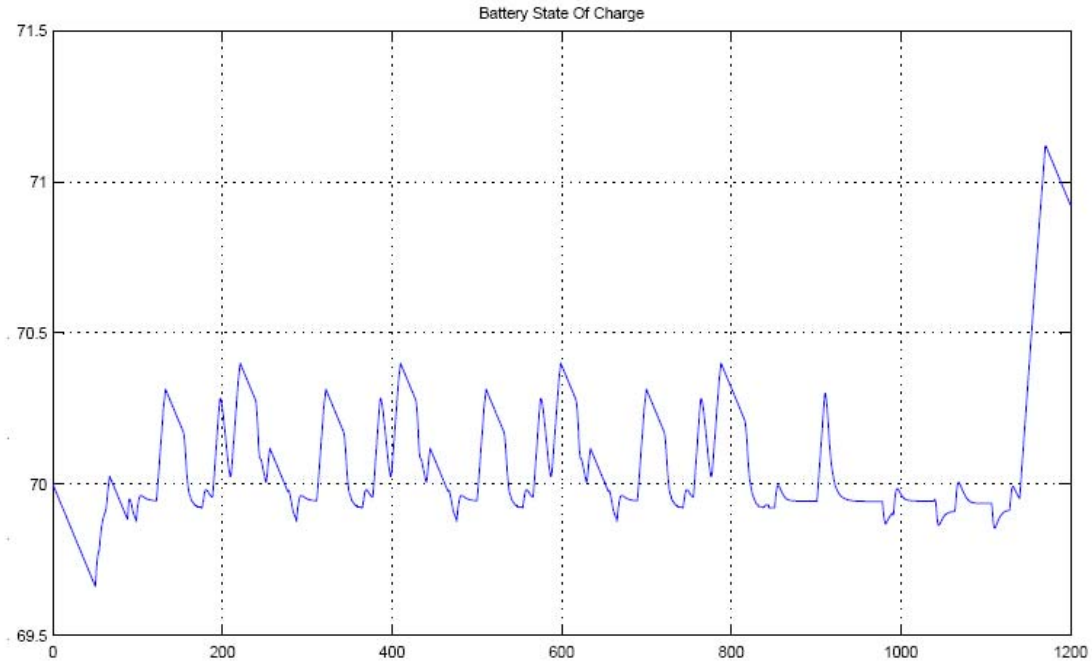

Figure 3.11: Battery SOC over NEDC

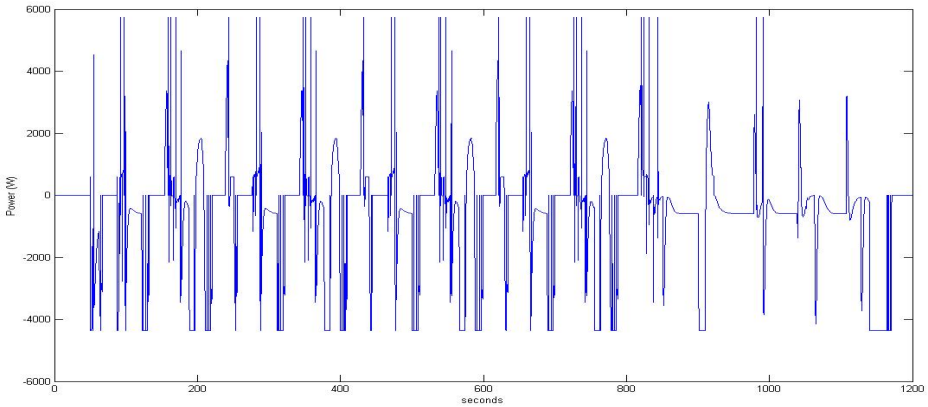

Figure 3.12: EM power flow over NEDC

3.4.2 US06

Apart from the significantly greater use of the electric machine and therefore the converter over a highway driving cycle, the charge controller can always keep the SOC around its reference value.

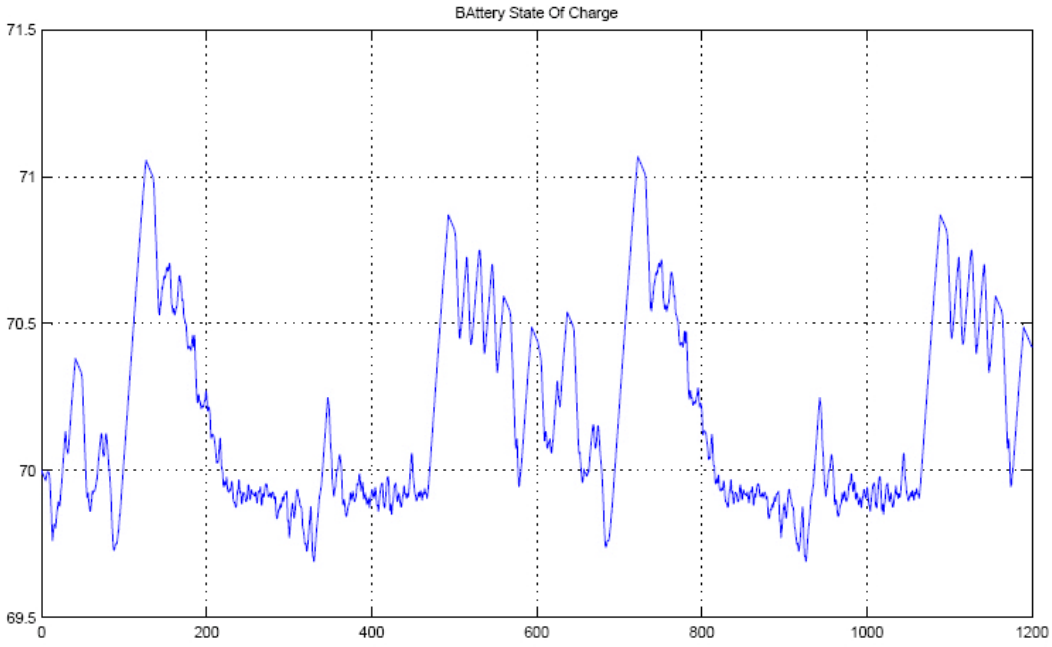

Figure 3.13: Battery SOC over US06

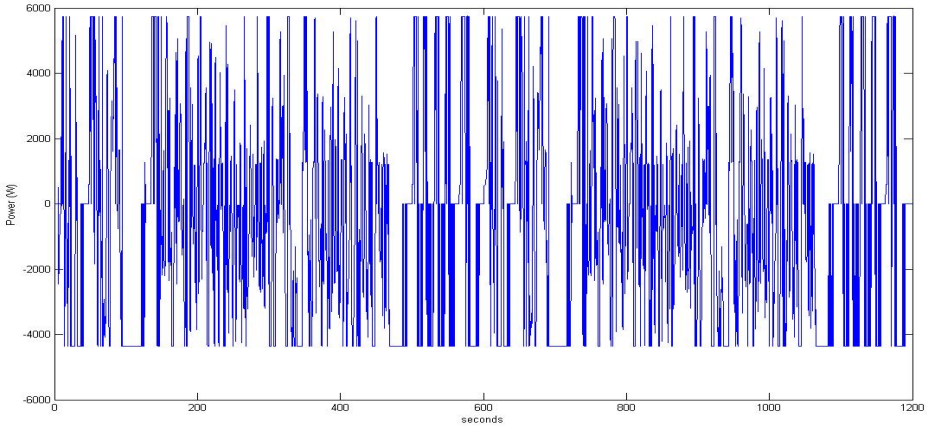

Figure 3.14: EM power flow over US06

3.5 Conclusion – fuel consumption

We present the results in fuel consumption that the model has produced in table 3.2:

Table 3.2: Fuel consumption improvement

Fuel consumption (lt/10km)			
	ICE standalone	ICE+BAS	% consumption reduction
NEDC	0,7664	0,5393	29,63
US06	0,783	0,7081	9,57

We conclude that we have a considerable reduction in fuel consumption and that it is more important (up to 30%) over the NEDC. The significant difference between the two cycles is a result of taking advantage of the "stop & go" function, as in a city driving cycle we have many periods during which the car is not moving. Our goal is that we have in both cases an important reduction in fuel consumption and that is achieved only by using a small (only 5kW) and cheap electric machine.

4. Calculating energy and power losses of the power converter over the NEDC and US06 driving cycles

Now that we have our model ready, we can proceed with the losses estimation. The most important output of the simulink model is the power consumption and generation of the electric machine during a driving cycle that is given as an input. The most common driving cycles are the NEDC and US06, that represent an urban and a highway driving cycle respectively.

4.1 NEDC

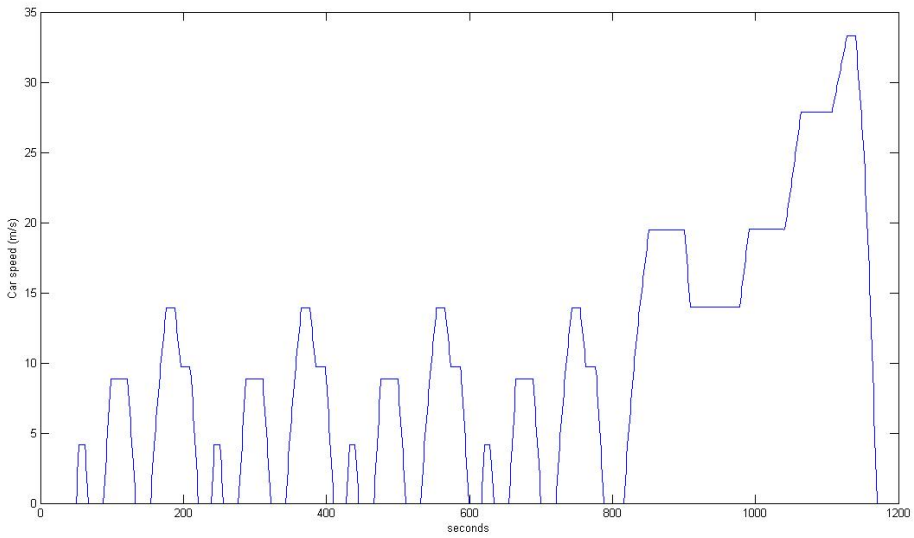

Figure 4.1: The New European Driving Cycle

At first we run the Simulink hybrid model with the alternated characteristics, as to operate like the BAS. The electric power that flows through the inverter can be seen on the diagram below:

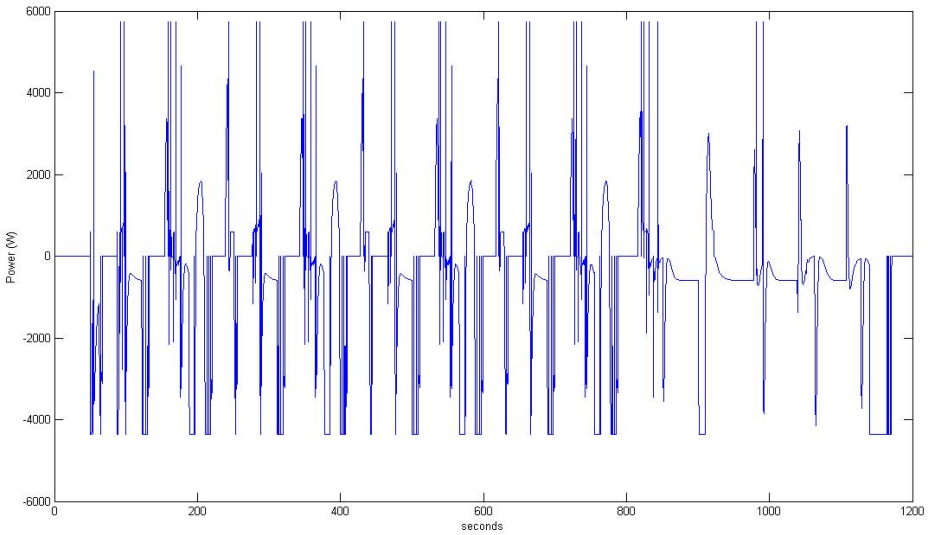

Figure 4.2: Mechanical power over NEDC

The power is greater than 0 when the electric machine operates as a motor and is below 0 when the machine operates as a generator and charges the battery. As stated in chapter 2, a SMSM is less inductive than an EMSM, which operates normally with a power factor greater than 0.9. Assuming then that the power factor of the SMSM equals 1, we consider the current flowing only through the BJTs during motor operation. During the generator operation the transistors remain switched off as only the diodes conduct during the AC to DC rectifier operation. For the inverter square pulse mode, we estimate the conducting losses as they represent the majority of the losses. The switching losses are considered to be less than 1%, as the SiC components have a really good switching response, so these losses are not taken into account. We study the PWM losses in a next chapter, where it is also shown that the switching losses are not remarkable.

4.1.1 112 Volts DC

For a load with a power factor that equals 1, the $V_{ce,sat}$ (green) and the current through a semiconductor I_F (red) can be seen below:

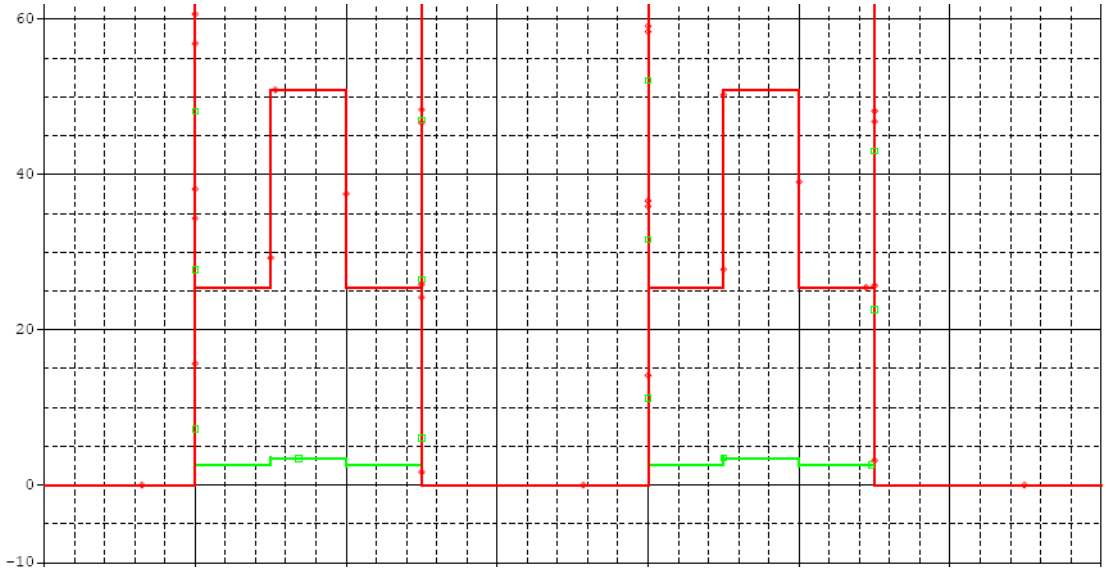

Figure 4.3: $V_{ce,sat}$ (green), $I_{forward}$ (red)

The current levels are determined by the output power (figure 4.2) and of course the output voltage of the inverter. Then we can also calculate the $V_{ce,sat}$ levels, as they are proportional to the forward current of the transistors. In order to estimate this ratio, we use the I_c-V_{ce} curves for the BiTSiC, shown in figure 4.4:

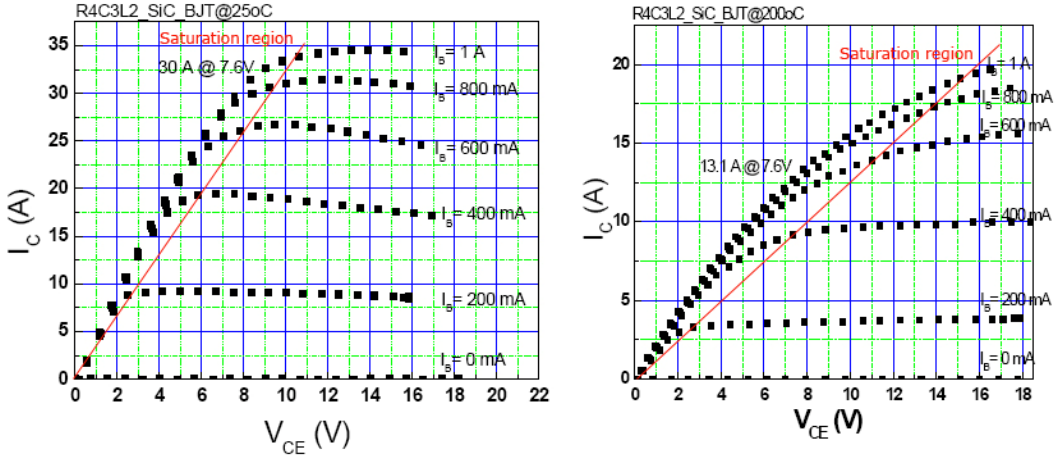

Figure 4.4: BiTSiC Vce - Ic @ 25°C - 200°C

Taking into account the 400mA base current, as a collector current of 10 Amperes is sufficient in any case for our application and can be driven even under 200°C by that base current, we can have now a linear approximation for the ratio V_{CE}/I_C in the saturation area. The result for 150°C is $V_{CE}/I_C = 0.42\Omega$. Now we know the saturation voltage level, depending on the collector current, so we can estimate the power losses over the transistors for the whole driving cycle. The conducting losses of the square pulse modulation can be estimated as below:

$$t_{on}/T_{SW} = 0.5 \Rightarrow P_{S,cond} = 0.5 \cdot V_{ce,sat} I_F$$

Now we can estimate the average power losses over every time step (0.1 sec). The losses over the transistors are shown on the next figure:

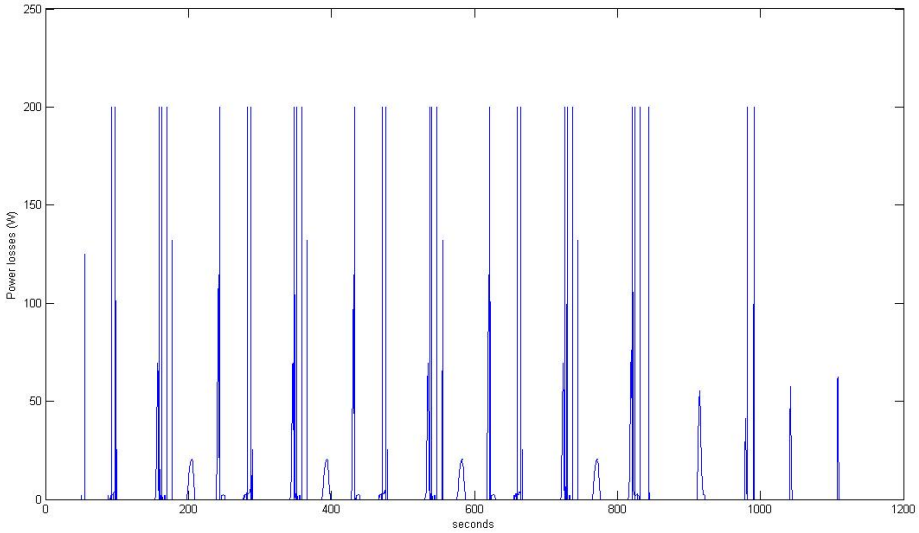

Figure 4.5: Power losses over BJTs, 112V NEDC

It is worth to have a look at the average efficiency of the inverter during that operation. We can easily calculate the energy transferred through the inverter to the electric motor, by integrating the positive part of the power graph. Integrating also the power losses over the transistors diagram we have the complete energy losses over the inverter for the NEDC driving cycle.

$$\eta_{BJT} = \frac{E_{BJT} - E_{losses}}{E_{BJT}} = \frac{293kJ - 3.6kJ}{293kJ} \approx 0.9875$$

We have now to estimate the rectifier operation losses that result from the generator operation. In this case, we keep the transistors always in their cutoff region and we use just the schottky diodes to rectify the current and charge the battery. The power transferred through the power electronic modules is the negative part of the power graph.

In that estimation, we assume that the DC voltage and current of the inverter are constant. We ignore any ripple on the signals, as it is too low to affect our calculations. We approximate then linearly the forward resistance for the diodes at the junction temperature of 150^{o}C.

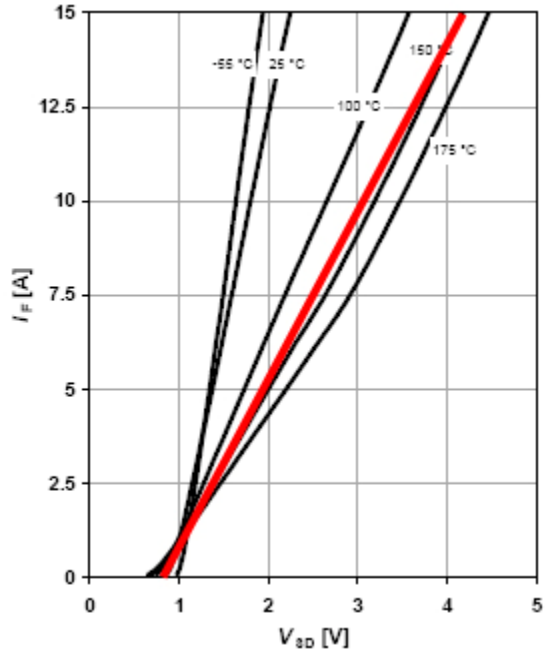

Figure 4.6: Diode I_F-V_F (red -> 150°C)

We have the DC link voltage level, so from the power flow diagram we can estimate the current that flows through the inverter. Knowing the current per diode, leads us to the forward voltage drop of the diodes, according to the diagram above and as a result to the power losses over the diodes. The corresponding diagram that shows the power losses over the diodes for the NEDC is shown below:

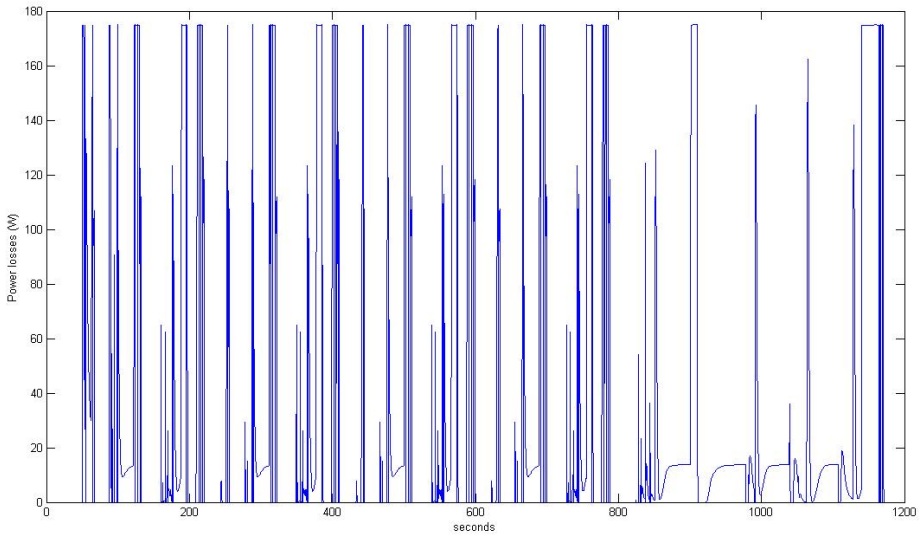

Figure 4.7: Power losses over diodes, 112V NEDC

Even though it seems that we have greater energy losses, when the EM operates as a generator, the maximum power losses are lower

than in motor operation. From the efficiency point of view, this operation is less efficient:

$$\eta_{diode} = \frac{E_{diode} - E_{losses}}{E_{diode}} = \frac{1055kJ - 37.15kJ}{1055kJ} \approx 0.9648$$

The overall efficiency of the converter for the 112 Volts design is then:

$$\eta = \frac{E_{BJT} + E_{diode} - E_{losses}}{E_{BJT} + E_{diode}} = \frac{293kJ + 1055kJ - 40.75kJ}{293kJ + 1055kJ} \approx 0.97$$

4.1.2 300 Volts DC

It is important to have a look at a different battery model that can provide higher DC link voltage to the inverter, as it is shown that silicon carbide has many more benefits in higher voltage levels. We use the 300 V standard to make the same losses' estimation for the inverter. In that design we use much less semiconductors (1/3 compared to the 112 V design), but on the other hand the forward current is slightly greater. We have to estimate once again the forward voltage drop of the transistors and diodes. The outcome we expect is that the losses might be slightly greater per component, but significantly lower for the whole converter. We now expect better efficiency over the converter.

For the same driving cycle we estimate the average power losses over every time step and we present them in the figure below:

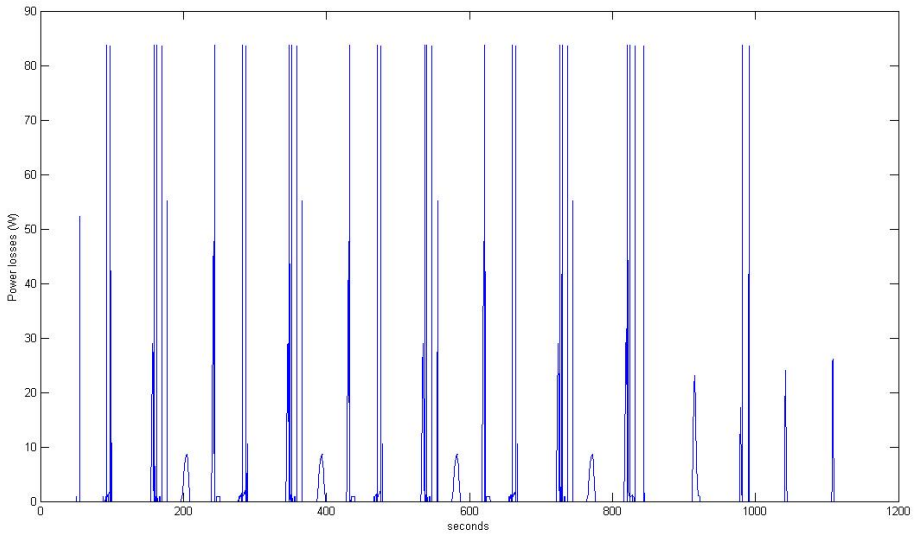

Figure 4.8: Power losses over BJTs, 300V NEDC

As we see the maximum power losses are significantly less than the power losses of the 112V design. The efficiency in this case is:

$$\eta_{BJT} = \frac{E_{BJT} - E_{losses}}{E_{BJT}} = \frac{293kJ - 1.5kJ}{293kJ} \approx 0.9948$$

As far as the generation mode is concerned, the conducting losses over the diodes for the 300 Volt design is shown on the next graph:

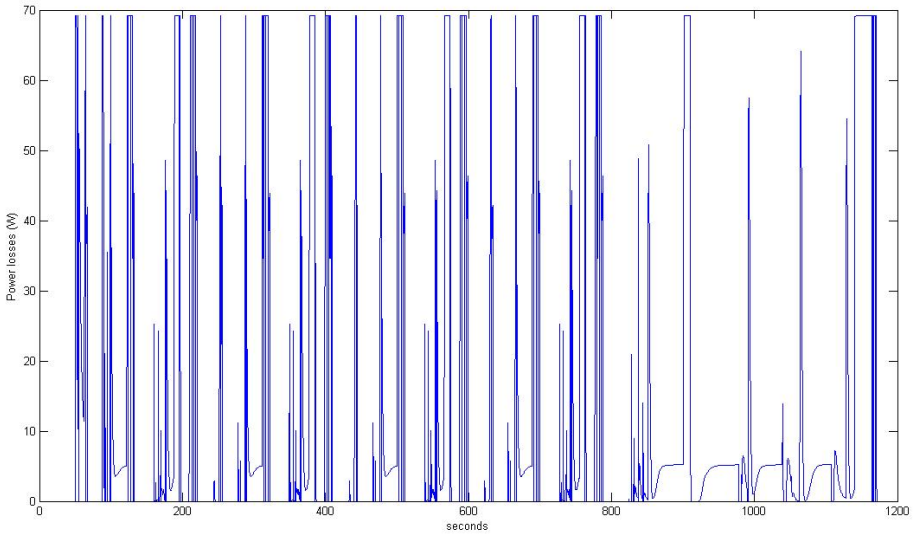

Figure 4.9: Power losses over diodes, 300V NEDC

The power losses seem to be lower compared to the BJT power losses, but the efficiency is expected to be lower, as the diodes operate for longer period than the transistors.

$$\eta_{diode} = \frac{E_{diode} - E_{losses}}{E_{diode}} = \frac{1055kJ - 14.6kJ}{1055kJ} \approx 0.9862$$

The overall efficiency of the converter for the 300 Volts design is then:

$$\eta = \frac{E_{BJT} + E_{diode} - E_{losses}}{E_{BJT} + E_{diode}} = \frac{293kJ + 1055kJ - 16.1kJ}{293kJ + 1055kJ} \approx 0.988$$

We understand now that in a higher voltage design we have much better efficiency over the inverter. We have to comment that this efficiency we have estimated does not include any power losses over the driving circuit of the transistors. Taking into account the driving circuit, we will conclude in slightly lower efficiency of the inverter than what we have estimated. However, in this study, we

are not interested in the driving circuit, as this circuit is built both with Si and SiC components, so it cannot be placed on the same heat sink with the transistors. Because of the Si parts, it still needs its own heat sink, as it cannot be cooled by the combustion engine's water temperature. As a result, a different study is needed to evaluate the driving circuit's losses and its own heat sink.

4.2 US06

Apart from the New European Driving Cycle, there is another driving cycle, US06, which corresponds to the highway driving style. The speed over time graph of this driving cycle is shown below:

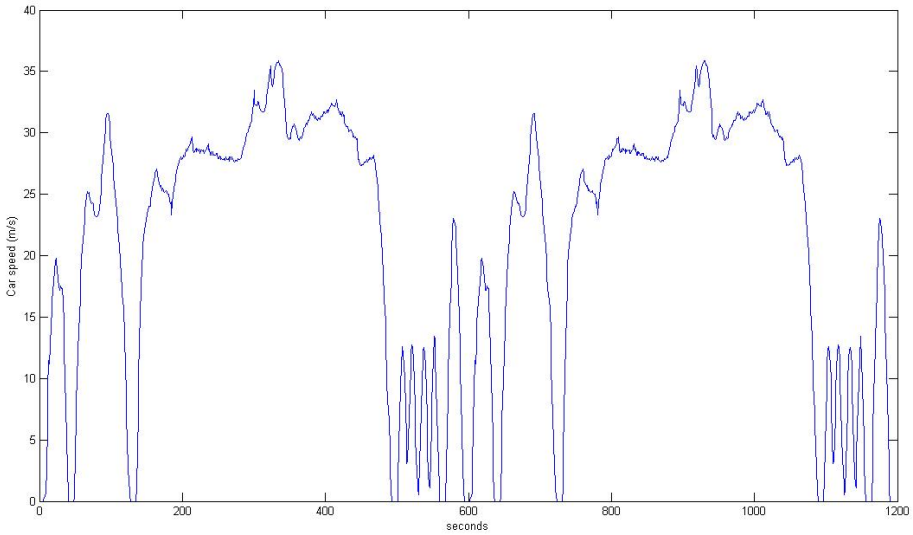

Figure 4.10: The US06 Driving Cycle

After running the simulink BAS model we have the power consumption and generation of the electric machine. Added some thermal losses over the electric machine, this is the power that flows through the inverter and can be seen below.

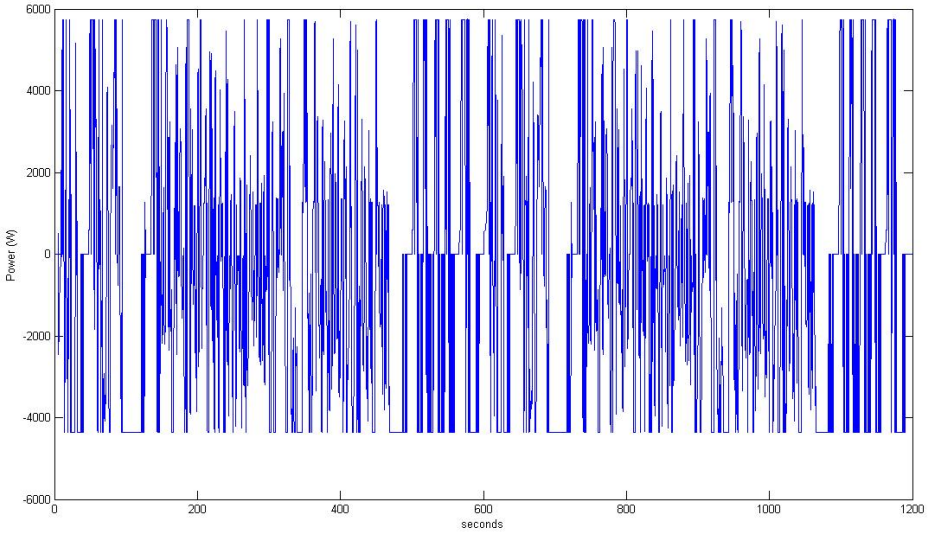

Figure 4.11: Mechanical power over US06

Even though we do not have so many accelerations during a highway driving cycle, some of the ones we have are heavier. Apart from the accelerations, the simulink model results in more significant use of the electric machine over the US06 driving cycle.

We still assume a load with a power factor 1 in this chapter and we don't consider any switching losses. During this driving cycle we don't have many start and stop functions, at least not as many as in NEDC. However, we will study these losses and add them in a next chapter. At the moment we estimate the square pulse mode, conducting losses in the two different dc link voltage designs.

4.2.1 112 Volts DC

At first we present the losses over the transistors. These losses occur when the electric machine operates as a motor. We do not expect the maximum power losses to be higher than the corresponding NEDC losses, as the maximum losses appear for the maximum load, which is not different between the two cycles, as it is limited by the electric machine's specifications. On the other hand, the efficiency of the inverter is not only a matter of the maximum power, but depends on the power of any single operating point. In case of US06 we have more operating points at full power production, where the losses are greater, so the efficiency is expected to be lower.

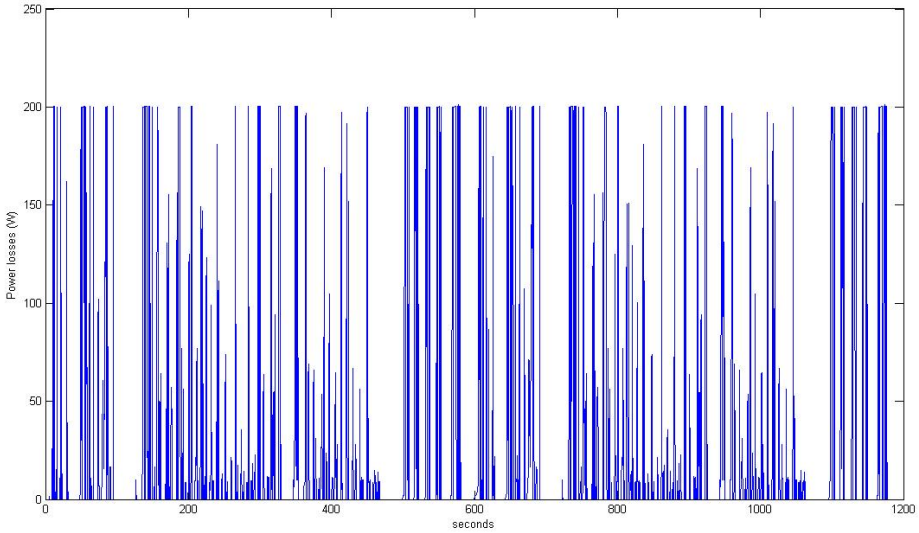

Figure 4.12: Power losses over BJTs, 112V US06

We also estimate the efficiency of that operation:

$$\eta_{BJT} = \frac{E_{BJT} - E_{losses}}{E_{BJT}} = \frac{1343kJ - 31.54kJ}{1343kJ} \approx 0.9765$$

To present the diode losses, we use the negative part of the power flow through the converter diagram (figure 4.11), that corresponds to the AC to DC rectifier. Using also the datasheets for SiC diodes (figure 4.6), results to the following diagram:

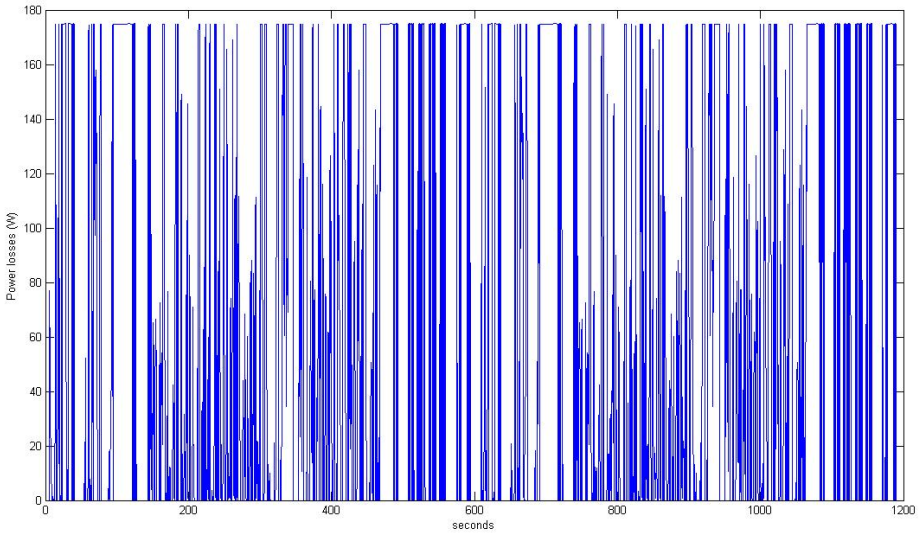

Figure 4.13: Power losses over diodes, 112V US06

The power losses are still not higher than the NEDC, but the use of the inverter will lead to lower efficiency:

$$\eta_{diode} = \frac{E_{diode} - E_{losses}}{E_{diode}} = \frac{2019kJ - 75.17kJ}{2019kJ} \approx 0.9628$$

The overall efficiency of the converter for the 112 Volts design, over the US06 driving cycle is then:

$$\eta = \frac{E_{BJT} + E_{diode} - E_{losses}}{E_{BJT} + E_{diode}} = \frac{1343kJ + 2019kJ - 106.71kJ}{1343kJ + 2019kJ} \approx 0.9682$$

4.2.2 300 Volts DC

In the 300 Volts design we expect lower power losses and much better efficiency. We can confirm our assumptions with the following graphs, showing the losses over the inverter and rectifier operation:

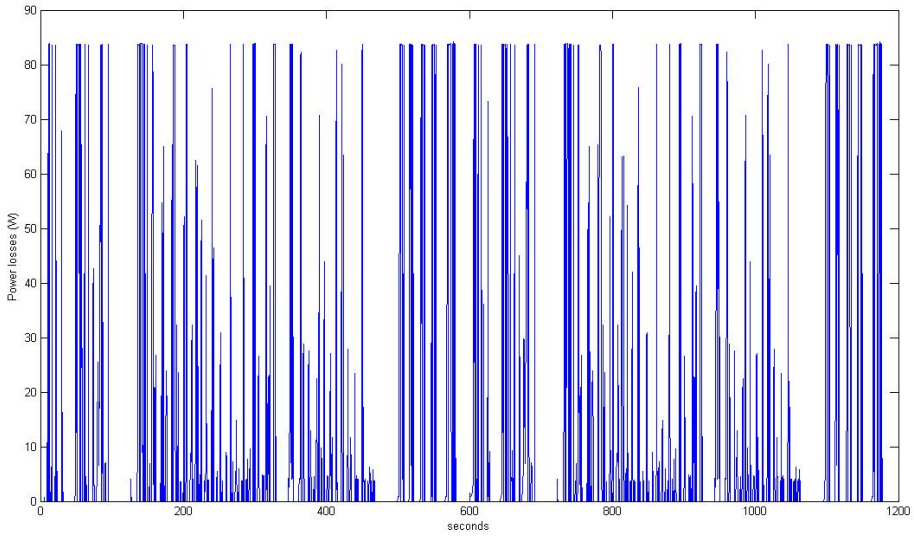

Figure 4.14: Power losses over BJTs, 300V US06

The efficiency is expected to be lower than the corresponding NEDC, but higher than the US06 112 Volts design.

$$\eta_{BJT} = \frac{E_{BJT} - E_{losses}}{E_{BJT}} = \frac{1343kJ - 13.19kJ}{1343kJ} \approx 0.99$$

For the rectifier operation, when the diodes are conducting, we conclude to the graph below:

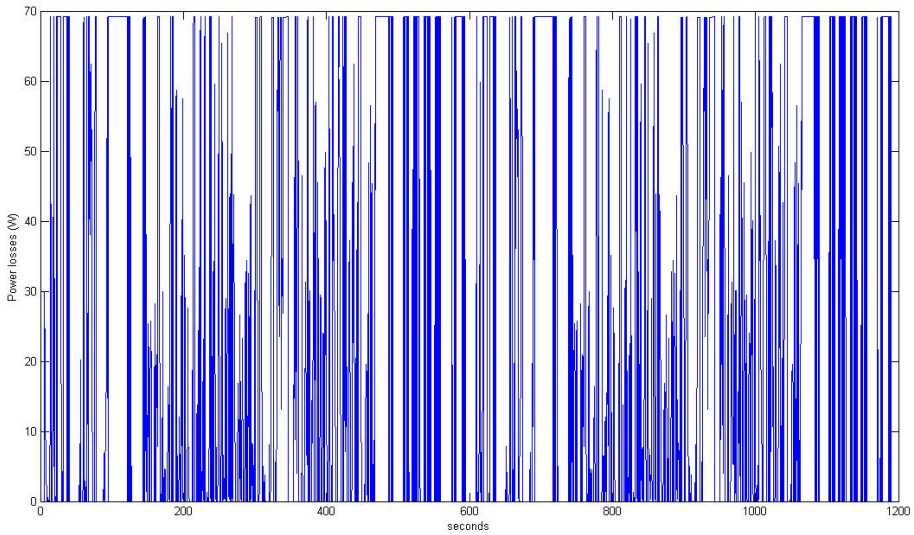

Figure 4.15: Power losses over diodes, 300V US06

$$\eta_{diode} = \frac{E_{diode} - E_{losses}}{E_{diode}} = \frac{2019kJ - 29.6kJ}{2019kJ} \approx 0.985$$

The overall efficiency of the converter for the 300 Volts design is then:

$$\eta = \frac{E_{BJT} + E_{diode} - E_{losses}}{E_{BJT} + E_{diode}} = \frac{1343kJ + 2019kJ - 42.8kJ}{1343kJ + 2019kJ} \approx 0.987$$

4.3 Conclusion

The conclusion of all above is presented in table 4.1. To design the heat sink for such an inverter we need to know just the maximum power losses, but it is also useful to know how the temperature varies over a driving cycle, especially when a thermal time constant is involved. In addition to these, in order to design the inverter it is good to know how efficient it is going to be in use. As far as the efficiency is concerned, the solution is definitely the 300 Volts design. Its lower losses improve also the heat sink dimensions and cost as we will show later.

Table 4.1: Power losses and efficiency

		NEDC	US06
112 V	max power losses	200.06	201.2
	efficiency	0.97	0.968
300 V	max power losses	83.65	84.13
	efficiency	0.988	0.987

In the next chapter we have a closer look at the starting operation and the PWM losses and we conclude to the complete power losses diagram of the converter for every driving cycle. So then we can proceed with the temperature calculations.

5. Starting operation and PWM losses

5.1 Starter operation

Apart from the torque additional supply and the braking regenerative mode, another important operation of the electric machine is the starter operation. It needs to produce the torque needed to start the ICE under even the most unsuitable circumstances. It is important then to design the electric motor to be able to provide such high torque, even for a small period of time. Furthermore, the starting operation takes place several times in an urban driving cycle, as the aim of the BAS is to reduce the emissions by stopping the ICE operation when the car is not moving. To reduce polluting emissions during the engine cranking, we don't have just to start the ICE, but it would also be preferable to raise its speed up to 400-500 rpm.

5.1.1 Starting at low temperatures

In northern countries the temperature can reach during the winter values between -30 ~ -50^{o}C. At these temperatures engine cranking is much more difficult, as the load torque of the engine is greater. This is due to very high oil viscosity. There are several models to describe viscosity, a simplified one is the exponential model [6], where:

$$\mu(T) = \mu_0 e^{-bT}$$

This is shown just to prove that oil viscosity becomes a very important factor under low temperatures.

It is also suggested [CAI, 2004] that in order to overcome the engine's static torque under low temperatures, the machine has to provide a break away torque about 1.5 ~ 1.8 times the nominal cranking torque. We assume that even under these circumstances, 180 Nm of torque are enough to start the ICE. We can see in figure 5.1 the torque and power requirement of a belt driven Integrated Starter Alternator machine. Let us focus on the starting process, which includes operation under 1000 rpm.

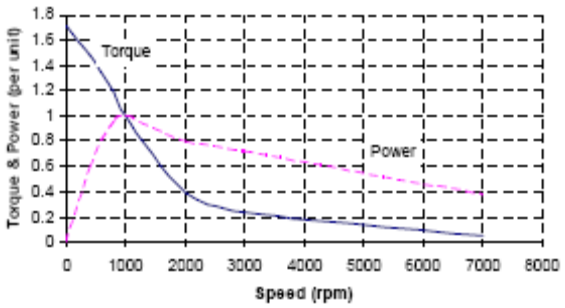

Figure 5.1: Load torque and power over ICE speed

Considering this as the maximum load torque over the speed, we can estimate the maximum speed we can drive the ICE during the cranking period. Assuming that the load torque falls linearly over the speed and that the initial torque can be to 180 Nm, (180 Nm = 1.7 pu), we can estimate its grade:

$$a = \frac{106 - 180}{1000 - 0} = -0.074\,Nm/rpm$$, and then:

$$T_l\left(n_{ICE}\right) = -0.074 n_{ICE} + 180\,.$$

From the electric motors characteristics we take the electric motor torque diagram and compare it to the load torque. We drive the ICE until it reaches almost 500 rpm (maximum), or as far as we are able to drive it with the electric machine. For the low temperature cranking we have the following graph, showing the load torque and the maximum torque the electric machine can provide.

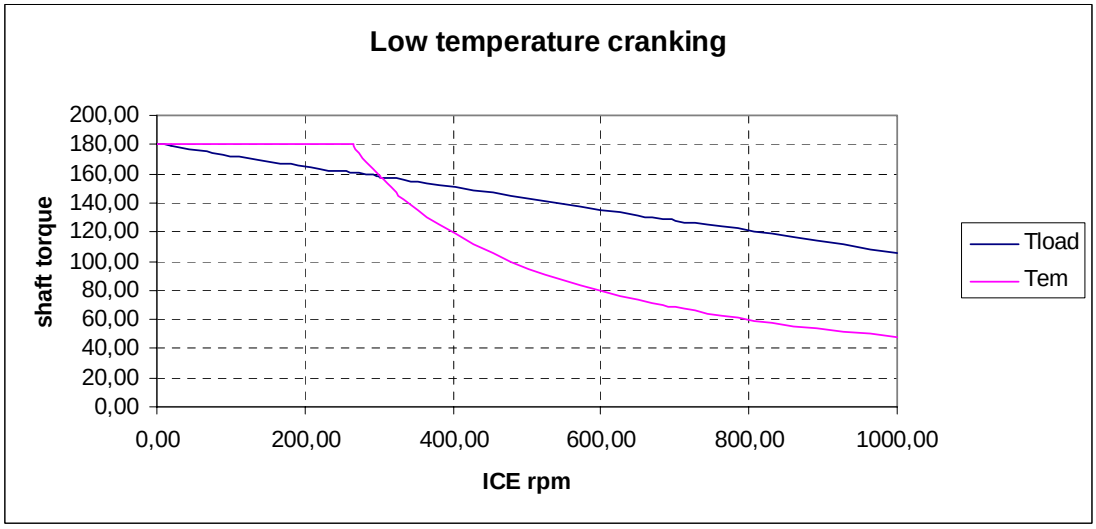

Figure 5.2: Low temperature cranking

The result is that in low temperatures we can drive the ICE up to almost 300 rpm. This is acceptable for the cranking operation, but not the best possible for polluting emissions' reduction, as stated above.

Dividing this torque difference by the rotating inertia of the ICE, which is $J = 0.0287 kg \cdot m^2$, we estimate the rotating acceleration of the ICE, according to:

$$T_{em} - T_l = J \frac{d\omega}{dt}$$

This rotating acceleration, over the ICE speed, is shown in figure 5.3:

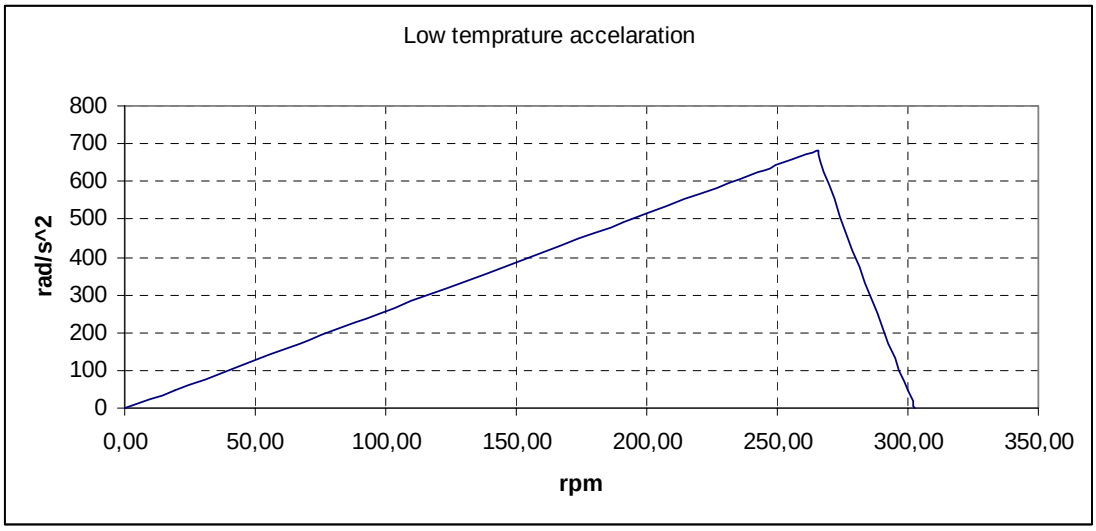

Figure 5.3: Accelaration under cold temperature

For the constant torque operation, the equation that describes the acceleration over the speed is:

$\frac{d\omega}{dt} - A\omega(t) = \varepsilon$, with $A = 24.5$ and ε: small (we can assume $\varepsilon = 1$)

The solution of this equation is: $\omega(t) = \frac{\varepsilon}{A} e^{At} - \frac{\varepsilon}{A}$. Solving by time, it seems that this operation (0 up to 265rpm – base speed for EM) lasts for 0.226 sec. We conclude then that we can start the ICE and raise its speed up to 1000 rpm in less than 1 second, even under the most severe temperatures.

5.1.2 Starting at normal temperatures

In such case we have a cranking load torque that is much lower compared to very low temperatures. We expect that the BAS will be able to start the ICE much faster. We can also take advantage of that and drive the ICE up to 450 rpm, avoiding a great amount of

cranking polluting emissions. To prove this statement, we present the corresponding torque graphs to that case:

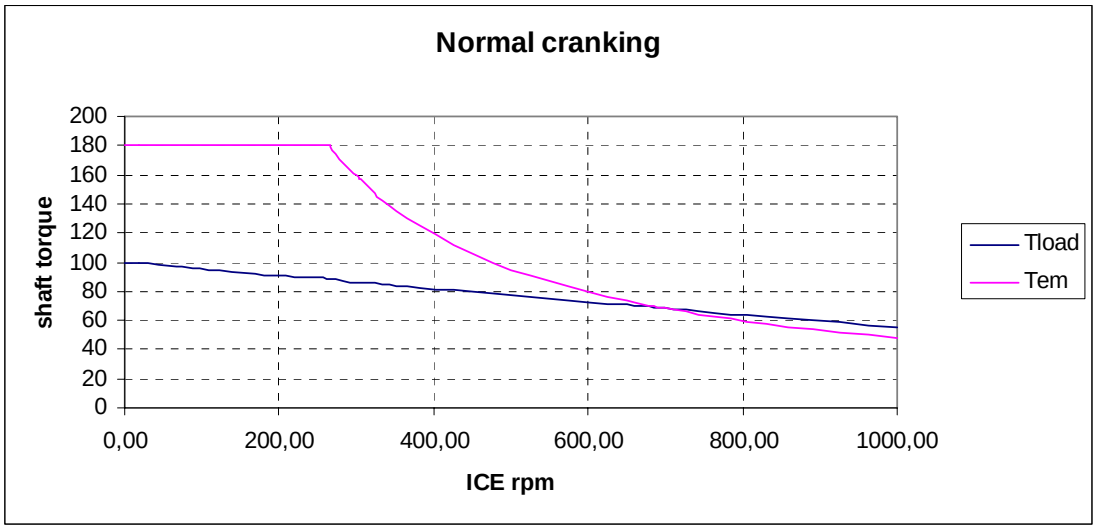

Figure 5.4: Load and provided torque in a normal temperature cranking

It is shown that we can drive the ICE even up to 650 rpm, but it is not really needed and also would cause further reduction to the battery's SOC.

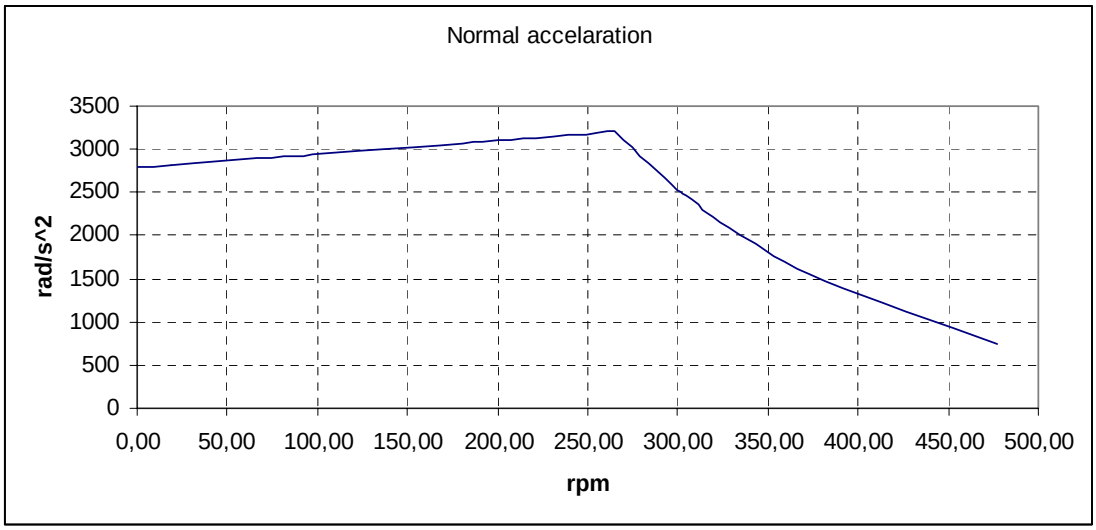

Figure 5.5: Acceleration under normal temperature

Estimating the acceleration as above, we conclude that it takes the ICE 0.07 seconds to reach the base speed of the EM and almost 0.2 seconds to reach the speed of 1000 rpm. For almost half of this time we consume energy, coming from the battery. During the first 0.07 seconds the power consumed is proportional to the speed of the motor, which is related exponentially to the time. A linear approximation of this relation would result in a greater amount of power needed than what is really used for each working point, but is preferred due to simplifications on the calculations. For the rest of

the time (0.07-0.1 sec) the power is constant on the time domain and its value is 5 kW, as we have already entered the field weakening area of the EM. We can also consider an efficiency factor of 90% for the EM. This is a rather low value, realistic though if we refer to such low power machine. These facts point at the energy consumption:

$$E = 1.1\left(0.07 \cdot 2500 + 0.03 \cdot 5000\right) = 358J$$

It seems that a normal starting does not consume a great amount of energy, because it lasts almost for 0.1 second and also the controlled modulation over the constant torque area results in a constant current rather than an initial spike current.

5.2 Losses over PW modulation

Now that we have a view of how the ICE operates with the BAS system, we can estimate the losses over the inverter. To begin with, we look at the PWM modulation. At the end of this operation (after 0.07 sec under normal temperature conditions) the frequency has to be up to 40 Hz. Because of the fact that this operation lasts for less than 0.1 sec, we don't need to have a continuous view of the power losses. Instead we can estimate the power losses at three different operating points and then consider the average power losses over this operation for our needs.

5.2.1 Characteristics of the PW modulation

The carrier signal is a triangular pulse. Its frequency is 1080 Hz, 27 times greater than the maximum reference frequency and its peak to peak voltage is 112V, equal to the DC link voltage. As reference we use the symmetrical sinusoidal wave, as we can achieve greater output voltage, before entering the overmodulation area, compared to the simple sinusoidal reference.

During this operation the ratio between voltage amplitude and frequency is supposed to be kept constant. We choose then 3 different operating points of the inverter and estimate the power losses for each. Let us consider the operating points:
$\left(VoltageAmplitude, Frequency\right)$

- $\left(112V, 36Hz\right)$
- $\left(78V, 25Hz\right)$
- $\left(31V, 10Hz\right)$

5.2.2 Switching losses

Under the PW modulation the switching losses can be considerably high, because of the high switching frequency. In order to estimate these losses over the BJTs, we use the model previously created [Haraldsson-Andersson, 2007]. The turn on and turn off are shown in figures 5.6 and 5.7 respectively.

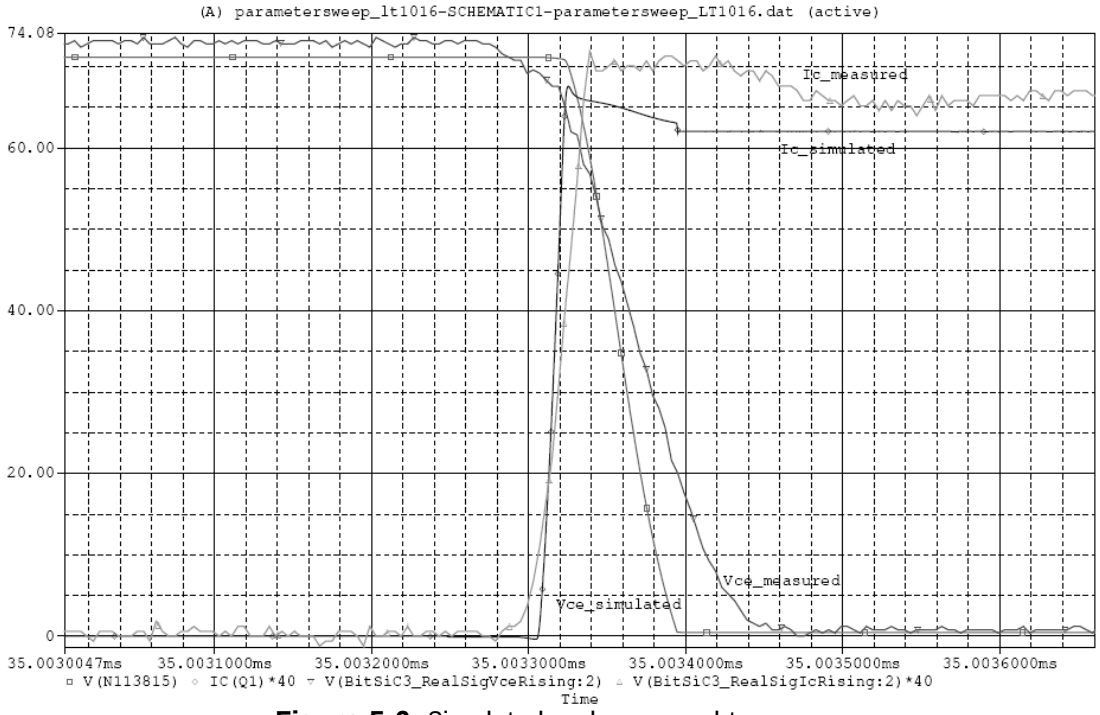

Figure 5.6: Simulated and measured turn on

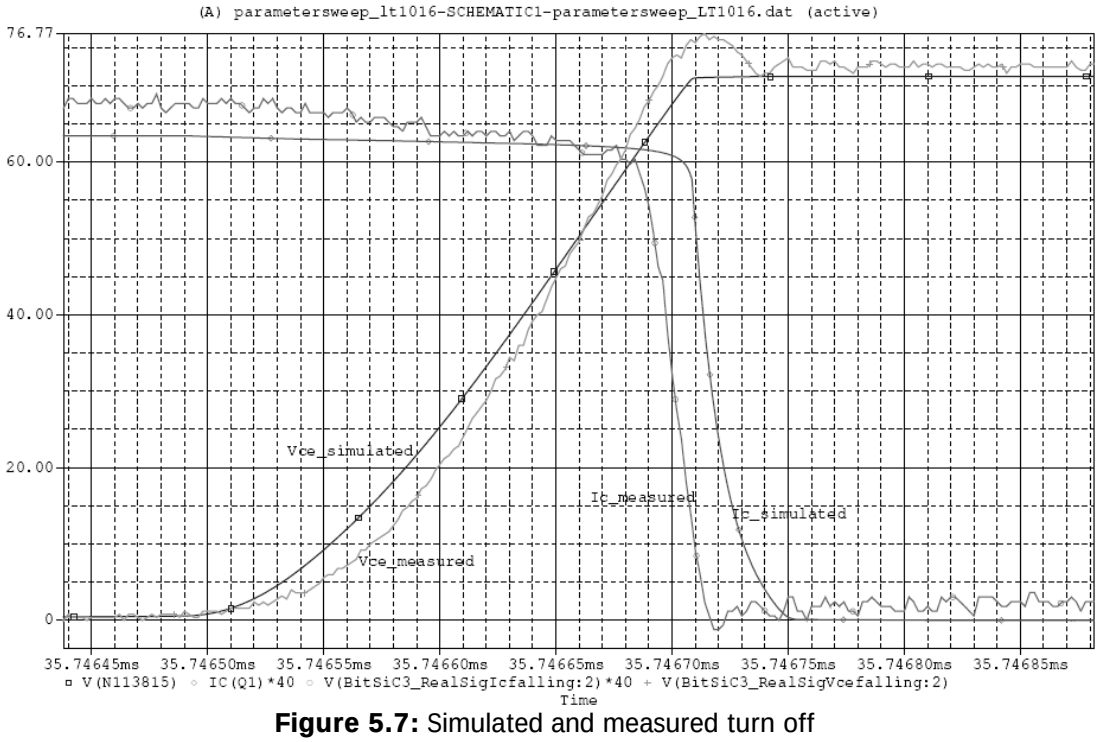

Figure 5.7: Simulated and measured turn off

To estimate the losses we use two M-files (appendix B2), one for the each switching operation. As the switching times are improved in the BiTSiC's new generation, we use the same model, changing the duration of each operation. Then we use these results to estimate the complete losses over a period in each of the tree cases.

5.2.3 PWM losses estimation – 112 Volts design

a. 112 Volt DC – 36 Hz

When we apply this voltage amplitude of the reference signal and the corresponding frequency, the pulses driving a couple of BJTs (high and low) are shown in figure 5.8:

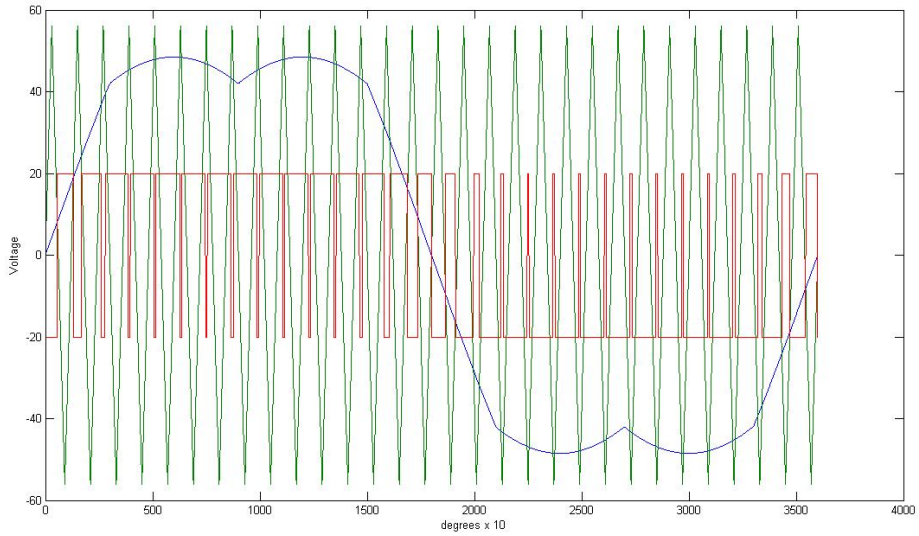

Figure 5.8: PWM reference, carrier signals and driving pulses (112, 36)

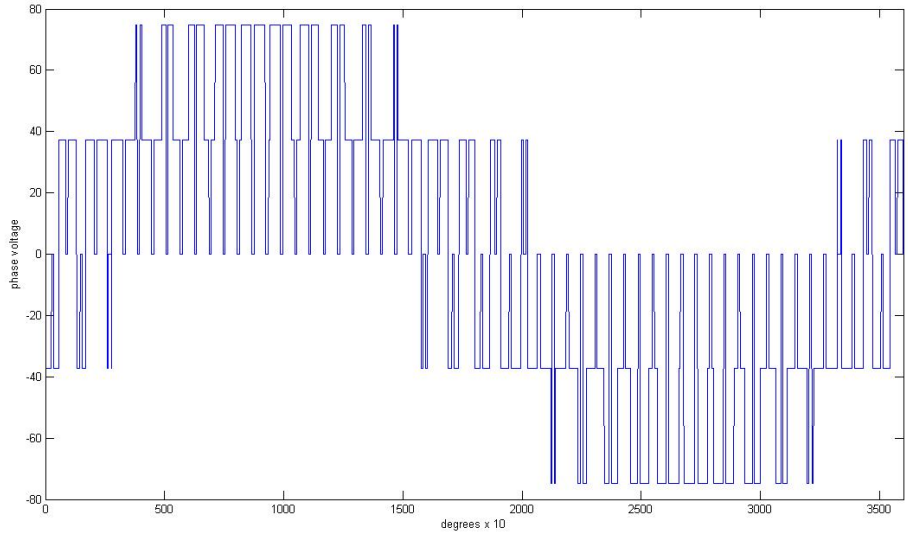

Figure 5.9: Phase voltage with reference to machine's neutral (112, 36)

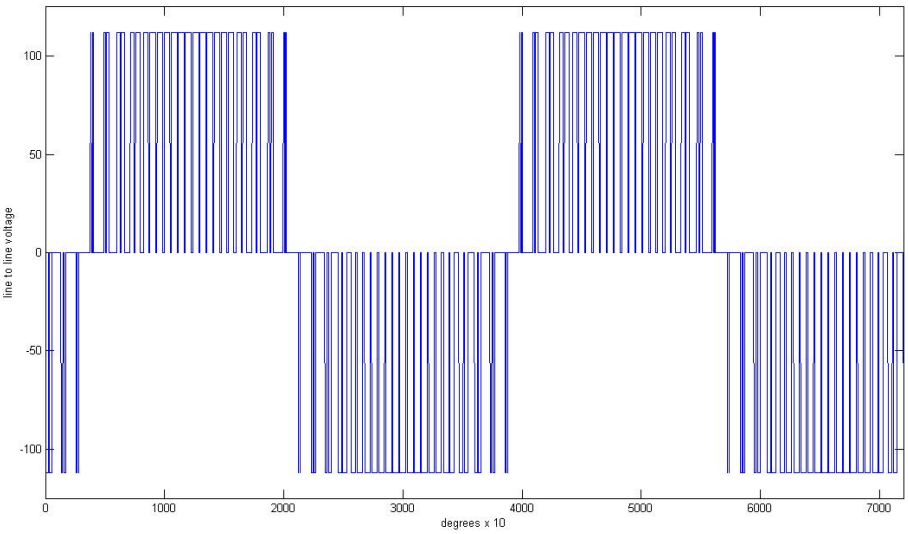

Figure 5.10: Line to line output voltage (112, 36)

The positive parts of these pulses (figure 5.8) drive the upper transistor, while the negatives drive the lower of the couple. We don't have any conduction period through the diodes. When we add the pulse's width over a whole period, the results equals the time of a half period. We conclude that the conducting losses for a period doesn't have any difference between the PWM and the square pulse modulation, as in both cases the whole conducting period is the same. However, the switching losses are more important at the PWM area, as we have as many turn-on and turn-off operations, as the frequency ratio is $\left(f_{car} / f_{ref}\right)$.

As the conducting losses do not differ under that modulation, we can take their value from the previous chapter. The average losses of the inverter for one period are:

$$P_{cond} = 200.1W$$

Switching losses can also be important in case of a PW modulation. In the frequency examined, we have 30 turn-ons and another 30 turn-offs. To estimate the switching losses we use the model previously created [Haraldsson-Andersson, 2007], but we apply on it the latest results from TranSiC [8] experiments, that show much better rise and fall times. For one cycle (turn-on & turn-off) the switching losses are:

$$P_{SW,avg} = \frac{\left(E_{turnon}^{losses} + E_{turnoff}^{losses}\right) \cdot k_{operations}}{T_{per}},$$

where

- $E_{turnon}^{losses} = 124uJ$
- $E_{turnoff}^{losses} = 352uJ$
- $k_{operations} = f_{car} / f_{ref} = 30$
- $T_{per} = 1/f_{ref} = 27.78ms$

$$P_{SW,avg} = \frac{(124uJ + 352uJ) \cdot 30}{27.78ms} = 514mW$$

It seems that the transistors have a really good switching behavior, as the switching losses are about 0.3% of the overall losses.

b. 78 Volts DC – 25 Hz

For that couple of voltage amplitude and frequency we can see the waveforms, the pulses that drive a couple of high and low transistors (phase voltage) and the output, line to line voltage:

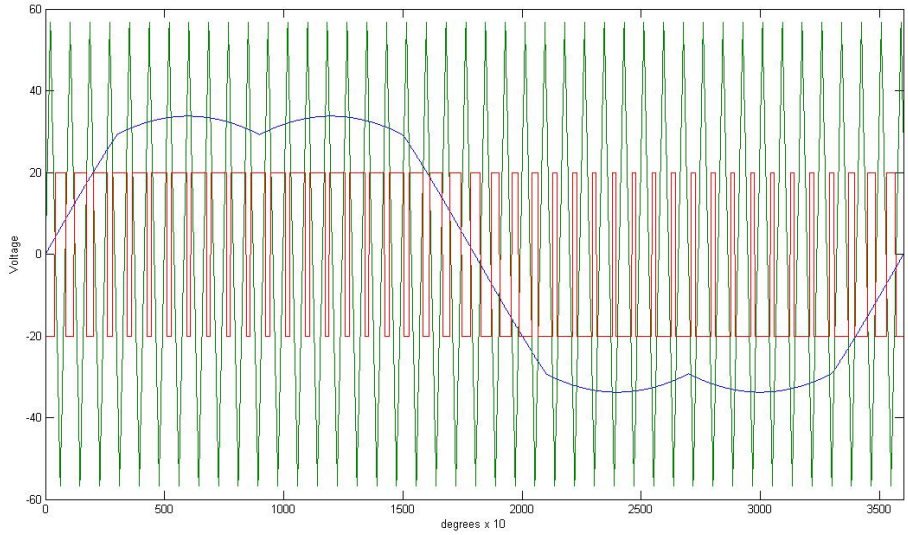

Figure 5.11: PWM reference, carrier signals and driving pulses (78, 25)

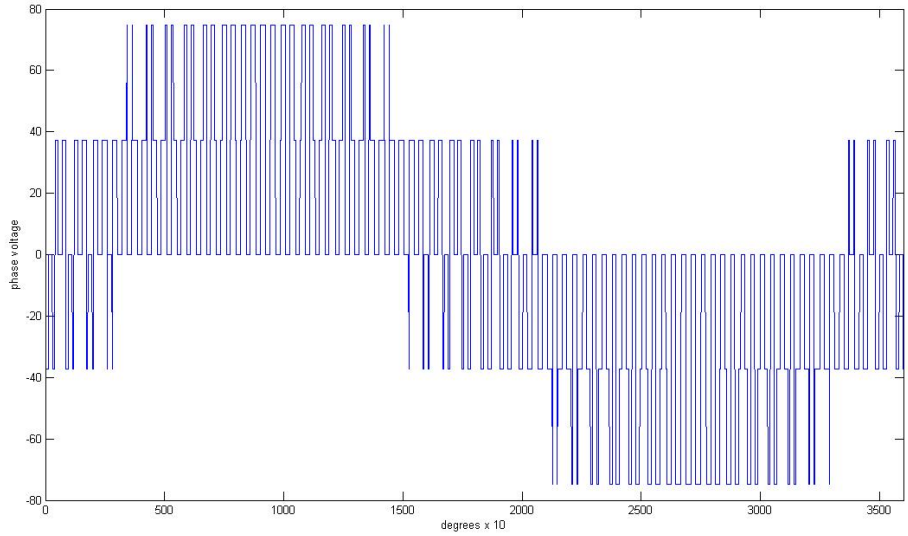

Figure 5.12: Phase voltage with reference to machine's neutral (78, 25)

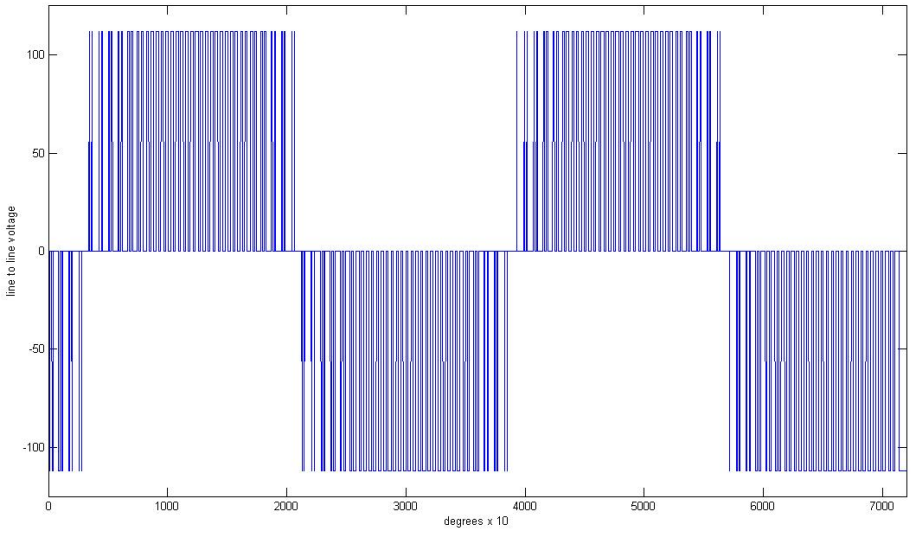

Figure 5.13: Line to line output voltage (78, 25)

To calculate the losses, we use the same method as above. The direct current is the same, as it is constant throughout the PWM period, and so the saturation voltage is the same, as it depends on the current. So the conducting losses are the same as above. As far as the switching losses are concerned, we have the same DC voltage level, so the energy lost per turn-on or turn-off is the same. The higher switching frequency compensates the longer period time, so the mean power losses over a period are the same as above.

c. 31 Volts – 10 Hz

As stated above, we do not expect any difference in the losses during this switching state. We can now claim that the average power losses over the 0.1 second that the Pulse Width Modulation takes place, over the whole inverter are:

$$P_{losses} = P_{cond} + P_{SW,avg} = 200.6W$$

5.2.4 PWM losses estimation – 300 Volts design

It is worth to have a look at the losses in case we use the 300 Volts battery model. In that case, the conducting losses per component are relatively higher, as we have a slightly increased current per component, however, the overall losses are much lower, as the number of components is 1/3 compared to the 112 Volt model. The conducting losses are known from the previous chapter as well. Using the $(212.1V, 36Hz)$ operating point to estimate the switching losses, we have:

$$P_{cond} = 83.65W$$

$$P_{SW,avg} = \frac{(363uJ + 1052.3uJ) \cdot 30}{27.78ms} = 1.53W$$

$$P_{losses} = P_{cond} + P_{SW,avg} = 85.18W$$

In that case, the switching losses are the 1.8% of the overall losses.

5.3 Overall losses

Now we can make a complete diagram of all kind of losses (PWM, transistor, diode) over a driving cycle. All these losses are presented as positive, because as far as the heat dissipation is concerned, it makes no difference if the losses derive either from a transistor or from a diode. Of course we separate the cases of the two driving cycles and the two different DC link voltage designs.

5.3.1 112 Volts DC – NEDC

On the next figure overall losses are presented over the NEDC. In red color we present the starting operation (PWM) losses, in green the generator mode (diode) losses and in blue the motor operation (transistor) losses.

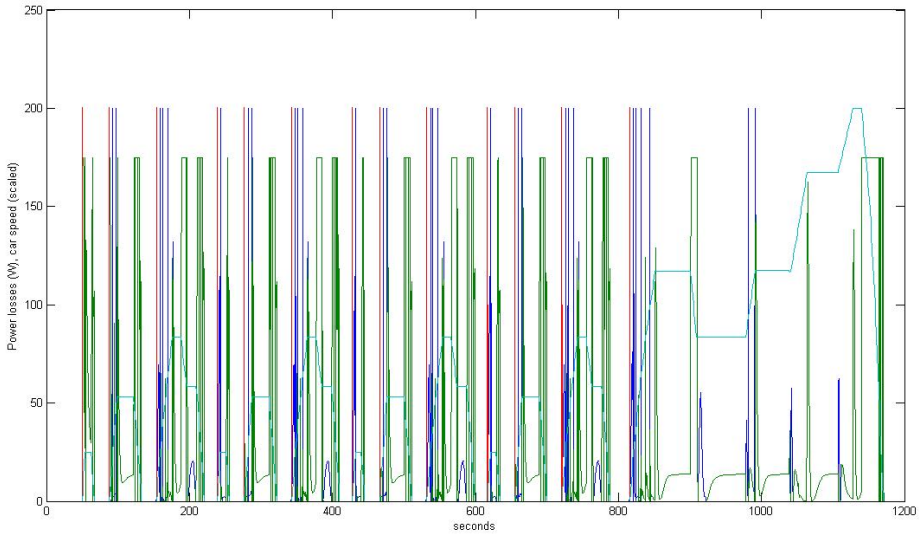

Figure 5.14: Overall losses over NEDC – 112V

We can take a closer look to an urban cycle to see how the hybrid operates.

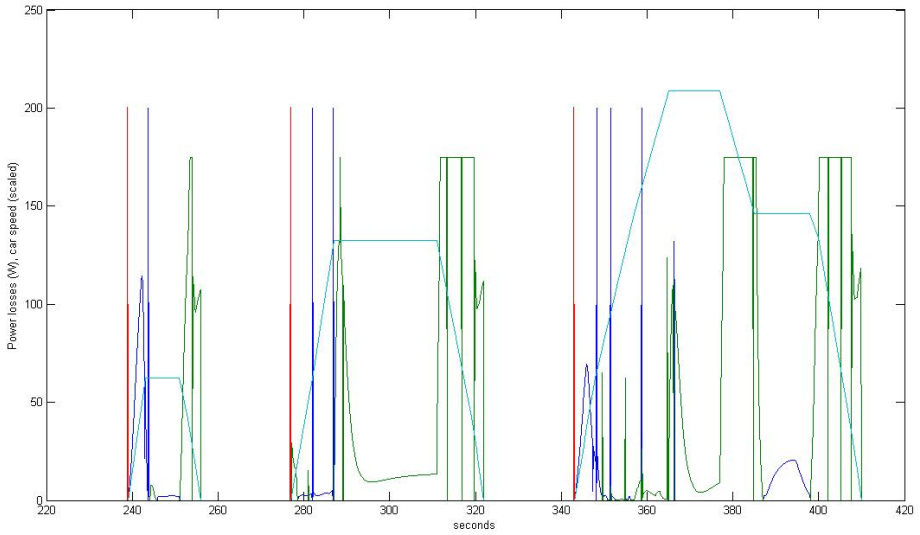

Figure 5.15: Overall losses over an urban cycle -112V

In light blue is shown the speed of the hybrid, scaled to fit the power losses diagram. The red parts are the losses during the starting operation, as estimated previously. In blue we can see the inverter (over BJTs) losses, that appear only during accelerations, while the diode losses over the battery charging (regenerating) mode are shown in green. We clearly understand that the diode losses appear during decelerations, as expected.

5.3.2 300 Volts DC – NEDC

In case of 300 Volts DC link, we don't expect any difference in the shape of these graphs, we just expect the values to be lower, as the power losses are lower in this case.

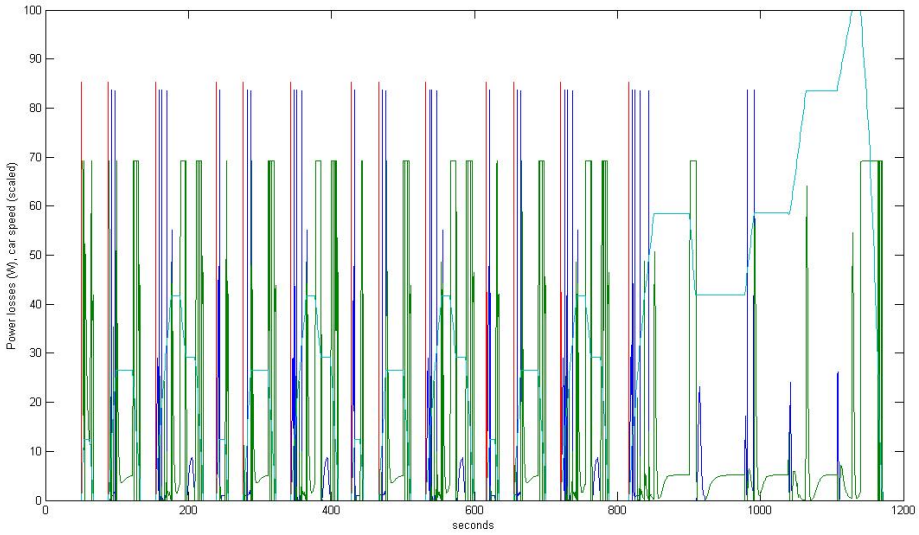

Figure 5.16: Overall losses over NEDC – 300V

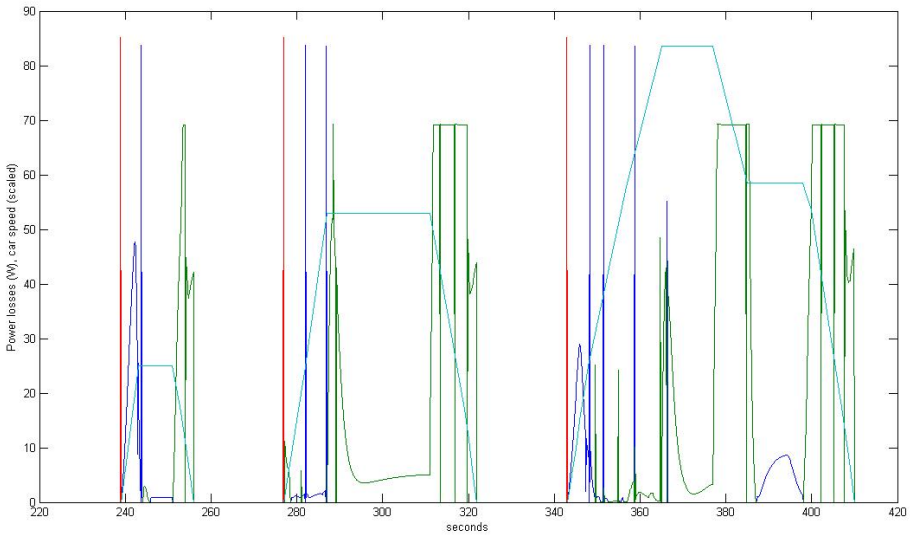

Figure 5.17: Overall losses over an urban cycle -300V

5.3.3 112 Volts DC – US06

Over the highway driving cycle, we do not have so many start and stop functions. We still have accelerations and decelerations though, where we can clearly see the different operations of the electric

machine. In order to achieve better distinctness we present 600 seconds of the US06 driving cycle, that is still a complete US06 cycle.

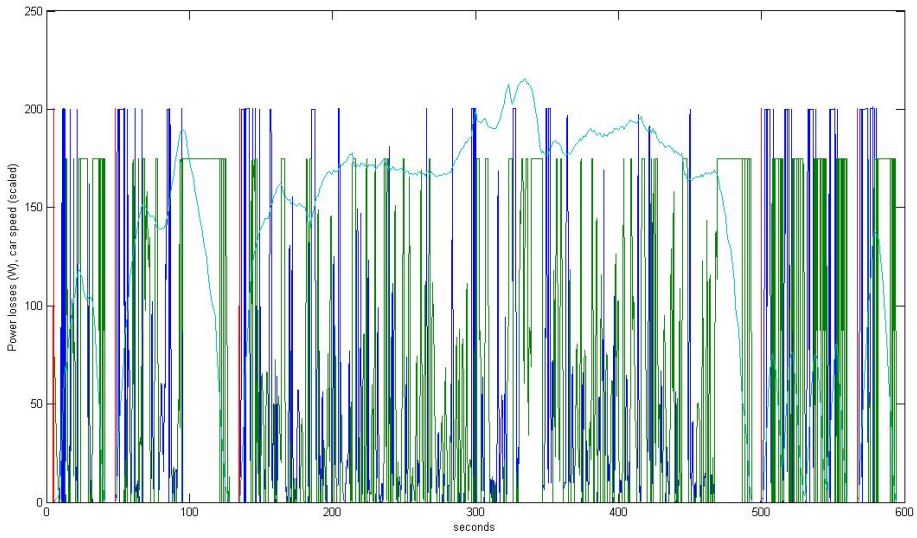

Figure 5.18: Overall losses over US06 – 112V

We can zoom into some interesting areas of that diagram, just to have a more clear view of the different operations. We zoom at first at the area around 100 seconds, where we have a full acceleration and deceleration and then we can also zoom around 300 seconds, where we have a smaller speed variance.

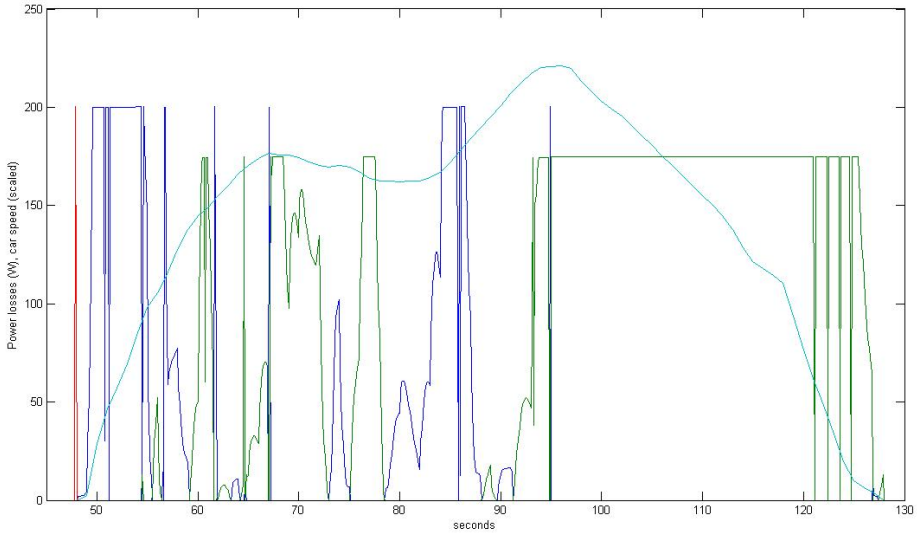

Figure 5.19: Losses over US06, 45-130 sec

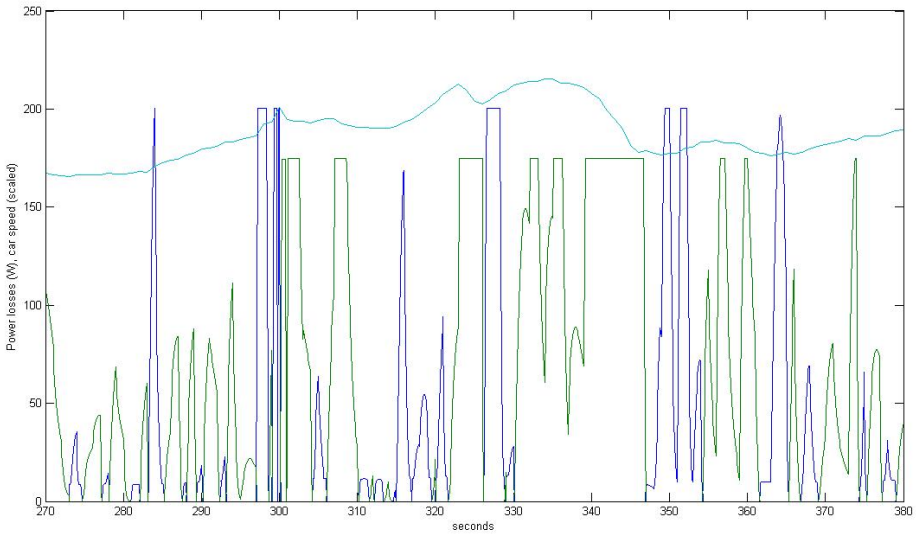

Figure 5.20: Losses over US06, 270-380 sec

5.3.4 300 Volts DC – US06

We have also to present the alternate design of 300 Volts DC link:

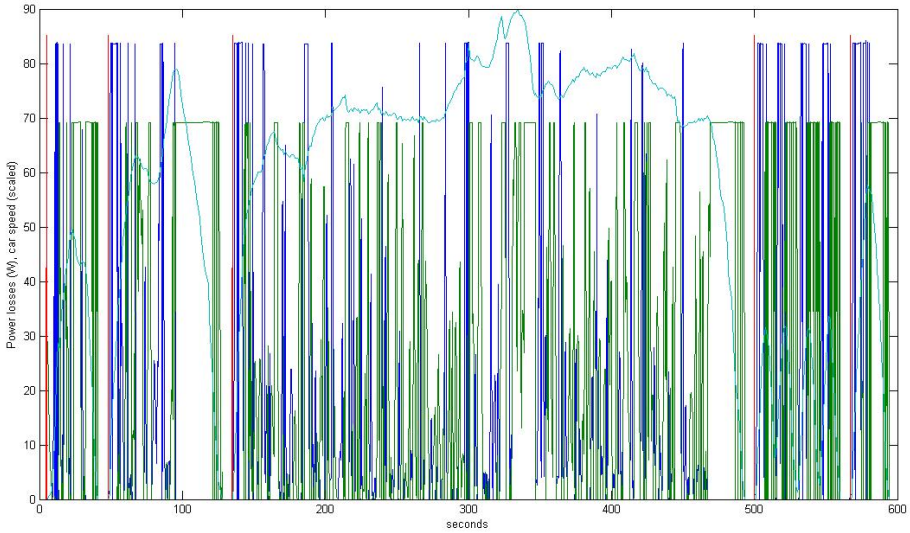

Figure 5.21: Overall losses over US06 – 300V

We can zoom now to several other areas, for example the area after 500 seconds, where we have continuous accelerations and decelerations.

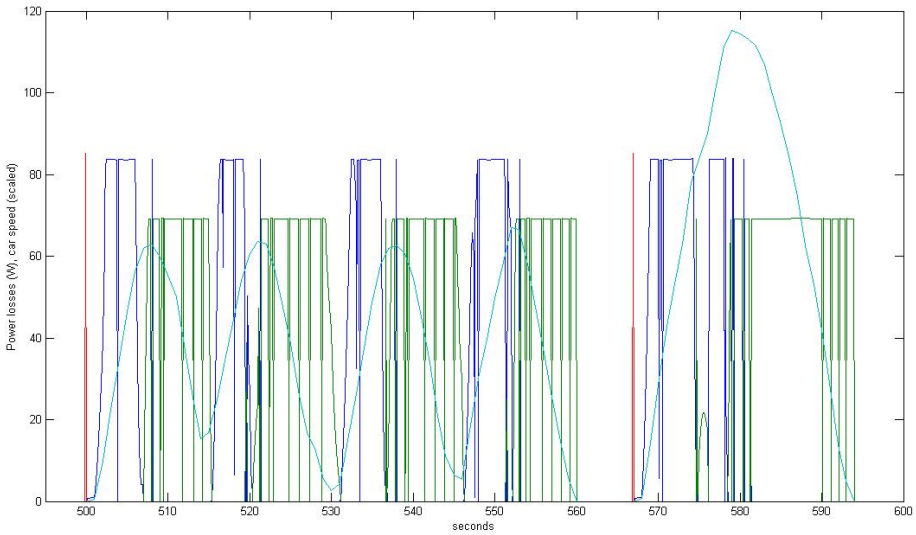

Figure 5.22: Losses over US06, 500-600 sec

It is clear now that the maximum power losses do slightly differ between the two driving cycles and that is because they are not dependant on the driving style, but the electric machine's power.

The next step is to create an image of the temperature deference between the semiconductors' junctions and the case and then estimate an appropriate heat sink for each case. We notice in all the diagrams above that the maximum power losses are in each case the transistors conducting losses and as a result we can use the values previously calculated to estimate the heat sink.

6. Thermal calculations

6.1 Introduction

Under a conventional car's hood the temperature conditions are not appropriate for electronics to operate. Air temperature can rise up to more than 200°C at which the electronics can be destroyed. A conventional car's combustion engine normally uses a liquid cooling system to dissipate the heat produced during its operation. The liquid's temperature is normally around 100°C, but can reach temperatures up to 130°C where the ICE can still operate. So, if we want to place any electronic circuit under the hood, without using a separate cooling system, it has to be able to withstand higher temperatures than the operating limits of a normal semiconductor.

Silicon carbide's advantage is that a pn-junction made of this material is able to operate in higher temperatures than common silicon. According to TranSiC [8], a SiC junction can operate even up to 225°C, high enough to be cooled with a water temperature of 130°C. Knowing the thermal properties of a SiC component and the power it dissipates over operation, we can estimate the heat sink needed to keep the inverter inside its temperature limits.

6.2 Junction-heat sink temperature difference, heat sink estimation

This temperature difference depends not only on the power losses during operation that are estimated previously, but also at the components thermal resistance between junction – case and case – heat sink. As far as the SiC diodes are concerned, we can find this value by having a look on the datasheets. For the BJTs there is no complete datasheet at the moment, so we have to make the following admission [Haraldsson-Andersson, 2007]: Si and SiC do not have the same thermal specifications. SiC actually has almost three times better thermal conductivity, but today Si wafers are three times thinner than the SiC wafers as well. Compared to an Si-IGBT module with the same electrical characteristics, an SiC module entering the market today, would have similar thermal characteristics. An Si module that fits our needs is the SKM 22GD123D, by Semikron [9].

The temperature difference between the heat sink and the junction of a single component can be found according to the equation:

$$T_{j,comp} - T_{h,comp} = P_{d,comp} \cdot \left(R_{thjc,comp} + R_{thch,comp} \right),$$

where $R_{thjc,BJT} = 0.86\ ^oC/W$, $R_{thjc,diode} = 1.5\ ^oC/W$, $R_{thch} = 0.6\ ^oC/W$.

The maximum temperature difference appears when we have the maximum losses over a component. Of course these losses differ between the two different designs (112V, 300V) and over the two driving cycles (NEDC, US06). We can proceed to a heat sink design for each DC link potential, taking into account the maximum losses that appear in each case.

Now that we know the thermal resistance of each component, we can estimate the maximum heat sink resistance, according to the method taught at the power electronics course at LTH [10]. This method follows these three steps:

1. Determine the needed heat sink temperature for all the components, assuming a maximum junction temperature:
$$T_{h,i} = T_{j,i} - P_{d,i} \cdot \left(R_{thjc,i} + R_{thch,i}\right)$$

2. The component requiring the lowest heat sink temperature will determine the allowed maximum temperature:
$$T_h = \min\left(T_{h,i}\right)$$

3. This selection of heat sink temperature means that some components will have a junction temperature lower than the maximum allowed. The maximum allowable thermal resistance for the heat sink is calculated from:
$$T_h = T_a + R_{thha} \cdot \sum_{i=1}^{n} P_{d,i} \Rightarrow R_{thha} = \frac{T_h - T_a}{\sum_{i=1}^{n} P_{d,i}}$$

Of course we have to take the worst case water temperature $\left(T_a\right)$, which is 130°C. The diodes' junction temperature limit is 175°C [4]. The transistors can operate with a junction temperature of 250°C [8], but for efficiency reasons and to have lower driving current, we prefer using them with a junction temperature of utmost 175°C. We can use a margin of 25°C, which is common in practical designs and reduce the junction temperature to 150°C, where we have made all our previous estimations as well. It is obvious that a silicon module that cannot operate reliably over 125°C, cannot be cooled by a water temperature of 130°C.

When estimated the power losses for the whole inverter, we estimated the power losses per single component as well. Multiplying the losses per component with its thermal resistance between heat sink and junction we have the temperature difference

between these two layers. The results for each design are shown in table 6.1:

Table 6.1: Temperature difference between junction and heat sink

		112 V		300 V	
		NEDC	US06	NEDC	US06
BJT (R_{thjc}=0.86)	losses (W)	2,78	2,79	3,49	3,51
	T_{jh} (^oC)	4,06	4,07	5,10	5,12
Diodes (R_{thjc}=1.5)	losses (W)	2,43	2,43	2,89	2,89
	T_{jh} (^oC)	5,10	5,10	6,07	6,07

Even if the power dissipation over a diode is lower than over a transistor, because of the diodes' thermal resistance its junction temperature is higher for the same case temperature. As a result, the components that need more cooling are the diodes, as the junction temperature is the same for both transistors and diodes (150^{o}C).

The maximum heat sink temperature is then for each case:

Table 6.2: Maximum heat sink temperature

	112 V	300 V
$T_{h,max}$ (^oC)	144,9	143,9

Our aim is to mount the whole inverter on the same heat sink plate. In that case, to estimate the heat sink's thermal resistance, we need to take into account the maximum losses of the whole circuit, not only the diode losses that come from the components which need cooling most. These losses, according to table 4.1 are:

Table 6.3: Maximum power losses of the whole inverter

	112 V	300 V
$P_{losses,max}$ (W)	201,2	85,18

Proceeding to the third step of the heat sink estimation, we result to the following thermal resistance for each case:

Table 6.4: Maximum heat sink thermal resistance

	112 V	300V
R_{thha} ($^oC/W$)	0,074	0,165

These values are rather high for a thermal resistance of a heat sink, showing that it is possible to place every component on the same heat sink. Searching on the Internet we found a common heat sink from Tykoflex that has much lower thermal resistance, as shown in figure 6.1, taken from the datasheet [11]:

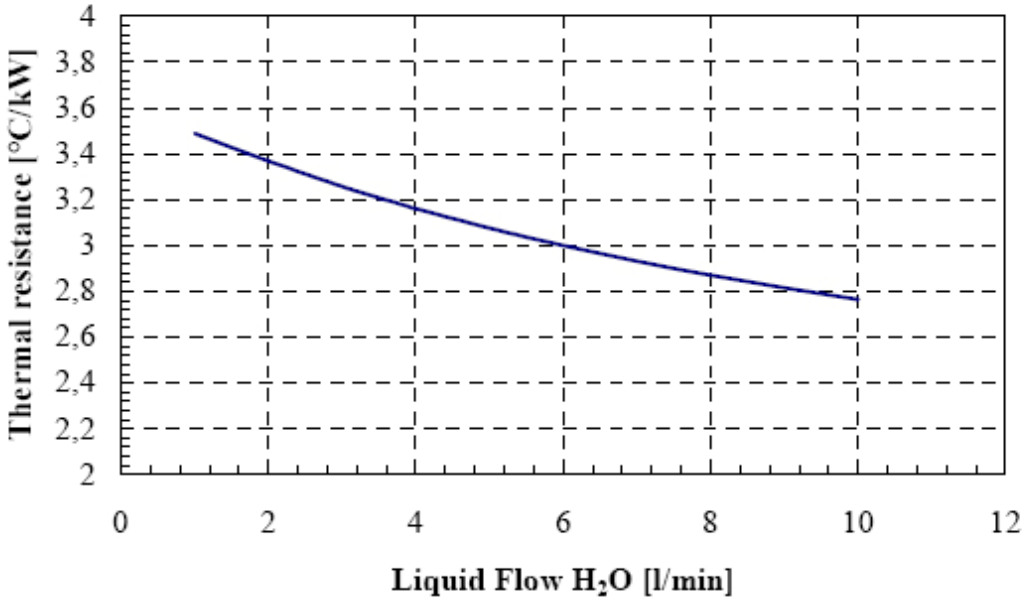

Figure 6.1: Heat sink to ambient thermal resistance over liquid flow

Considering a normal liquid flow now, say 5 l/min, the thermal resistance of the heat sink is $3.1 \cdot 10^{-3}\ ^{o}C/W$. With that value we can estimate the junction temperatures of the diodes or the transistors during a driving cycle.

6.3 Junction actual temperature over a driving cycle

Using the heat sink from Tykoflex and following the reverse procedure we can compare the results on the junction temperature for the two designs. The heat sink's low thermal resistance will result in low temperatures, much lower than the limit of 150°C. This happens because with a thermal resistance of 0.003 we do not consider the effect of the complete power losses over the inverter, as they are multiplied with a very low value. This will result into no difference between the two designs, so to prove the 300 Volts design's benefits we are going to use a thermal resistance value of $0.06\ ^{o}C/W$, almost 20 times greater, that will force the junctions' temperature to rise up to 150°C in the 112 Volts design.

On the other hand, forgetting at all the heat sink and considering a thermal resistance close to 0, will result in the junction-case temperature difference of each component. This temperature difference is slightly higher on the 300 Volts design, as it is affected only by each component's power dissipation, which is higher in that case because of higher current per component. The lower complete power losses of such a design are not of any importance when using an overestimated heat plate.

6.3.1 Transistor junction temperature over NEDC

During the NEDC a transistor's junction temperature rises up to 146°C for the 112 Volts design and up to 140°C for the 300 Volts design.

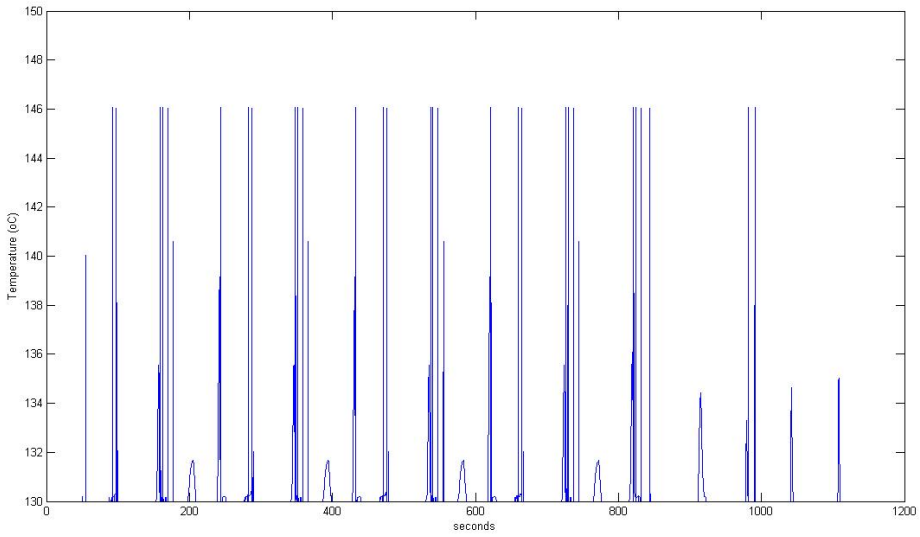

Figure 6.2: Transistor junction temperature - 112V

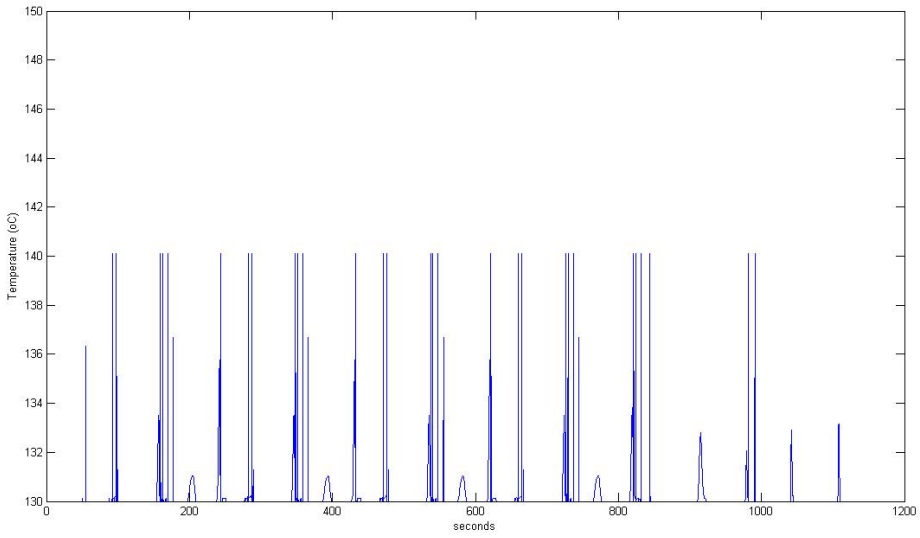

Figure 6.3: Transistor junction temperature - 300V

6.3.2 Diode junction temperature over NEDC

In figures 6.4, 6.5 we can see the junction temperature of a diode over the NEDC. The results for the maximum temperatures correspond to the BJTs' maximum temperatures.

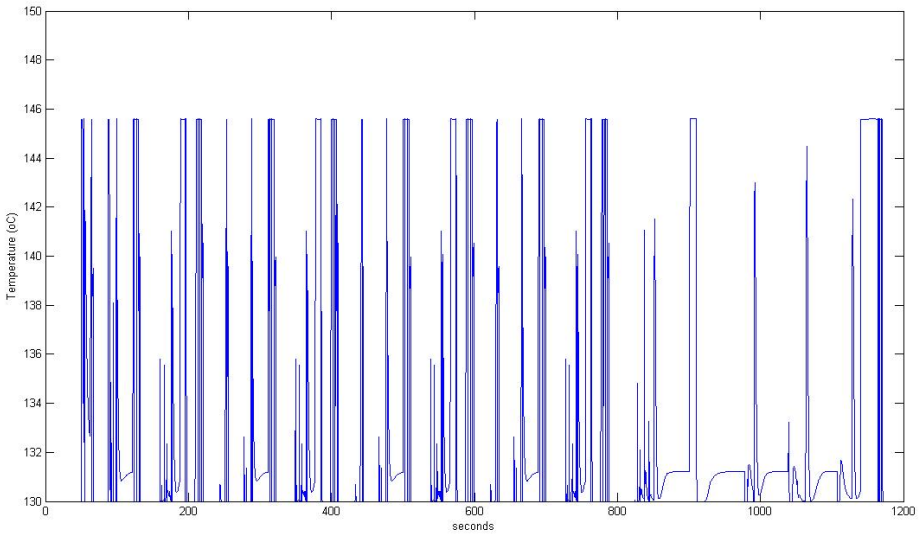

Figure 6.4: Diode junction temperature - 112V

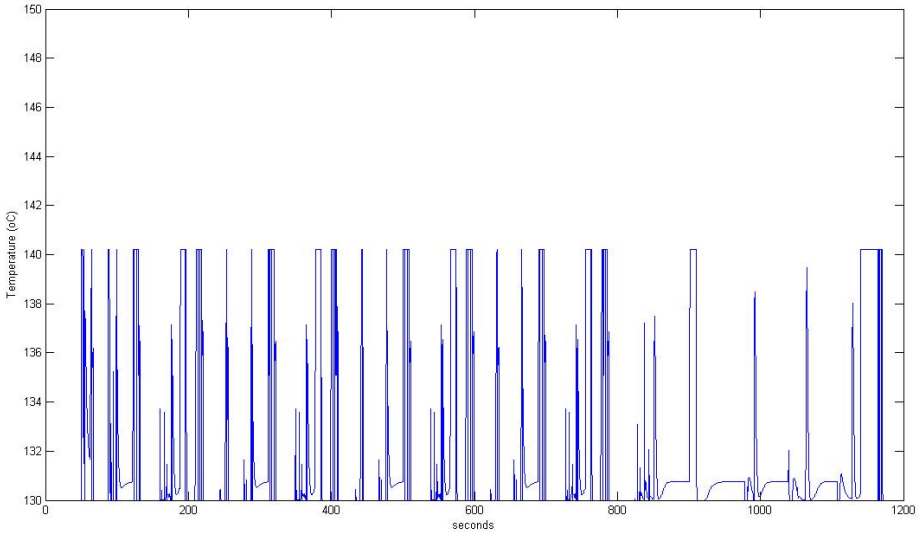

Figure 6.5: Diode junction temperature - 300V

6.3.3 Transistor junction temperature over US06

During the US06 we achieve slightly higher temperatures, compared to the NEDC. The junction temperature variation for a transistor is shown in figures 6.6, 6.7 for the 112 and 300 Volts design respectively.

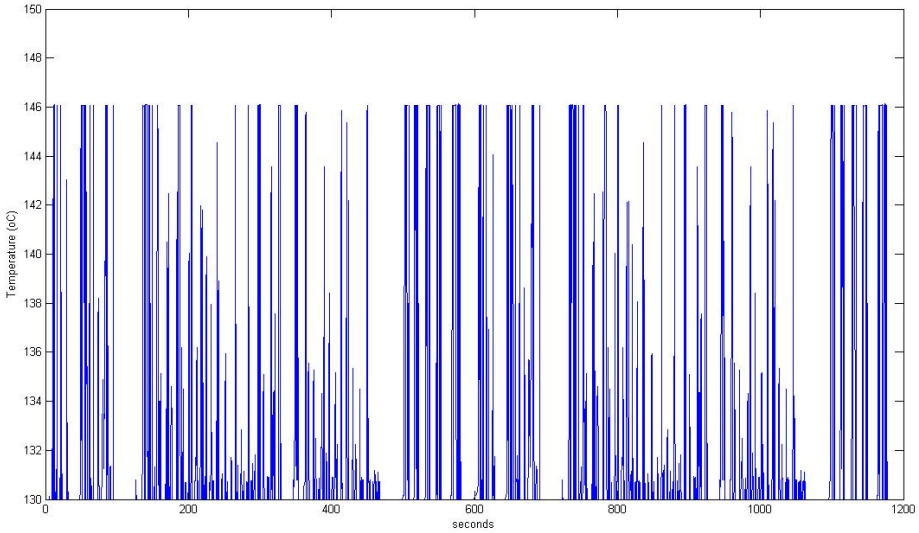

Figure 6.6: Transistor junction temperature - 112V

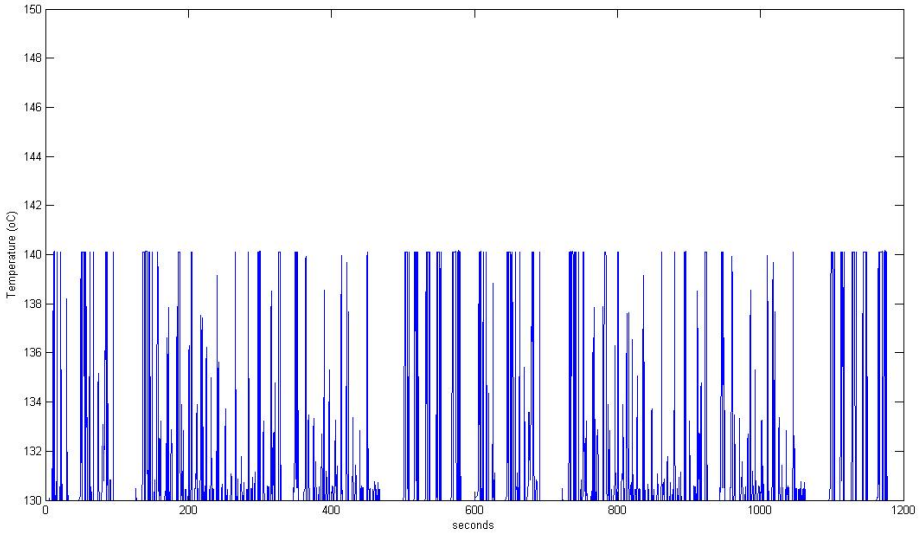

Figure 6.7: Transistor junction temperature - 300V

6.3.4 Diode junction temperature over US06

Last but not least, we present the corresponding graphs for a diode's junction temperature during the US06 driving cycle.

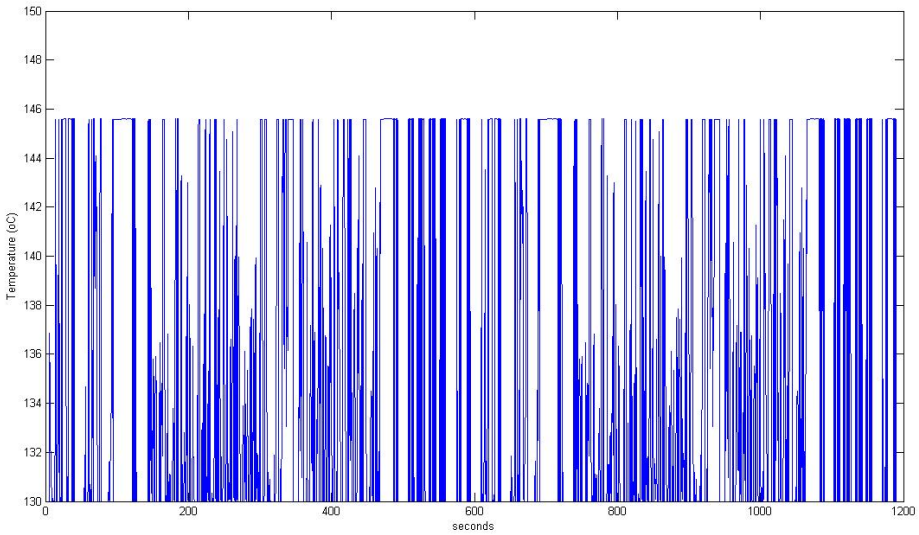

Figure 6.8: Diode junction temperature - 112V

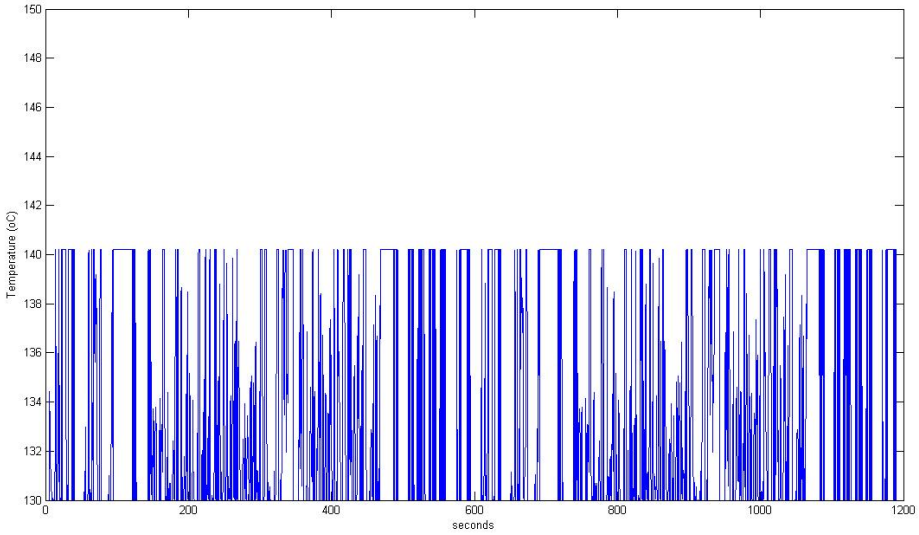

Figure 6.9: Diode junction temperature - 300V

We conclude that in both designs the heat sink needed is attainable, but in the 300 Volts design, apart from other benefits, we can use a much smaller and cheaper heat sink for that application.

7. More realistic models

7.1 Case of inductive load

In our previous estimations we assumed that the electric machine load was fully resistive. Actually it looks much like a resistive load, however it is still an electric machine, so there is an inductive part as well. It is not easy to determine the phase angle between the current and the voltage, as we were not able to run a machine of this kind, but in order to make a more realistic losses' model we assume a phase angle of 20 degrees.

This phase angle will lead to greater amplitude of phase current than what we have estimated for the resistive load in order to produce the same mechanical power on the shaft. On the other hand, this current will be much smoother without important high frequency harmonics, because of the inductance, so we cannot predict if the power losses will be increased or reduced.

We examine at first the case of a current without harmonics and we will later have a look at the impact of a fifth and seventh harmonic on the losses. These cases are examined for the square wave modulation, as it is shown before that there we have the greatest amount of losses and also this is the dominant modulation that is used in this application. Figure 7.1 shows the machine's winding voltage and current waveforms.

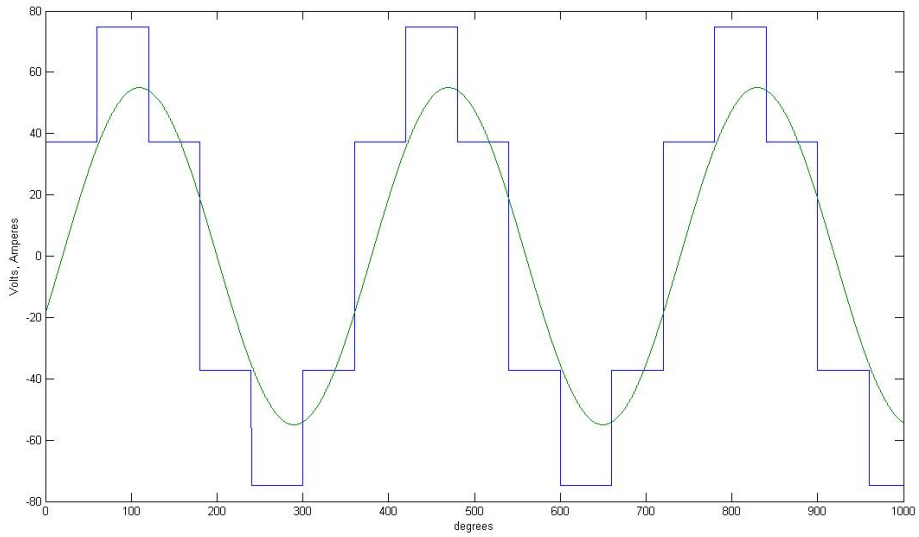

Figure 7.1: EM winding voltage and current

In this case, to achieve an output power of 5 kW from the machine and to overcome the power losses, the current rms value is around

55 A, for the 112 Volts on the DC link design. At first, we notice that the 12 transistors per module design can withstand this current, as the maximum current is less than 5 A per transistor.

The next step is to estimate the average power losses over one period. These losses derive both from the transistors and diodes. To be more specific, when the current and phase voltage waveforms are both positive or negative, then this current flows through a transistor (upper module for positive, lower for negative). In case one of the waveforms is positive and the other negative, the conduction is done through a diode. As a result we have to estimate different losses for each part, as transistors and diodes have different forward impedances. With the help of an M-file (appendix B4) we calculate the average power losses over a period for the whole inverter. These losses turn out to be:

$$P_{losses} = 159.74W$$

As we stated above, we have to include some harmonics on the current waveform, as we expect them to exist in our system. In case we add a fifth and a seventh grade harmonic, the current signal turn out to look like in figure 7.2:

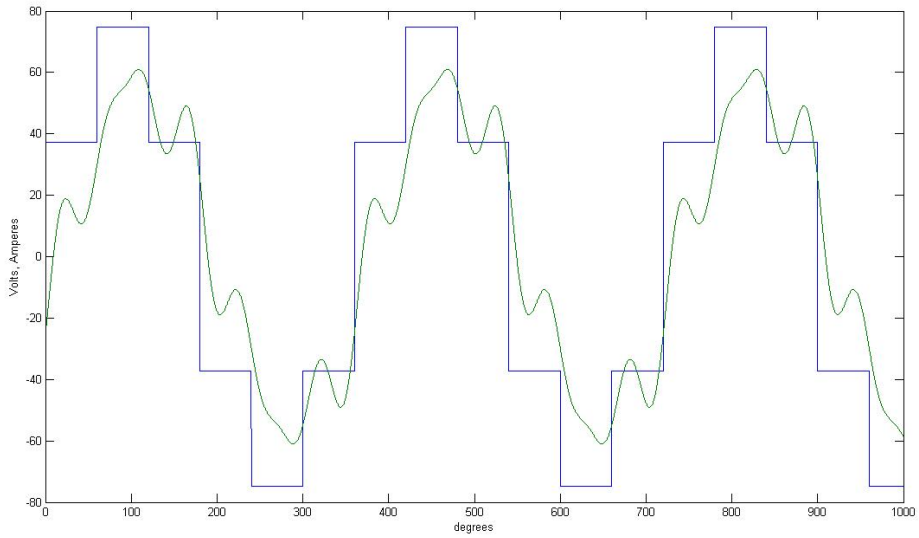

Figure 7.2: EM winding voltage and current, including 5th and 7th harmonics

We now conclude to slightly higher power losses, estimated to be:

$$P_{losses} = 168.79W$$

Adding more and more harmonics will increase that amount by some watts, but will not really affect our conclusion, which is that

the power losses do not vary a lot compared to our basic calculations in chapter 4.

This model, including the phase shift between voltage and current, seems more realistic as it includes the electric machine's inductive part. The power losses in that case seem to decrease rather than increase. This could be justified by considering that the current is looking more like a sinus, than having the voltage's shape. As a result, during a period, we have many points with lower saturation voltage on the transistors compared to the "step" looking current and some others that cause greater saturation voltage, as shown in figure 7.3. This could justify a slight difference in power losses.

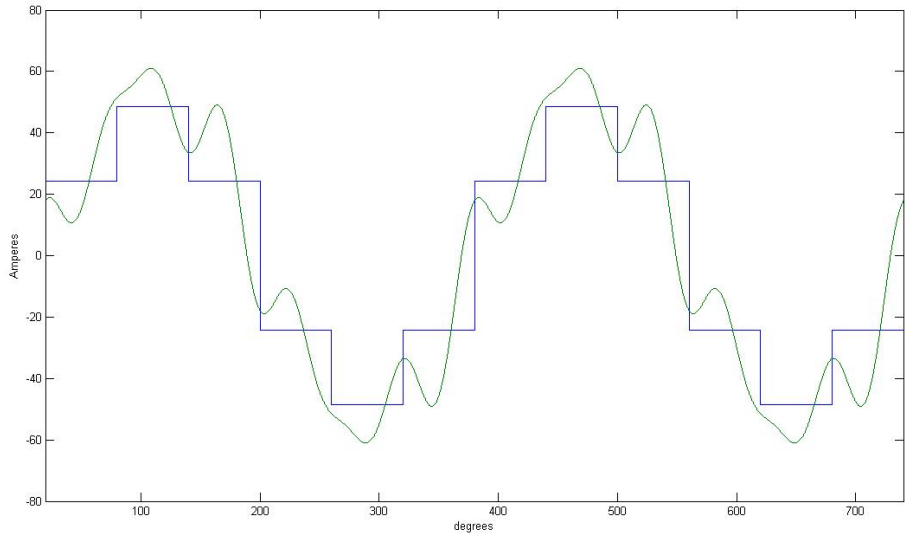

Figure 7.3: Current for a resistive and an inductive load

Apart from this difference there is another factor that can prove to be important in the losses reduction. As stated above, there is a part where the conduction is done through the diodes. As the transistors' saturation voltage is different from the diodes' forward voltage, we expect a different result. This difference could become greater in case of a more inductive load, as the diodes would conduct for longer periods.

It is proven then that our heat sink design is sufficient even for the case of an inductive load, as a motor, operating with a phase angle between current and voltage of 20^{o}.

7.2 Case of thermal capacitance in semiconductor elements

Another assumption we made in chapter 6 was that the thermal model of the semiconductors includes only a thermal resistance. A

more realistic thermal model includes a thermal capacitance as well, in parallel with the resistance. A rather complex thermal model that includes all kind of different stages between a junction and the ambient is shown in figure 7.4. This is a thermal model for an IGBT developed by Toyota for their last generation hybrid vehicles [12].

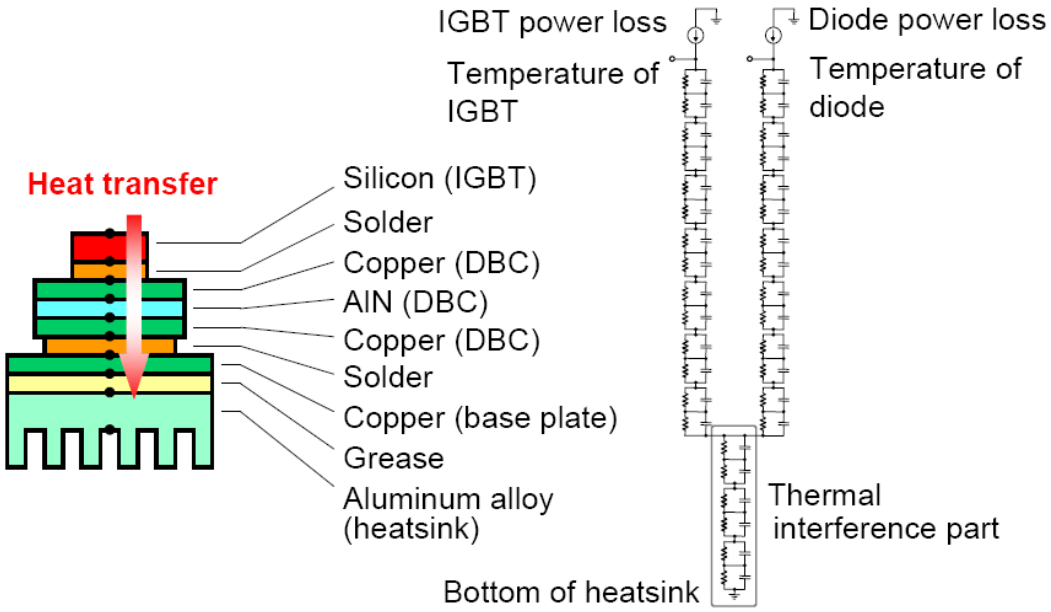

Figure 7.4: IGBT complete thermal model

This thermal capacitance introduces a time delay on the temperature rise and fall of the junction. Its effect is more important over a city driving cycle, where we have many continuous accelerations followed by corresponding decelerations. Depending on the thermal capacitance, the junction temperature may not reach the maximum values we have estimated, but also it may not be cool enough before the next acceleration if the stop time is not long enough.

In case of trains, thermal capacitance is more important, especially if the design is for a vehicle that stops at several stations every few minutes. For example in a metro design we have to include this thermal capacitance, as it is of great importance to know how the junction temperature is rising. This rise leads us to estimate for how long the locomotive can accelerate and for how long it has to wait in each station for the electronics to get cooled before the next acceleration.

In case of cars, however, we could make that study based on a driving cycle, but it is not really representative as a driving cycle is a theoretical behavior under certain circumstances. A real driver is free to accelerate for as long as he wishes and the power electronics should not discourage him of doing so. As a result, in our design, power electronics should be able to withstand the temperature rise

of any speed variation and so the heat sink design is made by taking into account this fact.

8. Conclusion

This work started just after Martin Andersson's and Oscar Haraldsson's thesis, who experimented on Silicon Carbide transistors and managed to create a model that simulated its behavior. The aim was, starting from that model, to design and construct a power converter prototype that can be used in hybrid vehicles. This project was limited to the design of the converter, as the components are not ready yet and, hence, we could not have enough semiconductors to proceed to construction.

This power converter is used to transfer electric power from the battery to the electric machine and vice versa. The idea of using SiC derived from its operating advantages in high temperatures. Moving the power electronics under the hood can eliminate significant costs that were intended for cooling systems. In this thesis is shown that the combustion engine's cooling system is sufficient to cool the power converter.

Another matter examined in this thesis was how the DC link voltage can affect the design. We used two different voltages, the 112 V that SAAB automobile desired and the 300 V standard. Our results showed many benefits from the higher DC link voltage design such as the use of less semiconductors and the need for a smaller heat sink, as the losses proved to be significantly lower. Of course the trade off in that case is a higher voltage battery, resulting in other disadvantages such as battery cost and safety precautions.

In any case, silicon carbide technology proves to be applicable and much profitable in the automobile industry, as it has much better performance compared to silicon.

9. Future work

This study emphasized on the thermal design of a power converter, made of silicon carbide semiconductors. We discussed advantages and disadvantages of two different designs. The next step is to decide on the design and build a converter to verify the results. Apart from the main part of the converter, there are many other things to be done. It is interesting to see how far we can go with silicon carbide. All driving circuits proposed so far are built both with silicon and silicon carbide components. The potential of building both the converter and its driving circuit from silicon carbide would be interesting as well. These are just the first steps in understanding and using the novel and really promising technology of silicon carbide.

References

1. Bio Power Hybrid presentation, GME-SAAB/KTH, 25/09/2006

2. A Silicon Carbide Inverter for a Hybrid Vehicle Application, Oscar Haraldsson-Andersson, Martin Andersson, Master thesis, IEA, Lund University, 2007

3. BiTSiC-1206 datasheet, rev. 0.91, TranSiC

4. IDH08S120 SiC Schottky diode datasheet, rev. 0.9, Infineon

5. Belt driver Alternator and Starter with a Series Magnetized Synchronous Machine drive, Tomas Bergh, Licentiate thesis, IEA, Lund University, 2006

6. Wikipedia: http://en.wikipedia.org/wiki/Temperature_dependence_of_liquid_viscosity

7. Comparison and Review of Electric Machines for Integrated Starter Alternator Applications, Dr Willian CAI, IEEE senior member, 2004

8. TranSiC, http://www.transic.com

9. SKM 22GD123D datasheet, Semikron

10. Power Electronics – Devices, Converters, Control and Applications, Mats Alakula and Per Karlsson, Lund University, 2006

11. Liquid cooled plate for railway IGBT converters, Tykoflex

12. Evolution of Hybrid Vehicle Electric System and its Support Technologies, APEC 2007 – System Design, Toyota Motor Corporation, 2007

Appendix A: Abbreviations

Abbreviation	Explanation
AC	Alternating Current
BAS	Belt-driven Alternator and Starter
BiTSiC	Bipolar Transistor in Silicon Carbide
BJT	Bipolar Junction Transistor
DC	Direct Current
EM	Electric Machine
EMF	Electromotive Force
EMSM	Electrically Magnetized Synchronous Macine
ICE	Internal Combustion Engine
IEA	Industrial Electrical Engineering and Automation
IGBT	Insulated Gate Bipolar Transistor
LTH	Lunds Tekniska Högskola
NEDC	New European Driving Cycle
PMSM	Permanent Magnet Synchronous Macine
PWM	Pulse Width Modulation
Si	Silicon
SiC	Silicon Carbide
SMSM	Series Magnetized Synchronous Machine
SOC	State Of Charge

Appendix B: The MATLAB code, M-files

B1. Initialization of Simulink model parameters

```
% ********************************************************
% * This file sets the parameters for the Simulink program
% * "Parallel" and must be run prior to runing simulations.
% *
% * Mats Alakula, January 2004.
% ********************************************************

%Driving Cycles
load eudc;
load us06;

ICEpower=110000;
EMpower=5000;

% Vehicle type ++++++++++++++++++++++++++++
Fuel=1;          % Defines if gasoline (Fuel=1) or Diesel (Fuel=2) is
used, (DEFAULT=1)
Hybrid=0;        % 0 for conventional, 1 for parallellhybrid  (DEFAULT
= 0)
Depletion=0;     % Depletion = 0 for Charge Sustaining mode and 1 for
depletion mode (DEFAULT = 0)
StopAndGo=0;     % 1 if stop & go is on (DEFAULT = 0)
Speedy=0;        % 1 for "sporty" driving  (DEFAULT = 0)

if Fuel==1, % Gasoline
    load EtaICE_OTTO;
    EtaICE = EtaICE_OTTO;
elseif Fuel==2, % Diesel
    load EtaICE_DIESEL;
    EtaICE = EtaICE_DIESEL;
else
    'Erroneous fuel choice'
end

[value,row]=max(max(EtaICE'));

Pice_max = ICEpower*Hybrid+110000*(1-Hybrid);
if Fuel==1,
    wice_max = 6000*2*pi/60;
elseif Fuel==2,
    wice_max = 4500*2*pi/60;
else
    'Erroneous fuel choice'
end
wice_min = 950*2*pi/60; % 950 rpm idle
Tice_max = Pice_max/(wice_max*row/(length(EtaICE)-1));

[PtoT,Tice,Wice,Tlim_ice,FuelConsICE]=CreateICEmap(Pice_max,wice_max,
Tice_max,EtaICE);
```

```
% Gear ratio for the final gear between the traction motor and the
wheels   *************'
gr2 = 1;
EtaGEAR=0.96;

% Mechanical parameters  +++++++++++++++++
Mv = 1645;          % Vehicle weight
rw = 0.317;         % wheel radius (m)
Cd = 0.26;          % air resistance
Cr = 0.007;         % roll resistance
Av = 2.52;          % Front area
rho_air = 1.22;     % Air density
grav = 9.81;
vmax=160/3.6;       % 160 km/h max speed

Pvehicle_max = (Cr*Mv*grav+1/2*rho_air*Cd*Av*vmax^2)*vmax;

Number_of_gears = 5;
v = [Inf 13.6818    7.1591    4.5036    3.4119    2.5215];
Utvx_vect = v(end:-1:1);


% Electric machine's parameters  +++++++++++++++++
Pem_max = EMpower*Hybrid+2000*(1-Hybrid)       % Peak continuous
power
Tem_max = 60*Hybrid+10*(1-Hybrid)  % Peak continuous torque
wem_max=3*wice_max      % EM mounted on cranc shaft
wem_min=3*wice_min

[EtaEM,Tem,Wem] = CreateEMmap(Pem_max,wem_max,Tem_max);

% Power Electronics efficiency (preset)
EtaPE = 0.96;

% Fuel energy density
if Fuel==1, % Gasoline
    Density = 32000000;
elseif Fuel==2, % Diesel
    Density = 35900000;
else
    'Erroneous fuel choice'
end

% Battery parameters +++++++++++++++++
Wbatt = 100*3600*25;   % 100 Wh/kg, 3600 sec/h, 25 kg
[EtaBATT,Pbatt]=CreateBATTmap(Pem_max,Wbatt);
SOC_batt_ref_value = 70;

% Controller parameters *********************************
Tau_charge = 1;
ksoc = max(Wbatt)/400/Tau_charge;
%ksoc = max(Wbatt)/400/Tau_charge;

% Auxilliary load power **********************
Paux = 600;    % Without AC
```

B2. Calculating switching losses

a. Turn-on

```
%*****************************************
%Calculating losses of a BJT during turn-on
%07/05/2007
%Antonopoulos Antonios
%*****************************************

%Initial input
Vnom=112;
%Inom=5;

%otherwise
load tWPem;
load freq_em;
for i=1:12001
Inom=tWPem(i,3)/(sqrt(3)*87.4*12); %I=Power/(sqrt(3)*Vll*Nsic);

%Other parameters
Ipeak=1.25*Inom;
Vcesat=2.1;

%Time parameters, according to graph, may need to be changed!!
tV0=0;      %before tV0 -> V=Vnom
tV1=0.09;   %after tV1 -> V=Vcesat

tI0=0.02;   %before tI0 -> I=0
tI1=0.05;   %at tI1 -> I=Ipeak
tI2=0.14;   %after tI2 -> I=Inom

%Graph model!
%  V
%------
%       \
%        \
%         \
%          \
%           \ +
%            \  +
%           + \   +
%          +   \    +      I
%         +     \     ++++++++++++
%        +       \
%       +         -------------------------
%+++++++%%%%%%%%%%%%%%%%%%%%%%%%%%%%%%%%%%%%%%%%%%%%
%     ||      |   |   |
%  tV0 tI0  tI1  tV1  tI2

%Calculating grades (λ)
lamdaI1=Ipeak/(tI1-tI0);        %between tI0, tI1
lamdaI2=(Inom-Ipeak)/(tI2-tI1);     %between tI1, tI2
lamdaV=(Vcesat-Vnom)/(tV1-tV0);     %between tV0, tV1

%Calculating line beta factors
bV=Vcesat-lamdaV*tV1;
bI1=-lamdaI1*tI0;
```

```
bI2=Inom-lamdaI2*tI2;

%Calculating trionym factors a, b, c
aP1=lamdaV*lamdaI1;
aP2=lamdaV*lamdaI2;
aP3=Vcesat*lamdaI2;

bP1=lamdaV*bI1+lamdaI1*bV;
bP2=lamdaV*bI2+lamdaI2*bV;
bP3=Vcesat*bI2;

cP1=bV*bI1;
cP2=bV*bI2;

%Integrating, energy losses per sector
E1=aP1*(tI1^3-tI0^3)/3+bP1*(tI1^2-tI0^2)/2+cP1*(tI1-tI0);
E2=aP2*(tV1^3-tI1^3)/3+bP2*(tV1^2-tI1^2)/2+cP2*(tV1-tI1);
E3=aP3*(tI2^2-tV1^2)/2+bP3*(tI2-tV1);

%Total energy losses during turn-on on inverter
%E=E1+E2+E3;
E_turnon(i,1)=tWPem(i,1);
E_turnon(i,2)=12*6*(E1+E2+E3)*freq_em(i,2)/10;  %factor 10 because we
have frequency sampling over 0.1 seconds

end;
```

b. Turn-off

```
%*****************************************
%Calculating losses of a BJT during turn-off
%07/05/2007
%Antonopoulos Antonios
%*****************************************

%Initial input
Vnom=112;
%Inom=5;

%otherwise
load tWPem;
load freq_em;
for i=1:12001
Inom=tWPem(i,3)/(sqrt(3)*87.4*12); %I=Power/(sqrt(3)*Vll*Nsic);

%Other parameters
Vpeak=1.1*Vnom;
Iknee=0.8*Inom;
Ilow=-0.15*Inom;
Vcesat=2.1;

%Time parameters, according to graph, may need to be changed!!
tV0=0;      %before tV0 -> V=Vcesat
tV1=0.14;   %at tV1 -> V=Vpeak
tV2=0.24;   %after tV2 -> V=Vnom

tI0=0;      %before tI0 -> I=Inom
```

```
tI1=0.14;   %at tI1 -> I=Iknee
tI2=0.16;   %at tI2 -> I=Ilow
tI3=0.3;    %after tI3 -> I=0

%Graph model!
%               /--
%              /    \--               V
%             /         \----------------------------
%            /
%           /
%++++      /
%    ++++/
%        /++++
%       /     ++
%      /       +
%     /         +
%---/           +
%                +                          I
%%%%%%%%%%%%%%%%+%%%%%%%%%%%%+++++++++++++++++++++++++++++++
%                 +   ++++++++
%                 ++++
%   |         |   |       |    |
%  tV0      tV1  tI2     tV2   tI3
%  tI0      tI1

%Calculating grades (λ)
lamdaI1=(Iknee-Inom)/(tI1-tI0);     %between tI0-tI1
lamdaI2=(Ilow-Iknee)/(tI2-tI1);     %between tI1-tI2

%calculating the area below 0
if lamdaI2~=0;
    Ilow=-Ilow;
    tempT=tI1-Iknee/lamdaI2;    %time
    tempT=tI2-tempT;            %difference
    tI2=tI2-2*tempT;            %new tI2
end;

lamdaI3=-Ilow/(tI3-tI2);
lamdaV1=(Vpeak-Vcesat)/(tV1-tV0);
lamdaV2=(Vnom-Vpeak)/(tV2-tV1);

%Calculating line beta factors
bV1=Vcesat-lamdaV1*tV0;
bV2=Vnom-lamdaV2*tV2;
bI1=Inom-lamdaI1*tI0;
bI2=Ilow-lamdaI2*tI2;
bI3=-lamdaI3*tI3;

%Calculating trionym factors a, b, c
aP1=lamdaV1*lamdaI1;
aP2=lamdaV2*lamdaI2;
aP3=lamdaV2*lamdaI3;
aP4=Vnom*lamdaI3;

bP1=lamdaV1*bI1+lamdaI1*bV1;
bP2=lamdaV2*bI2+lamdaI2*bV2;
bP3=lamdaV2*bI3+lamdaI3*bV2;
bP4=Vnom*bI3;

cP1=bV1*bI1;
```

```
cP2=bV2*bI2;
cP3=bV2*bI3;

%Integrating, energy losses per sector
E1=aP1*(tI1^3-tI0^3)/3+bP1*(tI1^2-tI0^2)/2+cP1*(tI1-tI0);
E2=aP2*(tI2^3-tI1^3)/3+bP2*(tI2^2-tI1^2)/2+cP2*(tI2-tI1);
E3=aP3*(tV2^3-tI2^3)/3+bP3*(tV2^2-tI2^2)/2+cP3*(tV2-tI2);
E4=aP4*(tI3^2-tV2^2)/2+bP4*(tI3-tV2);

%Total energy losses during turn-off on inverter
%E=E1+E2+E3;
E_turnoff(i,1)=tWPem(i,1);
E_turnoff(i,2)=12*6*(E1+E2+E3+E4)*freq_em(i,2)/10;     %factor 10
because we have frequency sampling over 0.1 seconds

end;
```

B3. Calculating conducting losses

a. Over transistors

```
%Calculating conducting losses over transistors
%over a specified driving cycle

%Driving cycle
load Pmech_US06;
load Pmech;
%Pmech=Pmech_US06;

P(:,1)=Pmech(:,1);
P(:,2)=Pmech(:,2);

%Distinguish transistor from diode losses
for i=1:12001
    if Pmech(i,3)<0
        P(i,3)=0;
    else
        P(i,3)=Pmech(i,3);
    end
end

Vdc=300;    %DC link voltage
VR_high=2*Vdc/3;    %phase voltage
VR_low=Vdc/3;

Vll=sqrt(6)*Vdc/pi; %line to line voltage, fundamental

Pcomp(:,1)=P(:,1);
Pcomp(:,2)=1.1*P(:,3);  %losses on the EM

%Calculating the phase current
Req_phase(:,1)=P(:,1);
for i=1:12001
    if Pcomp(i,2)>0
        Req_phase(i,2)=(Vll^2)/Pcomp(i,2);
    else
        Req_phase(i,2)=0;
    end
end

Iphase(:,1)=P(:,1);
for i=1:12001
    if Req_phase(i,2)>0
        Iphase(i,2)=VR_high/Req_phase(i,2);
        Iphase(i,3)=VR_low/Req_phase(i,2);
    else
        Iphase(i,2)=0;
        Iphase(i,3)=0;
    end
end

% Saturation Collector-Emitter Voltage (dependant on # of components)
Vcesat(:,1)=P(:,1);
for i=1:12001
```

```
    Vcesat(i,2)=0.42*Iphase(i,2)/4;
    Vcesat(i,3)=0.42*Iphase(i,3)/4;
end

Econd_losses(:,1)=P(:,1);
for i=1:12001
    Econd_losses(i,2)=Vcesat(i,2)*Iphase(i,2)*0.05/3;
    Econd_losses(i,3)=Vcesat(i,3)*Iphase(i,3)*0.1/3;
end

%Power losses and temperature calculations
Rthjc=0.86;
Rthch=0.6;
Rthha=0.06;
Ta=130;
Tja(:,1)=P(:,1);
Pcond_losses(:,1)=P(:,1);
for i=1:12001
    Pcond_losses(i,2)=Vcesat(i,2)*Iphase(i,2)*0.5/3;
    Pcond_losses(i,3)=Vcesat(i,3)*Iphase(i,3)/3;
    Pcond_losses(i,4)=Pcond_losses(i,2)+Pcond_losses(i,3);
    Tja(i,2)=Rthjc*Pcond_losses(i,4)/4;
    Tja(i,3)=Rthch*Pcond_losses(i,4)/4;
    Tja(i,4)=Rthha*Pcond_losses(i,4)*6;
    Tja(i,5)=Tja(i,2)+Tja(i,3)+Tja(i,4)+Ta;
end

EnergyLosses=0;
Energy=0;
for i=1:12001
   EnergyLosses=EnergyLosses+6*(Econd_losses(i,2)+Econd_losses(i,3));
   Energy=Energy+Pcomp(i,2)*0.1;
end

PowerLosses=0;
Power=0;
for i=1:12001
    PowerLosses=PowerLosses+6*Pcond_losses(i,4);
    Power=Power+Pcomp(i,2);
end
PowerLosses=PowerLosses/12001;
Power=Power/12001;

%Efficiency
efficiency=(Energy-EnergyLosses)/Energy;
Pefficiency=(Power-PowerLosses)/Power;
```

b. Over diodes

```
%Calculating conducting losses over diodes
%over a specified driving cycle%

%Driving cycle
load Pmech_US06;
load Pmech;
%Pmech=Pmech_US06;

P(:,1)=Pmech(:,1);
```

```
P(:,2)=Pmech(:,2);

%Distinguish diode from transistor losses
for i=1:12001
    if Pmech(i,3)<0
        P(i,3)=-Pmech(i,3);
    else
        P(i,3)=0;
    end
end

Vdc=300;    %DC link voltage

Pcomp(:,1)=P(:,1);
Pcomp(:,2)=P(:,3);

%Calculating the direct current
Rdc(:,1)=P(:,1);
for i=1:12001
    if Pcomp(i,2)>0
        Rdc(i,2)=(Vdc^2)/Pcomp(i,2);
    else
        Rdc(i,2)=0;
    end
end

Idc(:,1)=P(:,1);
for i=1:12001
    if Rdc(i,2)>0
        Idc(i,2)=Vdc/Rdc(i,2);
    else
        Idc(i,2)=0;
    end
end

% Forward Voltage
Vf(:,1)=P(:,1);
for i=1:12001
    Vf(i,2)=((Idc(i,2)/4)+3.261)/4.348;
end

Econd_losses(:,1)=P(:,1);
for i=1:12001
    Econd_losses(i,2)=Vf(i,2)*Idc(i,2)*0.05;
end

%Power losses and temperature calculations
Rthjc=1.5;
Rthch=0.6;
Rthha=0.06;
Ta=130;
Tja(:,1)=P(:,1);
Pcond_losses(:,1)=P(:,1);
for i=1:12001
    Pcond_losses(i,2)=Vf(i,2)*Idc(i,2)*0.5;
    Tja(i,2)=Rthjc*Pcond_losses(i,2)/4;
    Tja(i,3)=Rthch*Pcond_losses(i,2)/4;
    Tja(i,4)=Rthha*Pcond_losses(i,2)*6;
    Tja(i,5)=Tja(i,2)+Tja(i,3)+Tja(i,4)+Ta;
end
```

```
EnergyLosses=0;
Energy=0;
for i=1:12001
    EnergyLosses=EnergyLosses+6*Econd_losses(i,2);
    Energy=Energy+Pcomp(i,2)*0.1;
end

PowerLosses=0;
Power=0;
for i=1:12001
    PowerLosses=PowerLosses+6*Pcond_losses(i,2);
    Power=Power+Pcomp(i,2);
end
PowerLosses=PowerLosses/12001;
Power=Power/12001;

%Efficiency
efficiency=(Energy-EnergyLosses)/Energy;
Pefficiency=(Power-PowerLosses)/Power;
```

B4. Calculating power losses of an inductive load

```
% Calculating conducting losses over the inverter
% when the power factor is not 1

fi=pi/9;     % φ = 20 degrees
Vdc=112;     % DC link voltage

for i=1:10000   % degrees, not to be confused with seconds
    I(i,1)=i/10;
    I(i,2)=55*sin(I(i,1)*pi/180-fi);     %fundamental
    I(i,3)=11*sin(I(i,1)*5*pi/180-fi);   %5th harmonic
    I(i,4)=8*sin(I(i,1)*7*pi/180-fi);    %7th harmonic
    I(i,2)=I(i,2)+I(i,3)+I(i,4);
end;

% EM winding voltage
for i=1:10000
    VRN(i,1)=i/10;
    if sin(VRN(i,1)*pi/180)>0
        VRN(i,2)=Vdc/3;
    end;
    if sin(VRN(i,1)*pi/180)<0
        VRN(i,2)=-Vdc/3;
    end;
    if sin(VRN(i,1)*pi/180)==0
        VRN(i,2)=0;
    end;

    if abs(sin(VRN(i,1)*pi/180))>0.866
        VRN(i,2)=2*VRN(i,2);
    end;
end;

% Actual active power per phase
avgP=0;
for i=1:10000
    P(i,1)=i/10;
    P(i,2)=VRN(i,2)*I(i,2)*cos(fi);
    avgP=avgP+P(i,2);
end;
avgP=avgP/i;

for i=1200:10000
    P(i,3)=P(i-1199,2);
end;
for i=2400:10000
    P(i,4)=P(i-2399,2);
end;

avgPall=0;
for i=5001:10000
    avgPall=avgPall+P(i,2)+P(i,3)+P(i,4);
end;
avgPall=avgPall/5000;

% Vce,sat - Vforward
for i=1:10000
```

```
    Vcesat(i,1)=i/10;
    Vf(i,1)=i/10;
    Vcesat(i,2)=0.42*I(i,2)/12;
    Vf(i,2)=((I(i,2)/12)+3.261)/4.348;
end;

%Losses over BJTs and diodes
for i=1:10000
    Plosses(i,1)=i/10;
    if (I(i,2)*VRN(i,2))>0
        Plosses(i,2)=abs(Vcesat(i,2)*I(i,2));
    end;
    if (I(i,2)*VRN(i,2))<0
        Plosses(i,2)=abs(Vf(i,2)*I(i,2));
    end;
    if (I(i,2)*VRN(i,2))==0
        Plosses(i,2)=0;
    end;
end;

%Average within a period
avgPlosses=0;
for i=3601:7200
    avgPlosses=avgPlosses+Plosses(i,2);
end;
avgPlosses=avgPlosses/3600;

for i=1200:10000
    Plosses(i,3)=Plosses(i-1199,2);
end;
for i=2400:10000
    Plosses(i,4)=Plosses(i-2399,2);
end;

avgPlosses3=0;
for i=5001:10000
    avgPlosses3=avgPlosses3+Plosses(i,2)+Plosses(i,3)+Plosses(i,4);
end;
avgPlosses3=avgPlosses3/5000;
```

B5. PWM waveforms, pulses and output voltage

```
% PWM waveforms, pulses, output voltage
% winding voltage, line to line voltage

% Reference signal
for i=1:7200
    PWM(i,1)=i;      %degrees
    PWM(i,2)=56*sin(PWM(i,1)*pi/1800);        %sin
    PWM(i,7)=56*sin((PWM(i,1)+1200)*pi/1800);
    PWM(i,8)=56*sin((PWM(i,1)+2400)*pi/1800);

    phase(i,1)=56*sin(PWM(i,1)*pi/1800);
    phase(i,2)=56*sin(PWM(i,1)*pi/1800+2*pi/3);
    phase(i,3)=56*sin(PWM(i,1)*pi/1800+4*pi/3);
    phase(i,4)=max(phase(i,1),phase(i,2));
    phase(i,4)=max(phase(i,4),phase(i,3));
    phase(i,5)=min(phase(i,1),phase(i,2));
    phase(i,5)=min(phase(i,5),phase(i,3));

    PWM(i,3)=PWM(i,2)-0.5*(phase(i,4)+phase(i,5));    %symmetrical sin
    PWM(i,9)=PWM(i,7)-0.5*(phase(i,4)+phase(i,5));
    PWM(i,10)=PWM(i,8)-0.5*(phase(i,4)+phase(i,5));
end;

fratio=30;       %ftriang/fsin
Ttriang=round(3600/fratio);
Atriang=56;

% Triangular pulse
for i=1:2*fratio
    for j=1:round(Ttriang/4)
        PWM((i-1)*Ttriang+j,4)=(Atriang/(Ttriang/4))*PWM(j,1);
    end
    for j=round((Ttriang/4)+1):round(3*Ttriang/4)
        PWM((i-1)*Ttriang+j,4)=-(Atriang/(Ttriang/4))*(PWM(j,1)-
Ttriang/2);
    end
    for j=round(3*Ttriang/4):Ttriang
        PWM((i-1)*Ttriang+j,4)=(Atriang/(Ttriang/4))*(PWM(j,1)-
Ttriang);
    end
end

% pulses production
for i=1:7200
    if PWM(i,2)>PWM(i,4)         %pulses from sin
        PWM(i,5)=12;
    else if PWM(i,2)<PWM(i,4)
        PWM(i,5)=-12;
        end
    end

    pulses(i,1)=0;
    pulses(i,2)=0;
    pulses(i,3)=0;
    pulses(i,4)=0;
    pulses(i,5)=0;
```

```
    pulses(i,6)=0;

    if PWM(i,3)>PWM(i,4)         %pulses from symmetrical sin a
        pulses(i,1)=12;
    else if PWM(i,3)<PWM(i,4)
        pulses(i,4)=12;
        end
    end
    if PWM(i,9)>PWM(i,4)         %pulses from symmetrical sin b
        pulses(i,3)=12;
    else if PWM(i,9)<PWM(i,4)
        pulses(i,6)=12;
        end
    end
    if PWM(i,10)>PWM(i,4)         %pulses from symmetrical sin c
        pulses(i,5)=12;
    else if PWM(i,10)<PWM(i,4)
        pulses(i,2)=12;
        end
    end
end

% Output phase voltage, inverter's reference
for i=1:7200
    if pulses(i,1)>0
        VR(i,1)=56;
    else if pulses(i,4)>0
        VR(i,1)=-56;
        end
    end
    if pulses(i,3)>0
        VS(i,1)=56;
    else if pulses(i,6)>0
        VS(i,1)=-56;
        end
    end
    if pulses(i,5)>0
        VT(i,1)=56;
    else if pulses(i,2)>0
        VT(i,1)=-56;
        end
    end
end

% VR(i,2) : VRN, reference: machine's neutral
for i=1:7200
    if ((VR(i,1)==56)&&(VS(i,1)==56)&&(VT(i,1)==-56))
        VR(i,2)=37.33;
        VS(i,2)=37.33;
        VT(i,2)=-74.67;
    end
    if ((VR(i,1)==56)&&(VS(i,1)==-56)&&(VT(i,1)==56))
        VR(i,2)=37.33;
        VS(i,2)=-74.67;
        VT(i,2)=37.33;
    end
    if ((VR(i,1)==56)&&(VS(i,1)==-56)&&(VT(i,1)==-56))
        VR(i,2)=74.67;
        VS(i,2)=-37.33;
        VT(i,2)=-37.33;
    end
```

```
    if ((VR(i,1)==-56)&&(VS(i,1)==56)&&(VT(i,1)==-56))
        VR(i,2)=-37.33;
        VS(i,2)=74.67;
        VT(i,2)=-37.33;
    end
    if ((VR(i,1)==-56)&&(VS(i,1)==-56)&&(VT(i,1)==56))
        VR(i,2)=-37.33;
        VS(i,2)=-37.33;
        VT(i,2)=74.67;
    end
    if ((VR(i,1)==-56)&&(VS(i,1)==56)&&(VT(i,1)==56))
        VR(i,2)=-74.67;
        VS(i,2)=37.33;
        VT(i,2)=37.33;
    end
end

%=========================================================
```